Improving the Bone Forming Ability of Synthetic Bone Substitutes Using Trace Element Additions

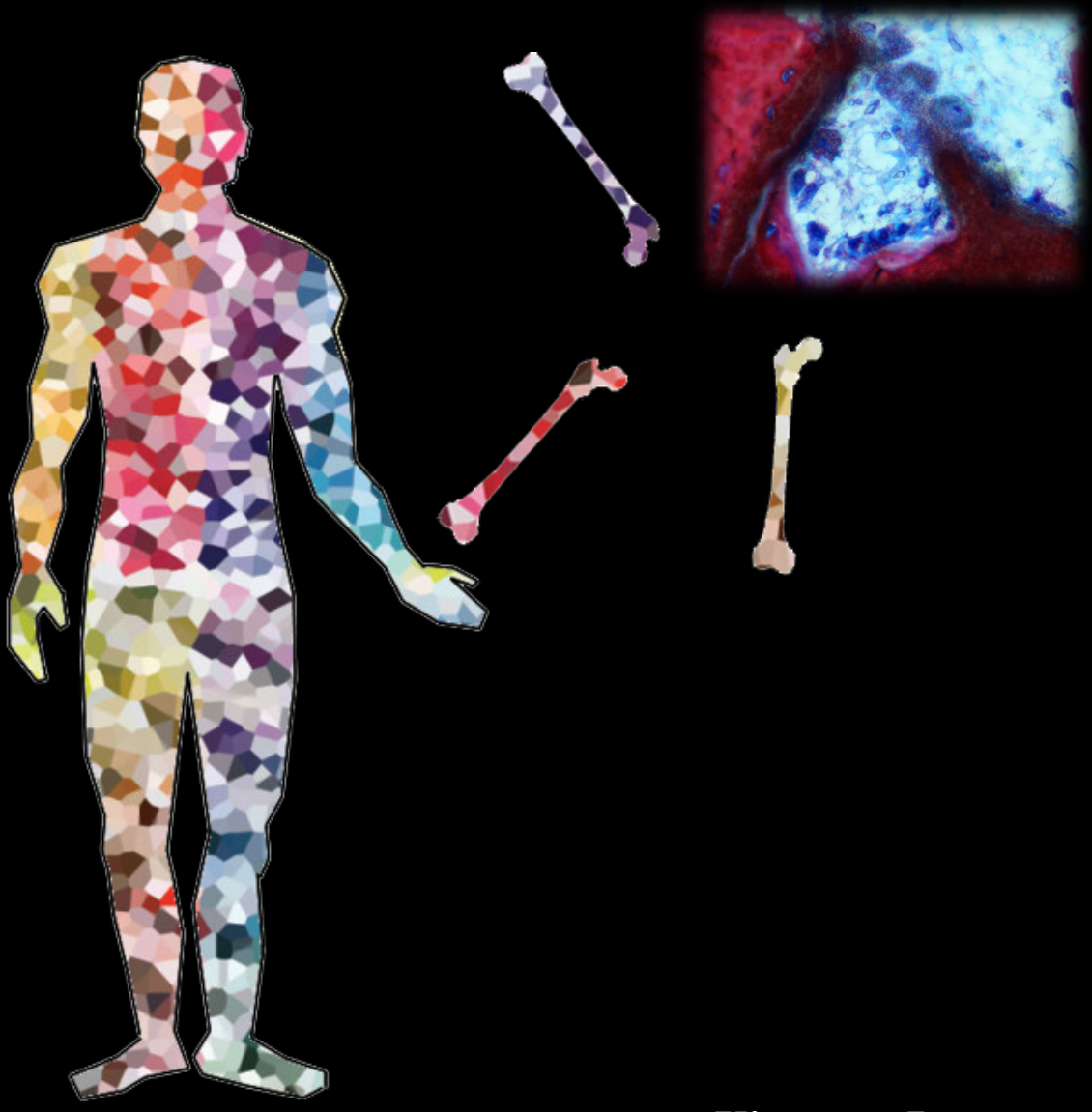

Xiaoman Luo

Improving the bone forming ability of synthetic bone substitutes using trace element additions

Xiaoman Luo

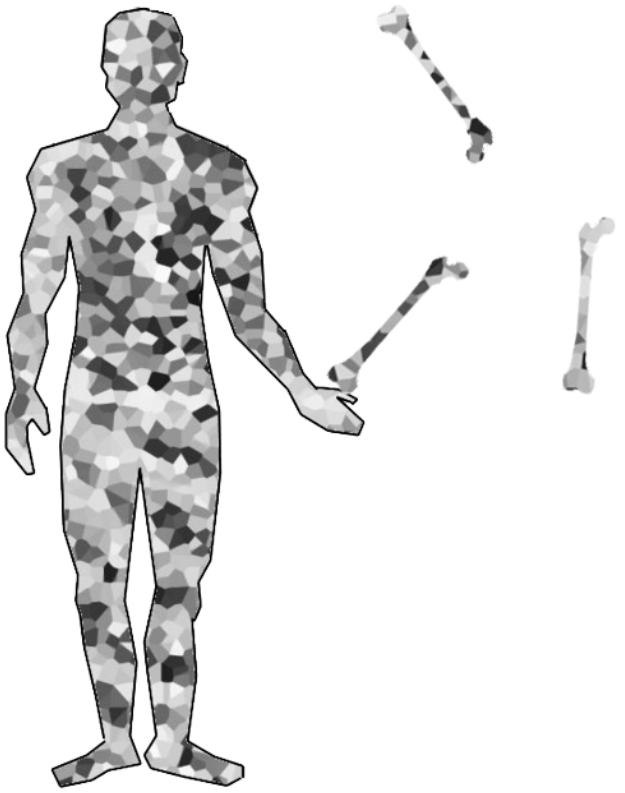

Members of the Committee

Chairman

Prof. Dr. Ir. J.W.M. Hilgenkamp

Promoter

Prof. Dr. J.D. de Bruijn

Assistant Promoter

Dr. Huipin Yuan

Members

Prof. Dr. Dirk Grijpma
Dr. Jeroen van den Beucken
Prof. Dr. Marc Bohner
Prof. Dr. Marcel Karperien
Prof. Dr. Pamela Habibovic
Prof. Dr. Yonggang Yan

Improving the bone forming ability of synthetic bone substitutes using trace element additions

Xiaoman Luo

PhD thesis, University of Twente, Enschede, the Netherlands
ISBN: 978-90-365-3966-1

The research described in this thesis was fully supported by

Xpand biotechnology

The printing of this thesis was generously sponsored by

MIRA BIOMEDICAL TECHNOLOGY AND TECHNICAL MEDICINE

PEPROTECH Manufacturer of Quality Cytokine Products

Anna Fonds

IMPROVING THE BONE FORMING ABILITY OF SYNTHETIC BONE SUBSTITUTES USING TRACE ELEMENT ADDITIONS

DISSERTATION

to obtain

the degree of doctor at the University of Twente

on the authority of the rector magnificus,

Prof. Dr. H. Brinksma,

on account of the decision of the graduation committee,

to be publicly defended

on Wednesday October 28th, 2015 at 12.45 hrs.

by

Xiaoman Luo

born May 22nd, 1984

in Chengdu, China

This dissertation has been approved by

PROMOTER Prof. Dr. Joost D. de Bruijn

ASSITANT PROMOTER Dr. Huipin Yuan

ISBN: 978-90-365-3966-1

Table of Contents

Chapter 1

Introduction

1.1 Classical elements

"What is everything in our world made of?" might be one of the deepest questions frequently asked when our ancestors started to look at the world they live in. Finding and understanding the world's basic building blocks turned out to be a long and difficult story until people could crack this intriguing code of the universe. Ancient Greeks believed that the world, including all lives, is composed of four fundamental elements: **Fire, Air, Water** and **Earth**. According to this theory, each of these elements is related to two of the four sensible qualities: cold, hot, dry and wet. For example, fire is hot and dry; air is wet and hot; water is cold and wet; earth is dry and cold. When these elements are mixed in different proportions, the product represents mixed qualities thus matters with various properties are formed. Likewise, various forms of life are caused by mixing appropriate amount of these saintly elements. Similar to the western people, in the east, the Chinese recognized the world as a system made of five primary "phases": **Metal, Wood, Water, Fire** and **Earth**. In this traditional theory, each phase mirrors a complex series of aspects of nature, based on which they could generate or inhibit each other. For example, Wood could feed Fire and part Earth while Water could control Fire and nourish Wood. The interactions between the five phases were analogized to the interdependence of all living things as well. Based on this theory, all matters, from herbs growing on the mountain to internal organs in human body, are structured and circled with these five phases. Plausibly people believed that by adding the deficiency or neutralizing the exceeded phases in patient, physically or orally, the circle of the five phases could be brought back to balance. In other words, the introduction of certain substances could be beneficial to the human body.

That the excess or deficiency of a certain substance in the human body could influence people's health is a plain concept that can be seen in the early stage of many medical theories. Humorism, claimed by Hippocrates around 400 BC, is a system of medicine closely related to the theory of the **Four Elements**. Hippocrates classified the body fluids in a person to four humors: black bile, yellow bile, phlegm and blood. When a patient suffers from a surplus or imbalance of one of these four fluids, it is said that the patient's personality and physical health could be negatively affected. Based on a patient's humoral complexion, medical treatment like bloodletting, emetics, administration of "cold" or "warm" food were used to counter the symptoms of disease. Although quiet deviated from what we know now, Hurmorism became the most common view and scientifically acceptable theory used in the medication of human body until early nineteenth century.

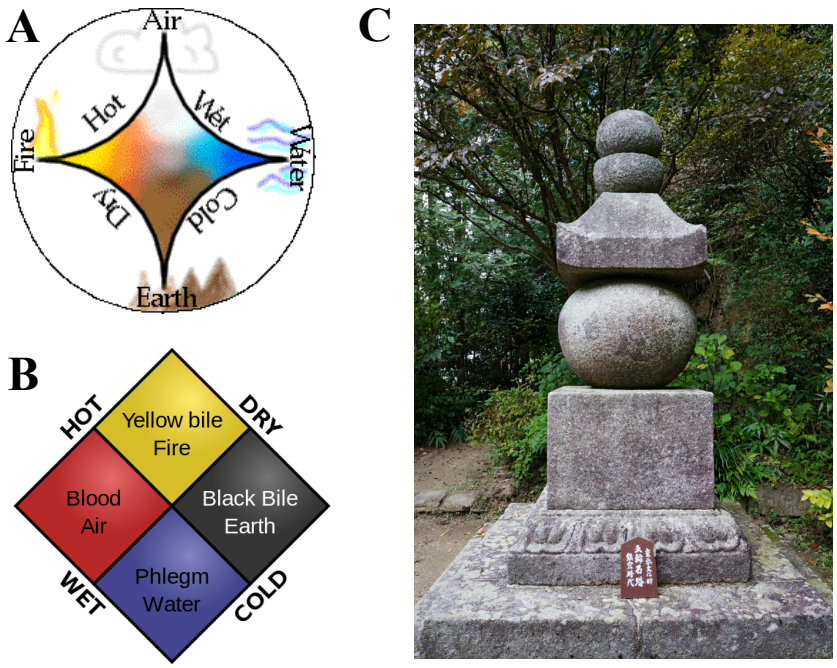

Figure 1. A: The ancient Greek concept of the Four Elements. **B**: A Buddhist Gorintō ("five-ringed tower") in Gansen-ji Temple, Japan, consisted of five rings from top to bottom, each representing one of the Five Elements that formed the world: ether (jewel-shape), wind (crescent), fire (pyramid), water (sphere) and earth (cube). **C**: The four humors, the most commonly held view of the human body among European physicians until the advent of modern medical research in the nineteenth century. Adopted by ancient Greek, it was tightly related to the theory of the Four Elements. All images are downloaded freely from the web using Google images filter.

1.2 Modern elements

Before the development of modern chemistry, people's concept of essential parts of matter is limited on what was visible around them. For example, the classical Four Elements theory is more like a description of four of the states of matter: earth for solid, water for liquid, air for gas and fire for plasma. Breakthroughs came from alchemists, who struggled to find an elixir by which base metals (e.g. lead) can be transmuted into noble metals (e.g. silver and gold). During their admixture or purification of various ingredients and potions, practical alchemists unconsciously funded a wide range of basis of modern medicine and chemistry [1]. In alchemy, the foundation of world is not any more abstract and anagogic "elements" but actual chemicals like mercury, sulphur and salt, where mercury giving volatility, sulphur

giving flammability and salt giving solidity [2]. Although they didn't realize, two out of three of these chemicals, mercury and sulphur, are already actual elementary substances. However, the concept of element was not clarified until Robert Boyle, who is regarded today as the first modern chemist and one of the founders of modern chemistry, defined elements as irresolvable constituents of various sorts in his book *The Sceptical Chymist* in 1661 [3][4][5]. In 1669, when alchemist Hennig Brand tried to search from residues of boiled urine for the elixir of life to produce gold, he accidentally isolated Phosphorus, an element that we now know exists in every cell of human body [6].

Figure 2. "*The Alchemist Discovering Phosphorus*" painted by Joseph Wright in 1771, depicting the discovery of the element phosphorus by German alchemist Hennig Brand in 1669. In search of the Philosopher's stone, a flash burst from the flask, in which a large quantity of urine was boiled down producing the hypergolic phosphorus in air. With the development of modern chemistry, we now understand that Water is actually composed of hydrogen and oxygen. Soil (Earth) is a mixture of liquids, organic matter and many complex minerals. Air is a combination of various gases. And Fire is not even a matter at all. But one thing in the Greek brief is true: everything in our world, including our entire body, is made of combinations of different elements. It is also true that one element can be transmuted to another, not by using the Philosopher's stone but via nuclear reactions. The image is adapted freely from Wikipedia.

Antoine Lavoisier recognized and named oxygen (1778) and hydrogen (1783) and realized that water is the combustion product of hydrogen and oxygen [7]. Thus, although had been thought for over 2000 years, water must be a compound but not an element. Instead of four, he listed 33 known elements of the time, including light and caloric [7]. Despite these flaws, the concept of modern elements was funded during this time, although the discovery of new elements was still random occurrence but not guided. In the beginning of 19th century, the ultimate building blocks of matter, atom, was described by John Dalton [8]. Afterwards, the discovery of new elements was boosted. Based on Dalton's atomic theory, in 1869, Dmitri Mendeleev presented his periodic table, a prefect map in which every element was ordered and grouped by their atomic number and recurring chemical properties [9]. This numerical pattern underlay the structure of matter, and decoded the mystery of the foundation of the whole world into a clear vision: that everything, from a diversity of nature to the complexity of man, was made from just 98 elements.

1.3 Origin and distribution of elements

There are so far 118 known elements. The first 98, from hydrogen (H) to Californium (Cf) are naturally-occurring elements and all of them have been found from Earth's crust. 80 of them are stable, while the rest are radioactive. The last 20 elements are produced artificially as the synthetic products of nuclear reactions.

Through the development of physical cosmology, it is known that Hydrogen (H) is the most abundant and lightest element in universe while Helium (He) is the second. They were mostly created from the Big Bang nucleosynthesis at the beginning of the universe (possibly together with small amount of Lithium) [10]. It is estimated that H and He make up roughly 74% and 24% of all baryonic matter in the universe respectively. Thus, from an astronomy point of view, all elements heavier than H, He and Li (so called "heavy elements"), are "trace" in the universe. For example, the mass fractions of all "heavy elements" in the solar system is about 1.3% of all elements [11]. Most heavy elements are generated in the core of stars through a process known as stellar nucleosynthesis, where H and He are fused into heavier nuclei [12]. When these heavier nuclei are produced, they too are burnt inside stars to synthesise heavier and heavier elements ranging from carbon (C) to iron (Fe) (e.g. C, N, O, F, Na, Si and Ca). Elements heavier than Fe (e.g. Cu, Zn and Sr) are all fused during the explosion of supernova when massive stars come to their end. The explosion also disperses different elements across the interstellar space, scattering matters which made up nebulae and planets including earth [13].

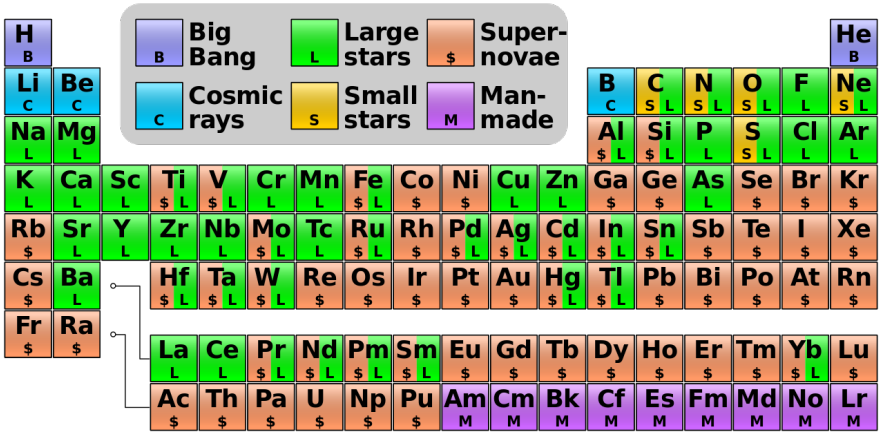

Figure 3. A periodic table indicating the origins of the elements. Note that many of the above elements can be also found in our body. This leads to a charming and poetic truth: that we are all made of stardust. The image is downloaded freely from Wikipedia.

All these elements can be found in the solar system. Although earth is made of the same nebula matter that formed the sun, the composition of earth is different from that of the sun because the formation of the planets acquired different concentration of elements. The most abundant element on earth is Fe (by mass, about 32%), basically because of its solid iron inner core. In its upper continental crust, oxygen is the most abundant element. A little more than 47% of the Earth's crust is consisted of oxygen because oxide compounds are common constituents of rocks [14]. Together with other elements (e.g. silicon (Si), alumina (Al), calcium (Ca), magnesium (Mg), sodium (Na), iron (Fe), carbon (C), phosphorus (P) and potassium (K)), these rock-forming elements comprised more than 99% of earth's crust. The other constituents occur in minute quantities, best known as the precious silver (Ag) and gold (Au).

Very few of these elements exist as simple substances; examples are the above mentioned silver and gold. Most elements that make up the Earth exist in different categories of minerals, including silicates (e.g. quartz and olivine), oxides and hydroxides (e.g. corundum and manganite), carbonates (e.g. calcite), sulphides (e.g. sphalerite), sulphates (e.g. celestite), halides (e.g. fluorite) and phosphates (e.g. apatite). In the last category, the most abundant phosphorus-bearing mineral in natural is apatite, which actually covers three different minerals (fluorapatite, chlorapatite and hydroxylapatite) depending on the predominance of either fluorine, chlorine or the hydroxyl group. This mineral is popular in the orthopaedic research field because hydroxylapatite is the main component of bone mineral.

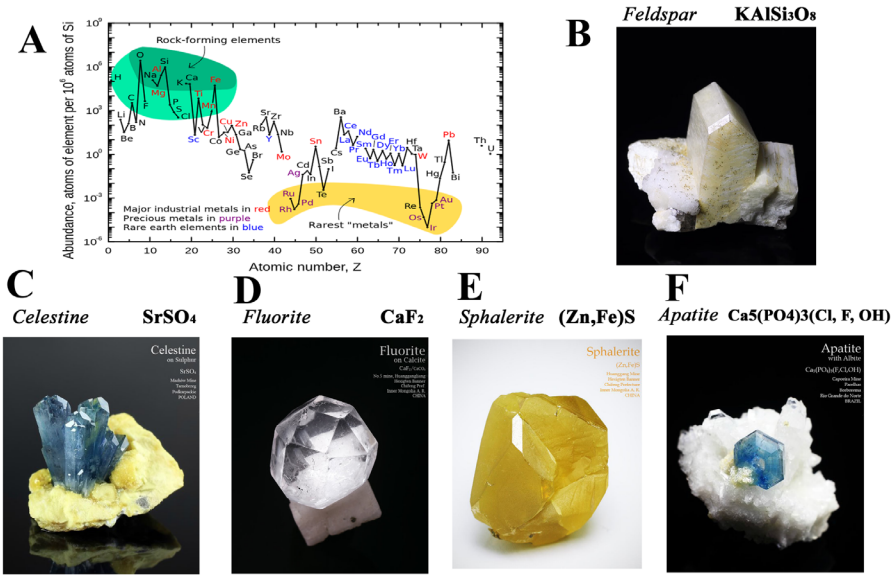

Figure 4. A: Abundance of the chemical elements in Earth's upper continental crust (atom fraction). B-F showing several natural-occurring gemmy mineral and their chemical formula: B. feldspar, the most abundant rock-forming mineral that makes up the Earth's crust; C: Celestine; D: Fluorite; E: Sphalerite; F: Apatite. Images B-F courtesy of Dr. Cao from Guokr.com.

1.4 Fundamental elements of living organisms

Most living organisms are common in their water-based cellular form, which is structurally supported by a carbon-based framework. Among the 98 natural-occurring elements, at least 60 can be detected in the human body. Nevertheless, approximately 99% of the mass of the human body is made up of six elements: oxygen, carbon, hydrogen, nitrogen, calcium, and phosphorus. Less than 1% is composed of another five elements: potassium, sulphur, sodium, chlorine, and magnesium. The remaining elements are trace in the mass of human body. Thus, according to their abundance in the body, biological elements can be classed as major and trace elements (Table 1).

Table 1. The abundance of elements in human body. The content is adapted from Wikipedia (http://en.wikipedia.org/wiki/Composition_of_the_human_body)

Major element	Fraction of mass	Trace element	Fraction of mass
Oxygen	0.65	Iron	60e-6
Carbon	0.18	Fluorine	37e-6
Hydrogen	0.10	Zinc	32e-6
Nitrogen	0.03	Silicon	20e-6
calcium	0.014	Strontium	4.6e-6
phosphorus	0.011	Bromine	2.9e-6
potassium	2.5e-3	Lead	1.7e-6
sulphur	2.5e-3	Copper	1.0e-6
sodium	1.5e-3	Iodine	160e-9
chlorine	1.5e-3	Selenium	190e-9
magnesium	500e-6	Manganese	170e-9

1.4.1 The CHONPS

Four most common elements in living organisms are **carbon**, **hydrogen**, **oxygen** and **nitrogen**. They are theoretically related to the chemical origins of life as shown in the famous "Miller-Urey experiment", where clusters of just these four elements, i.e. H_2O, CH_4, NH_3 and H_2, could spontaneously form organic compounds under electrical spark, including dozens of common amino acid now found in living systems as well as one of the four bases in RNA and DNA, adenine [15][16][17]. Together with two other important chemical elements, **phosphorus** and **sulphur**, they formed most biological molecules on earth. These six elements are elemental macronutrients for all organisms, and often referred as the acronym **CHONPS**.

Among the major elements, **carbon** forms the key component for all known life on earth. Carbon is the main component of sugars, proteins, DNA and fats. Almost all

living matters are composed of carbon-based organic molecules. Carbon is so crucial for all life forms in earth's biosphere, that people often class themselves as carbon-based life.

Phosphorus, the first element isolated from the human body (from urine), is also essential for life. Particularly, most phosphorus in human body is present in bone and teeth in the form of PO_4^{3-} (mainly in carbonated hydroxylapatite [18]).

1.4.2 Other abundant elements

Sodium is the most prominent cation in extracellular fluid (i.e. interstitial fluid and blood plasma) while **potassium** is the major positive ion inside animal cells. Together, they regulate blood pressure and play a key role in nerve transmission. The balance between sodium and potassium is mediated by an antiporter enzyme located in the cell membrane known as the sodium-potassium pump. This ion pump uses ATP to pump three sodium ions out of the cell and two potassium ions into the cell, thus generating the osmotic equilibrium and electrolyte balance.

Calcium is the most abundant metal in many animals. Roughly 99% of calcium in human body is present in bone and calcified cartilage in the form of bone mineral. The main component of bone mineral is carbonated hydroxyapatite. Therefore, calcium is essential for the growth, development and maintenance of healthy bones. About 1% of calcium is present in extracellular and intracellular fluids. Its concentration in blood plasma is tightly regulated but its intracellular concentration is subject to vary during many cellular functions.

Most **chlorine** in the human body is present in its anion form, chloride. It is an essential electrolyte located in all body fluids, and is responsible for maintaining acid/base balance, transmitting nerve impulses and regulating the osmotic equilibrium. It's also needed for the production of stomach acid, which is mainly composed of hydrochloric acid.

1.4.3 Trace elements in living organisms

Besides the major elements, over 60 chemical elements are trace by mass in the human body. More than a dozen of them are known to be essential for life in which they are required as key component of certain biomolecules or enzymes, or act as co-factors in biological reactions. For example, **iron** is an essential component of myoglobin and haemoglobin, which serve to bind and deliver oxygen in the biological fluids of vertebrates [19]; **zinc** activates many enzymes and maintains the metabolism of vitamin A, of which its deficiency may lead to night blindness [20];

selenium, in the form of selenoproteins, protects the organism from oxidative damage [21].

Apart from these crucial elements with known functions, some elements are not essentially required to support human biochemical processes, but have a positive effect in maintaining or improving health. For example, **fluorine** is not required for growth or to sustain life, but low level of fluoride hardens dental enamel and thus effectively prevents dental cavities; **strontium** is not an essential nutrient but it improves bone mineralization and thus bone density. The function of some trace elements found in the human body, e.g. caesium and titanium, are so far not clear and it is possible that they are simple contaminants from the environment and don't play any role in function. However, we should be cautious to give certain conclusions. For example, **bromine** has been believed for long to have no essential function in mammals until recently, a research carried by McCall *et al.* suggests that bromine is responsible for the assembly of collagen IV scaffolds and thus plays a vital role in tissue development and architecture [22]. Therefore, the possible functions of these "bystander" elements are still debatable.

The deficiency of essential trace elements may lead to diseases while overdose may result in toxicity. Examples are selenium, aluminium, cobalt, lead [23] and arsenic [24]. The over-dose toxicity issue applies to those elements which are not essential but are positive for health as well. For example, chronic high-level exposure to **fluoride,** a common and safe ingredient of tooth paste, can lead to accumulation of fluoride in bone, resulting in skeletal fluorosis and calcification of ligaments. Another example is **strontium**, although it is considered as a promotive element for bone health, over-dose of strontium may be associated with ricket disease and osteomalacia [25]. This indicates that the effects of elements on physiological activities in human body are tightly related to their doses. Further, it may be possible to stimulate or inhibit associated biochemical reactions in tissues by adding the deficient element or removing the excessive element at the site.

1.5 Trace elements in bone and their functions

1.5.1 The structure and composition of bone

From a structural point of view, bone is a bi-phasic material with a complex architecture, in which bone minerals are evenly distributed and organized in a matrix that is mainly composed of Type I collagen. Collagen provides a tensile framework while bone minerals add strength and hardness to it. This combination makes bone strong and flexible enough to withstand stress. At the micro level, bone minerals are long, rigid apatite crystals, primarily carbonated hydroxyapatite in its amorphous form.

These fine crystals were embedded in three parallel, staggered helices of collagen as the subunits of bone. When bone is initially formed, the organization of these subunits are haphazard, known as the woven bone. Woven bone is formed rapidly, but it is mechanically weak. However, woven bone can be gradually reconstructed to aligned, stronger lamellar bone. Mature bones are rigid organs in a variety of shapes. Together with skeletal muscles, tendons, ligaments and joints, they provide a frame to protect internal organs and to keep body supported and mobile.

From a different point of view, bone is a dynamic, growing tissue made up of living cells and non-living components. It is continuously formed and resorbed by coupled actions of mesenchymal stem cell-derived osteoblasts/osteocytes and monocyte-derived osteoclasts [26]. The formation of bone tissue involves multiple activities of the osteoblasts [27]. They firstly secrete an organic matrix of protein and then ossify it with deposition of minerals which are formed in their mitochondria [28]. During this process, some osteoblasts are embedded in bone that themselves produced and develop into osteocytes. Entrapped in lacunae, these mature bone cells are mechano-sensitive and are able to regulate the dynamic of bone formation and resorption by transmitting signals to osteoblast and osteoclast via microscopic canals between the lacunae. A complex series of parameters have been identified to play a role in regulating these cellular functions, including hormones, cell growth factors, mechanical physical forces, intracellular and extracellular concentrations of monovalent and polyvalent cations as well as anions [29][30].

Approximately 10% of the skeletal mass of an adult is renewed each year in bone remodelling [31][32], which means that there is continuous depletion and reprecipitation of bone minerals. During remodelling, osteoclasts attach to mature bone and create a low pH environment under their membrane to provoke bone mineral dissolution. Bone mineral is thus removed and released, resulting in a transfer of ions (e.g. calcium and phosphate) from the bone to the systemic circulation, which can be used as raw materials for the formation of new bone. Hence in tandem, bone remodelling repairs the micro-fractures in bone and regulates the calcium homeostasis in body fluid [33].

1.5.2 Trace elements in bone

Approximately 99% of the body's calcium is stored in bone minerals, making bones the reserve site of calcium, along with a series of trace elements such as magnesium, fluoride, manganese, zinc, silicon and strontium [34,35]. Although trace elements only represent a small fraction in bone mineral as compared to calcium, they are considered prominent for the growth, development and maintenance of healthy bones [29,35,36]. For example, strontium and magnesium have been reported to

influence the mineralization processes [37,38] as well as osteoblast and osteoclast activities [39,40] while zinc is considered essential in the growth and mineralization of bone tissue in which its deficiency may lead to bone growth retardation [41].

1.5.3 Trace elements and bone mineral

Biomineralization is a process in which biological apatite is synthesized by cells like osteoblast, emeloblast and odontoblast to ossify the certain protein matrix. It has been shown that the mineral phases of bone, enamel and dentin exhibit different ion concentrations and crystallinity [42,43], indicating that the distribution of trace elements in the body is purposively organized by nature to serve the different functional demands of certain tissues. When foreign ions are presented in the environment, they can participate in the nucleation and growth of biological apatite, being incorporated into the crystal lattice or be absorbed on the crystal structure. For example, Dahl *et al*. and Marie *et al*. reported that Sr can incorporate in bone mineral in newly formed bone after oral treatment of strontium [44,45].

The position of Ca^{2+} in the crystal lattice of apatite can be replaced by bivalent cations, such as Sr^{2+}, Zn^{2+} and Mg^{2+}, but monovalent and trivalent cations such as Na^{+}, K^{+} and Al^{3+} can be hosted as well [43]. Common substitutes of the anion group in apatite are CO_3^{2-}, SiO_4^{4-} for PO_4^{3-} and F^{-}, Cl^{-} for the OH^{-} group [46,47] Because of their different ionic radius, the foreign ion substitution in biological and synthetic apatites usually provokes changes in the lattice constants, the growth of apatite crystal in terms of crystal size and shape and thereby alter the solubility [42]. For example, the incorporation of silicon in hydroxyapatite leads to a decrease in crystallinity and crystallite size but an increase of solubility [48,49] while substitution of fluoride for OH^{-} increases the crystallite size and decreases the solubility [50–52]. Furthermore, the maximal amount of trace elements that can be contained in synthetic apatite lattices varies according to the radius and valence state of ions. Strontium substitution towards calcium can happen in a range varying from 0 to 100 at% in apatite [53], but this value is limited to about 15 at% for zinc [54].

1.5.4 Trace elements and bone cells

The importance of calcium and phosphate ions in regulating of cellular activities and bone metabolism is well known [55–61]. Many trace elements are often a part of the active centres of enzymes, e.g. zinc in the super family of zinc finger transcription factors, copper in superoxide dismutase and selenium in thioredoxin reductase and glutathione peroxidise. A zinc finger protein, Schnurri-2, is shown to regulate the activities of critical transcription factors required for bone remodelling [62]. Further, many trace elements, e.g. silicon, zinc, fluorine, magnesium and strontium are found

to be important for bone health [35][63]. It has been found that these bioactive ions can induce various responses of bone cells (i.e. osteoblasts, osteocytes, osteoclast and their progenitors). For example, fluoride stimulates the proliferation and osteogenic differentiation of osteoblastic cells in vitro [64–70] and silicon enhances the proliferation, metabolic activity and the synthesis of collagen type I in osteoblast-like cells [71,72]. Moreover, zinc [73–78] and strontium [40,79] were found to have dual effects that they favour osteogenesis while suppressing osteoclastic activity, indicating their potential in modulating bone growth. These findings indicate that the application of trace elements in the orthopaedic field has enormous potential.

1.6 Improve the bone forming ability of orthopaedic materials

1.6.1 Bone graft and their synthetic substitutes

For the repair of bone defects, the "gold standard" is autograft, which is sourced from a patient's own bone. It specifically possesses all imperative properties required for a bone graft material. For example, it is biocompatible and contains growth factors like bone morphogenetic proteins and osteogenic cells (i.e. osteoprogenitors and osteoblast) [80]. However, autologous bone is limited in quantity and harvesting can cause donor-site morbidity. Alternatively, bone graft harvested from donors (allograft) or animals (xenograft) are used but, have the risk of immunological reactions or disease transmission. Synthetic bone graft substitutes are not as efficient as compared to bio-derived bone grafts since they do not contain cellular components or growth factors, but they are not limited in quantity, which is more future-oriented considering the growing needs of the orthopaedic market [81]. Current commercial synthetic substitutes in the field include metals, alloys, polymers, coral-derived ceramics, and synthetic calcium phosphates. Among all artificial bone substitutes, calcium phosphates such as hydroxyapatite (HA), tricalcium phosphate (TCP) and their combinations (biphasic calcium phosphate, BCP) are considered the most attractive synthetic bone graft due to their chemical similarity to bone minerals and their ability to allow direct bone binding and growth on their surface [82].

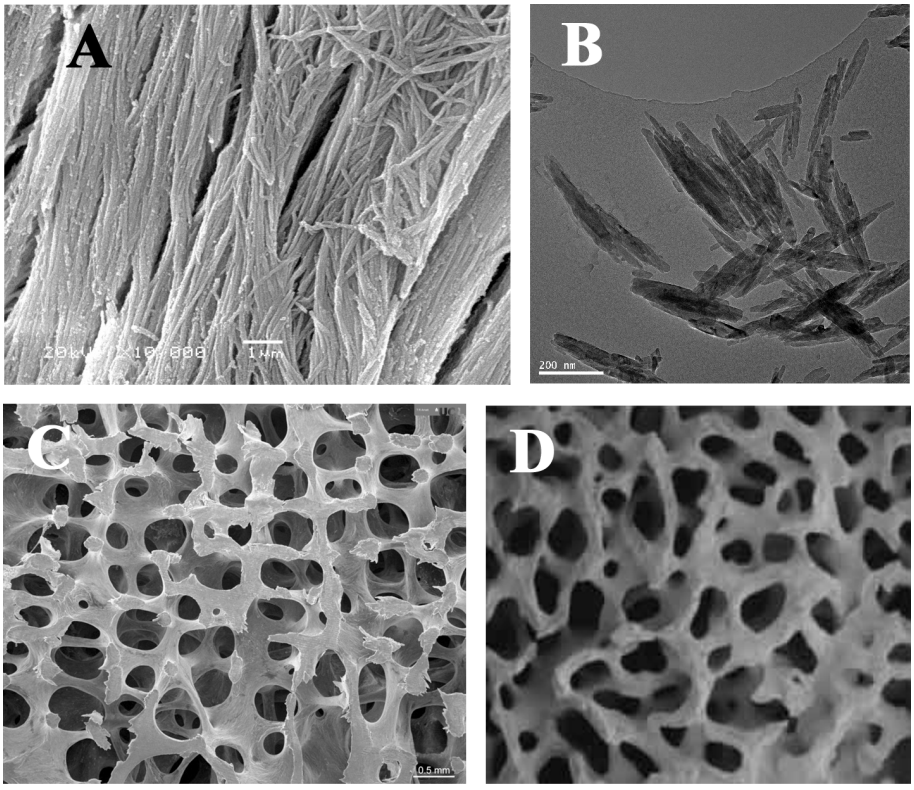

Figure 5. A: SEM image of bone mineral on collagen fibres in bone; B: TEM image of synthetic hydroxylapatite crystal; C: SEM image showing the architecture of spongy bone; D: SEM image of a porous calcium phosphate scaffold. Images are downloaded freely from web using Google images filter.

1.6.2 Approaches to improve the bone forming ability of synthetic bone graft substitutes

Synthetic calcium phosphate-based materials have been demonstrated to be non-toxic, biocompatible and osteoconductive that they serve as scaffolds or templates allowing new bone to form along their surface [42,82,83] However, when a bone defect exceeds a critical size, osteoconductive materials cannot fully regenerate the defect thus additional stimulation is required.

One attempt to overcome this drawback is tissue engineering, in which cells having osteogenic potential, e.g. bone marrow stromal cells (BMSC), are loaded into materials [84–87]. This approach raises the bone forming ability of the materials, but its efficiency is hampered due to possible host immunisation of the graft area and the

lack of vascularisation in the engineered tissues, which may lead to the poor survival of implanted cells [88].

Combining materials with growth factors such as bone morphogenetic protein-2 (BMP-2) is another approach to improve their bone forming ability. Being efficient and promising to trigger bone formation, the treatment is however costly and concerns about complications and adverse events exist [89–95].

Besides adding stimulus such as osteogenic cells and growth factors, it is also possible to improve the bone forming ability of synthetic materials by modifying their physicochemical properties such as solubility, porosity, microporosity pore size and grain size [96][97]. Among these features, the geometry of synthetic bone substitutes was shown to have an impact that specific surface topography could spontaneously induce osteogenesis, evidenced by the de novo bone formation in the materials when they are implanted at non-osseous site, i.e. osteoinduction. This outstanding feature has been reported for calcium phosphates ceramics [87,98–101], bioglass [102], calcium phosphate cement [103], calcium phosphate-based composites [104–107] and porous titanium [108]. The efficiency of osteoinductive calcium phosphate ceramics in bone repair was reported to be equal to autografts when implanted in critical-sized defects, suggesting their potential as promising alternatives of autologous bone crafts [109]. Nonetheless, it is not fully understood so far how surface microstructure could bring such responses, but protein adsorption [110], osteogenic differentiation of osteoblast progenitors [108,111–115] as well as early activation of osteoclastogenesis [116–119] on the surface have been suggested. Moreover, there are multiple routines to obtain synthetic bone substitutes with such desired property [120].

1.6.3 Improve the biological performance of calcium phosphates with trace elements

As mentioned previously, many trace elements such as silicon, zinc, fluorine, magnesium and strontium can regulate cellular activities of bone cells [64–78,40,79]. In view of this, there are growing interests to incorporate various trace elements in orthopaedic materials, aiming to achieve a release of these ions from the materials and thus enhance their bone forming ability. A lot of work has been done to incorporate trace elements (e.g. silicon [121,122], zinc [123–126], strontium [122,127,128]) into synthetic bioceramics and improved biological performance was observed both in vitro and in vivo (e.g. silicon [49,121,129], zinc [39,123–125,130–140], strontium [141,122,127,128,131,140,142–153] and fluoride [64,65,67,69,154–157]). Yamada and Legeros *et al.* introduced zinc in β-tricalcium phosphate and observed decrease of resorbing activity of osteoclasts [134]. Julien *et al.* reported

calcium phosphate cements doped with magnesium, zinc and fluoride [158]. Ito and Otsuka *et al.* demonstrated that the administration of calcium phosphate compounds containing magnesium (Mg^{2+}), zinc (Zn^{2+}) and fluoride (F^-), either by injection or orally, enhanced the bone mineral density and mechanical strength of ovariectomized (OVX) rats [159][160]. However, although there is expectation that one day the effectiveness of ion-containing materials could be comparable with autograft [161], to which degree the trace elements can improve the bone forming ability of synthetic bioceramic is still pending.

1.7 Ion-substituted calcium phosphates

1.7.1 The effect of ion substitution on the physicochemical properties of ion-containing materials

Considering calcium phosphates' great capacity in containing foreign ions, the concept of using calcium phosphates as carriers of pharmaceutical ions has enormous potential in promoting the biological performance of these materials [81,161]. One example is the silicon-substituted calcium phosphates where numerous articles have suggested enhanced biological performance of calcium phosphates with silicon addition [49,71,129,162–165]. However, the effect of silicon in substituted calcium phosphate materials was claimed to be overstated because a lack of experimental evidence linking the improved biological performance to silicon release [166]. For example, Coathup *et al*. have reported osteoinductive silicate-substituted calcium phosphate, but the stoichiometric counterpart in the study also triggered bone formation [167]. Additionally, the role of resorption and surface geometry, which might be provoked by silicon substitution, in the enhancement was not evaluated.

Likewise, this assertion could be tenable for all trace element-containing materials because the introduction of foreign ions in calcium phosphates always provokes additional physicochemical changes to the materials. This is because foreign ions have different radius than the replaced ion, e.g. Sr^{2+} (1.12Å), Zn^{2+} (0.74Å), Mg^{2+} (0.72Å) as compared to Ca^{2+} (0.99Å), therefore the introduction of these ions more or less causes alterations in their lattice structure, leading to changes of their crystallinity, solubility and microstructure. These changes in turn would affect other characteristics of the ion-doped material such as ion release property and protein adsorption. For instance, the introduction of zinc in HA causes the increase of specific surface area but decreased adsorption of proteins [168]. Similar to the situation of silicon-substituted calcium phosphates, it is thus scientifically difficult to associate the biological improvement to the doped ions solely [166].

1.7.2 The release of ions

Foreign ions are fixed in the lattice of calcium phosphate scaffold thus cannot take in part of cellular reactions directly. Logically, the doped ions must depart from their scaffold and enter the fluid environment, i.e. ion release, in order to interact with cells [166]. In body, lymph and blood flows may continuously renew the body fluid around the implants reducing the local accumulation of released ions. Therefore, an effective ion-substituted material should meet two criteria: (1) it should provide a continuous release of the ions; (2) the concentration of released ions should be sufficient to provoke a local stimulation. The demonstration of the latter could be complicated since it is difficult to monitor such release in vivo. So far most studies investigated the release profiles of ion-containing materials in vitro and it is generally agreed that the release of ions should be stable and consistent to ensure a controlled treatment.

In order to obtain a stable and consistent release profile, the quantity of trace elements in the material and the intensity of release need to be engineered.

As mentioned in 3.2.1, calcium phosphates can contain abundant foreign ions of various kinds in their lattice and release them when the lattice collapses. The doped ions depart from the scaffold through two main pathways, i.e. chemical dissolution and cell-mediated resorption. The first parameter is largely influenced by the chemistry and stability of calcium phosphates [169,170]. For example, TCP has a Ca/P ratio of 1.5 and is more soluble than HA (which has a Ca/P ratio of 1.67) under physiological condition (pH=7.4), while biphasic calcium phosphate exhibits intermediate Ca/P ratio and dissolution behaviour [171,172]. Additionally, sintered ceramics are more stable than their un-sintered counterparts. Thus, the three kinds of calcium phosphates release Ca^{2+} and PO_4^{3-} at different rate. For instance, the release of ions from TCP is rapid while that from HA is relatively slow under physiological condition. Based on this, it is proposed to indicate the in vivo behaviour of a calcium phosphate implant by looking at its solubility in physiological fluid [169,170]. However, since the dissolution mechanisms of calcium phosphates are still poorly understood [173] and the in vitro evaluations are based on simplifications of the real situation in vivo, so far the only way to assess the in vivo behaviour is to implant the material [174].

The degradation behaviour of calcium phosphate materials in the body could be largely different from in vitro because the in vivo environment is rich in glucose, proteins and various of cells including phagocytes, e.g. osteoclast-like resorbing cells [175]. Similar to the dissolution of bone mineral during bone resorption, these cells attach to the surface of calcium phosphates and dissolve them under the membrane.

Ions in the lattice are hence dissolved and evacuated to the resorptive site [176,177]. In case of ion-containing substitutes, the doped ions are thus released as well. Here the release rate of ions is controlled by the activity of resorbing cells, thus (1) the release of ions would not be feasible until the resorption occurs;(2) substitutes that are difficult to be resorbed (e.g. sintered apatite) might have poor ion release. Therefore, an ideal ion-releasing biomaterial should be either resorbable or release ions spontaneously under physiological condition to guarantee the treatment with a consistent release profile.

1.7.3 Control the release of ions

As mentioned previously, the release rate of doped ions can be roughly determined by the dissolution rate of the calcium phosphates skeleton (e.g. TCP for rapid release or HA for tardy release) and the content of substituted ions [146,178]. However, whether a clear relation between the two parameters and the releasing profile can be drawn is questionable since the substitution of foreign ions in calcium phosphates commonly leads to a change of their chemical stability and dissolution rate [52,135,153,179].

Further, the dissolution of ion-containing calcium phosphates can be controlled by embedding granular calcium phosphates into a biocompatible organic matrix (e.g. collagen [180,181], polyetheretherketone [143], alginate[182], poly-amino acid[183], poly-amide [184]). In such composite materials, the polymer phase would not only provide sufficient elastic and viscoelastic properties [185] but also regulate the water penetration to the composite's bulk. This latter property may slow down, but not block, the dissolution of the embedded calcium phosphates [104] prolonging in this way the release of doped ions. Furthermore, in case of a degradable matrix, the degradation of the polymer matrix would expose the embedded calcium phosphate to body fluids progressively, letting the release of doped ions continue. Thus, the release rate of ions is restrained by both the dissolution rate of the inorganic filler and the degradation rate of the polymer matrix.

1.7.4 Ion-substituted-apatite/polylactide composites as long-term ion-releasing materials

Among these organic matrices, polylactide attracted a lot of interest due to its availability, simple hydrolysis and nontoxic degradation products [186–188]. Apatite/polylactide composites can be obtained with various processing methods. One method is solvent-cast, in which the apatite particles were dispersed in polymer solution and followed by the removal of solvent by evaporation [105,189–191] or freeze-drying [192]. The advantage of this method is that the dissolution process

does not alter the chemistry of both polymer and apatite phase. However, it might lead to agglomeration of nano-apatite and result in inhomogeneous composites [105,185].

Alternatively, thermal extrusion is a well-developed solvent-free and efficient technique in manufacturing polylactide-based composites [193,194]. In this method, polymers are hot melted and finely blended with apatite fillers through an extruder. Barbieri *et al*. extruded apatite particles into polylactide with twin-screw compounder and observed homogenous distribution of apatite particles in the polymer matrix at the sub-micro level [185]. It is also reported that the fluid uptake, degradation rate as well as the mechanical properties of the composites could be controlled through the character of polylactide and their weight proportion in the composites [104,105,185]. This clearly indicated a direction to obtain composites with tailorable release rate.

1.8 Aim of the thesis

The aim of this thesis is to answer the following questions:

(1) Can the introduction of trace elements in synthetic bone graft substitutes result in inductive bone formation and, if so, to what extent is the bone formation attributed to the doped ions?

It has been reported that trace element containing calcium phosphates are biocompatible, osteoconductive and beneficial for bone repair [195–197]. However, few studies have demonstrated the possible role of trace elements in osteoinduction. Since the osteogenic differentiation of mesenchymal stem cells can be promoted by trace elements in vitro [198,199], we hypothesise that their addition in calcium phosphate-based materials can result in inductive bone formation. As the incorporation of these elements will also change the physical parameters of the calcium phosphate material (e.g. surface morphology and grain size), this may attribute to the altered biological behaviors. The question is therefore to what extent any enhanced bone formation can be attributed to the doped ions? To study these objectives, **zinc** is introduced in a non-osteoinductive tricalcium phosphate to study the influence of zinc addition on the biological behaviour as well as the physicochemical changes of the doped tricalcium phosphate using both in vitro and in vivo models, in **Chapter 2**.

(2) Can ion-containing materials that vary only in their trace element content be synthesized by introducing ion-containing apatite into polymeric matrices? Meanwhile, how will the polymeric matrices influence the release of doped ions, and how will these parameters influence the osteoinductivity of the ion-containing composites?

It is difficult to introduce foreign ions into calcium phosphate materials without provoking physical changes such as the alteration of surface geometry. However, scientifically, materials that vary only in their ion compositions are desired in order to pinpoint the role of trace elements in bone formation on ion-substituted materials. A potential method is to incorporate trace elements in granular apatite and introduce the apatite in a biocompatible polymer matrix. In this way, the polymer matrix will conceal the effect of apatite surface differences, while ion release properties will be retained. Will the introduction of trace elements change other physicochemical properties of the composites and in turn impact their bone forming ability? To answer this question, fluoride, as an example of anions, and strontium, as an example of cations, are introduced in apatite and further embedded in polylactide matrices respectively in **Chapter 3** and **Chapter 4**, to demonstrate the influence of ion substitution on the physicochemical properties such as ion release behaviours and in turn the osteoinductivity of the ion-containing composites. Further, **Chapter 3** focused on the effect of fluoridation on the degradation and resorbability of an osteoinductive composite while **Chapter 4** aimed more at investigating the potential role of polymer matrix on ion release and osteoinductivity of the strontium-containing composites.

(3) *Can the doped trace element release from the composites occur in a consistent and sustained fashion? If so, can the ion release dose-dependently induce osteogenic differentiation of mesenchymal stem cells and enhance inductive bone formation?*

The release of trace element ions might be continuously diluted by body fluid in vivo thus a sustained release profile of the ion-containing material is desired to guarantee a constant stimulation. Further, numerous studies have reported that the introduction of trace elements in synthetic bone substitutes could guide the cell differentiation to the desired direction (e.g. osteogenesis) but few of them have corroborated the real performance of ion-doped materials using both in vitro and in vivo assessments. In **Chapter 5** strontium-doped apatite and a hydrophilic polylactide were chosen to obtain composites that may provide consistent release of strontium. The ion release profile of the strontium-releasing composites is monitored for up to 24 weeks to verify their long-term release capacity. Furthermore, the effect of strontium on the differentiation fate of stem cells is studied by culturing murine mesenchymal stem cells on strontium-containing composites in vitro while its influence on bone metabolism is investigated in vivo using an rhBMP-2 induced ectopic model.

(4) *Can ion-containing materials provide significant improvement in osteoporotic individuals where bone metabolism is impaired?*

Many patients that require bone graft substitutes are aged people with impaired bone metabolism, e.g. patients suffering osteoporosis. It has been shown that osteogenesis in these patients is reduced [200], which may be enhanced by the addition of trace element-containing bone grafts. In **Chapter 6**, the influence of strontium-containing composites on rhBMP-2 induced bone formation in an osteoporotic environment is studied using the ectopic model developed in **Chapter 5**.

Finally, the results are generally discussed and perspectives for future studies are given in **Chapter 7**.

Chapter 2

Zinc in calcium phosphate mediates bone induction: in vitro and in vivo model

Zinc in calcium phosphate mediates bone induction: in vitro and in vivo model

Xiaoman Luo[a], Davide Barbieri[a], Noel Davison[a], Yonggang Yan[b], Joost D. de Bruijn [a, c, d] and Huipin Yuan[a, c*]

[a] *Xpand Biotechnology BV, Prof. Bronkhorstlaan 10, bld 48, 3723MB Bilthoven, The Netherlands*

[b] *College of Physical Science and Technology, Sichuan University, No.24 South Section 1, Yihuan Road, 610065 Chengdu, China*

[c]*MIRA Institute, University of Twente, Drienerlolaan 5, 7522 NB Enschede, The Netherlands*

[d] *School of Engineering and Materials Science, Queen Mary University of London,Mile End Rd, E1 4NS London, United Kingdom*

Abstract: Zinc-containing tricalcium phosphate (Zn-TCP) was synthesised to investigate the role of zinc in osteoblastogenesis, osteoclastogenesis and in vivo bone induction in an ectopic implantation model. Zinc ions were readily released in the culture medium. Zn-TCP with highest zinc content enhanced the alkaline phosphatase activity of human bone marrow stromal cells and the tartrate-resistant acid phosphatase activity as well as multinuclear giant cell formation of RAW264.7 monocyte/macrophages. RAW264.7 cultured with different dosages of zinc supplements in medium with or without zinc-free TCP showed zinc could influence both the activity and formation of multinuclear giant cells. After a 12-week implantation in the paraspinal muscle of canines, de novo bone formation and bone incidence increased with increasing zinc content in Zn-TCP – up to 52% bone in the free space. However, TCP without zinc induced no bone formation. Although the observed bone induction cannot be attributed to zinc release alone, these results indicate that zinc incorporated in TCP can modulate bone metabolism and render TCP osteoinductive, pointing to a novel way to enhance the functionality of this synthetic bone graft material.

Key words: Zinc, Calcium phosphate, Macrophage, Stem cell, Osteogenesis

Published in Acta Biomaterialia 2014, 10(1), 477-85

2.1 Introduction

Bone mineral is comprised of carbonated apatite crystals that contain a series of trace elements [34,35] such as magnesium (Mg), fluoride (F), manganese (Mn), zinc (Zn), silicon (Si) and strontium (Sr). Although they only represent a small fraction of bone mineral, they are considered essential for bone metabolism [36]. For example, Mg and Zn have been reported to influence osteoblast and osteoclast activity [76,201], while strontium ranelate is used clinically to reduce osteoporosis [202].

For the repair of bone defects, calcium phosphate ceramics (CaP) such as hydroxyapatite (HA), tricalcium phosphate (TCP) and their combination (biphasic calcium phosphate, BCP) are widely used due to their chemical similarity to bone mineral. After implantation, they allow migration of bone cells on their surface followed by bone deposition, in a phenomenon called osteoconduction [83]. However, when a bone defect exceeds a critical size, osteoconductive materials are not able to fully regenerate the defect and osteoinductive materials, which trigger the osteogenesis of mesenchymal stem cells [203] thus inducing bone formation even in non-osseous tissues, is needed. Osteoinduction can be achieved by adding growth factors such as bone morphogenetic proteins (BMPs) or osteogenic cells to the material.

Inspired by the idea that calcium phosphate ceramics mimic bone mineral chemistry and that trace ions regulate bone metabolism, the introduction of trace elements in CaP was expected to provide a novel method to enhance the bone forming ability of a bone graft. An example of such a material is silicon substituted HA [129], although there is debate whether silicon plays a direct role in the functioning of these materials [166].

Zn, another important trace element, is considered as an important mineral in the normal growth and development of the skeletal system. Bone tissue contains approximately 30% of the total zinc in the body [204]. Indeed, Zn deficiency impairs the development of maximal bone mass [205]. It is associated with the pathogenesis of osteoporosis [206,207], while dietary supplementation of zinc showed positive effects on bone metabolism [205].

It has been shown that zinc can influence the behavior of (pre)osteoblast [73–75] and osteoclast [76–78], indicating zinc plays an important role in bone metabolism. Thereafter, zinc has been introduced in various calcium phosphates ceramics in expectation that the release of zinc may promote the bone forming ability of synthetic materials. Naturally it was found that zinc-containing materials would release zinc, and influence the differentiation of osteogenic cells [208] and hence promote the

regeneration of nearby host bone [132,135], suggesting their potential role in improving conductive bone formation at osseous site.

Mineralized Achilles tendon and cartilage calcification have been associated with high Zn tissue levels [209]. Furthermore, some researchers showed that zinc could induce osteogenic differentiation of mesenchymal stem cells (i.e. bone marrow stromal cells) [124,125]. These facts indicated a possible role of zinc in ectopic bone formation (osteoinduction). We hypothesized that the incorporation of Zn in CaP may render the ceramic osteoinductive due to the stimulation of osteogenic differentiation of mesenchymal stem cells (originating from either the local tissues or the blood stream [210,211]). To investigate the hypothesis, zinc-containing TCP (Zn-TCP) was synthesized and evaluated as a model.

As mentioned above, zinc plays its role not only in bone formation but also in bone resorption, which should continuously influence the ossification mass in osteoinductive model since bone metabolism is equilibrium between ossification and bone resorption. It is clear that zinc-containing ceramics can also inhibit resorption activity of osteoclast [134,136] while bone resorption is also up to the formation of osteoclasts. Osteoclasts are differentiated from monocyte/macrophages, which can fuse to form multinucleated, TRAP-positive, bone-resorbing giant cells in the presence of certain cytokines, in particular receptor activator of NF-κB ligand (RANKL) [212]. As a matter of fact, zinc is involved in this osteoclastic differentiation too [73,131]. Thus zinc may influences bone resorption via not only the resorption activity of osteoclast but also the formation of osteoclast from macrophage. To address the possible influence of Zn-TCP on osteoclastogenesis, monocyte/macrophages (RAW264.7) was cultured with the presence of RANKL on Zn-TCP and on zinc-free TCP with zinc supplement in culture medium.

2.2 Materials and Methods

2.2.1 Preparation and characterization of Zn-TCP

Tricalcium phosphate powder was synthesized by wet precipitation using $Ca(OH)_2$ (Fluka) and H_3PO_4 (Fluka) at a Ca/P molar ratio of 1.5. Zn-TCP slurries were made by mixing TCP powder with aqueous solutions containing various concentration of $ZnCl_2$ (Fluka): 0, 5, 15, and 45 mmol $ZnCl_2$/100 g TCP ("TZ00" control, "TZ05", "TZ15", and "TZ45" respectively). Slurries were vacuumed to remove air bubbles, dried at RT and sintered at 1100 °C for 480 minutes resulting in dense Zn-TCP blocks.

Zn-TCP discs (Ø10 x 1 mm) were machined from dense blocks using a diamond saw microtome (Leica SP1600); granules (212-300 μm) were prepared by grinding and

sieving the residual block particulate. Discs and granules were ultrasonically cleaned in sequential baths of acetone (Sigma), 70% ethanol (Prolabo) and demineralized water for 15 minutes each. Materials were dried at 80 °C, steam sterilized at a pressure of 2-4 bar (121 °C) for 30 minutes and dried at 80 °C afterwards.

Materials were characterized on the basis of their crystal chemistry, surface structure, and release of Zn ions. Chemical analysis was conducted using an X-ray diffractometer (MiniFlexII, Rigaku) with Cu Kα radiation（λ=1.5405Å, 30kV, 15mA） over the 2θ range of 25°-45°. The microstructure of the ceramics was analyzed using a scanning electron microscope (SEM) (Jeol JSM-5600). Grain and pore size were quantified using ImageJ software (NIH) by measuring and averaging the vertical length of > 40 grains and pores in a representative micrograph taken at 2,500x. Ion release was measured as follows: discs were soaked in 1 ml culture medium for 4 days at 37°C with 5% CO_2 (1ml medium per disc, n=5 per material, more details are mentioned in section 2.2.2) and the zinc concentration in medium was measured by atomic absorption spectrum (AAS) (SpectrAA 220FS). Ca^{2+} and PO_4^{3-} concentrations in the medium were measured using QuantiChrom (BioAssay Systems, USA) and PhosphoWorks (AAT BioQuest, USA) colorimetric assay kits, respectively. Assays were carried out following the manufacturers' instructions and absorbance (620 nm) was measured using a multimode plate reader (Zenyth 3100).

2.2.2 Materials used for in vitro experiments

All discs have been pre-incubated in corresponding basic medium for 4 hours prior to cell culture. Before the cell seeding, these medium were discarded to prevent potential pH impact to cells (also applied to ion release experiments with basic medium used in section 2.2.2).

Suspension culture plates (Greiner Bio-One Cat.677102) were used for cells cultured on discs while cell culture plates (Greiner Bio-One Cat.677180) were used for cells cultured on plastic.

2.2.3 Osteoblast differentiation of hBMSC

Basic medium: α-MEM (Invitrogen, UK) supplemented with 10% FBS (Lonza, Germany), 2 mM L-Glutamine (Invitrogen, UK), 0.2 mM L-Ascorbic acid 2-phosphate (AsAP, Sigma), 100 IU/ml penicillin (Invitrogen, UK) and 100 µg/ml streptomycin (Invitrogen, UK)

Growth medium: basic medium supplemented with 1 ng/ml basic fibroblasts growth factors (bFGF, Instruchemie, the Netherlands)

Osetogenic medium: basic medium supplemented with 10 nM dexamethasone (Sigma)

Human bone marrow stromal cells (Passage 3, PT-2501, Lonza, Netherlands) were expanded in flasks containing growth medium under humidified atmosphere of 5% CO_2 at 37°C for one week until they were harvested with 0.25% trypsin (Invitrogen, UK). 2.5 × 10^4 cells/well were cultured on Zn-TCP discs (n=5 per material at each time point) with osteogenic medium in 48-wells for up to 14 days. The medium was refreshed twice a week and samples were harvested after 1, 4, 7 and 14 days.

2.2.4 Osteoclast differentiation of RAW264.7

Basic medium: α-MEM (Lonza, Germany) supplemented with 10% FBS (Peprotech) and 1% penicillin and streptomycin (Invitrogen, UK)

Monocytes/ macrophage (RAW264.7) cells were seeded in basic medium for one week. Cells were then harvested by using a cell scraper (BD Falcon) and further cultured on discs with or without zinc content or on plastic (n=5 per material at each time point) with basic medium in 48-wells at the density of 2.5 × 10^4 cells/well for 4 days in the presence of 20 ng/ml RANKL (Peprotech). Zinc supplement was applied on zinc-free group by adding zinc chloride in the medium range from 0 to 18ppm. These mediums were refreshed once at day one.

2.2.5 Biochemistry

Cell lysis

Cells were rinsed one time with warm PBS (Lonza) and froze at -80 °C for 24 hours. Then they were thawed to 37 °C. 400 µl Cyquant lysis buffer was added and ultrasonicated for 2 minutes followed with 5 minutes shaking at 400 RPM.

DNA content

The poliferation of hBMSC was measured using a CyQuant cell proliferation assay kit (Invitrogen) following the manufacture's guidelines. In brief, 100 µl cell lysate was mixed with 100 µl 400-time diluted GR reagent and further incubated at room temperature in dark for 5 minutes. The fluorescent analysis was performed with wavelength of 480 nm for excitation and 520 nm for emission using a spectrophotometer (Zenith 3100).

Alkaline phosphatase (ALP) activity

Diethanolamine buffer was prepared by dissolving 10% (v/v) diethanolamine (Sigma) in demineralized water. Afterwards the pH of diethanolamine buffer was adjusted with HCl (Sigma) to 9.8. 150 µl buffer containing 5 mM p-Nitrophenyl phosphate

disodium salt hexahydrate (PNPP, Sigma) and 1 mM $MgCl_2$ (Merck) was added to 50 µl cell lysate, and then incubated at 37 °C for 15 minutes. The absorbance was measured at 405 nm. The ALP activity was defined as µmol of p-Nitrophenol released after a 15-minute incubation normalized to the DNA content in each well (µmol/ng).

Tartrate-resistant acid phosphatase (TRAP) activity

10 µl cell lysate was added to 90 µl reagent solution (100 mM NaAc buffer (pH 5.8) supplement with 0.15 mM KCl, 1.0 mM ascorbic acid, 0.1 mM $FeCl_3$, 10 mM potassium sodium tartrate and 10 mM PNPP), incubated in dark at 37°C for one hour. To stop the reaction, 100 µl 0.3 M NaOH was added and the absorbance was measured at 405 nm.

TRAP staining

The TRAP expression of RAW264.7 cells cultured on plastic is stained using a commercial kit (Leukocyte Acid Phosphatase Kit, Sigma). Cells were first rinsed with PBS, fixed with 4% formaldehyde for 10 minutes, and then stained following the manufacturer's instructions. Staining was visualized using a Nikon SMZ800 stereomicroscope equipped with a Nikon camera.

Osteoclast size determination

Cells were rinsed with PBS, fixed in 2.5% glutaraldehyde in PBS for 10mins and then dehydrated with a graded ethanol series (25, 50, 70, 80, 90, 95, 100% x2) following with a graded HMDS (Alfa Cesar) series (33, 50, 75, 100%). Cells were then sputter coated with gold for SEM observation.

The size of osteoclasts on TCP discs was measured with SEM images (>200 cells) and quantified by calculating the mean surface area of cells using automated threshold, edge detection, and particle analysis functions in ImageJ software (NIH).

2.2.6 In vivo experiments

Four adult male mongrel canines (average body weight 12.5 kg) were used. All surgeries were conducted in Sichuan University under general anesthesia by abdominal injection of sodium pentobarbital (Sigma, 30 mg/kg body weight) with the permission of the local animal ethics committee. Zn-TCP granules were prepared as one cubic centimeter aliquots under sterile condition in glass vials prior to the implantation. One cubic centimeter of each Zn-TCP granules were implanted in the same side (two canines in the left, two canines in the right) of paraspinal muscle along the direction of spine. In brief, muscular pouches were created by scalpel incision and blunt dissection, and then the granules were inserted to the pouch with a

syringe. The distance between each implants was about 2~3 cm. The pockets were then closed with non-resorbable sutures for identification at harvest. Following the surgeries, animals were intramuscularly given buprenorphine (0.1 mg per animal) for two days to relief pain and penicillin (40 mg/kg) by intramuscular injection for three consecutive days to prevent infection. After operation, animals were allowed for full weight bearing and received normal diet. Calcein (10 mg/kg body weight, Sigma) and xylenol orange (100 mg/kg body weight, Sigma) were intravenously injected 6 and 9 weeks after implantation respectively. Subsequently, animals were sacrificed with a celiac injection of excessive amount of sodium pentobarbital 12 weeks after implantation. Implants were fixed with 4% formaldehyde, embedded in PMMA after gradient ethanol dehydration. Three non-decalcified sections were made across the middle of the explants using a diamond saw microtome (Leica SP-1600, Germany) and stained with 1% methylene blue (Sigma) and 0.3% basic fuchsin (Sigma). Histological observation was performed with light microscopy. The histological slides were scanned with a scanner (DIMAGE Scan Elite5400 Ⅱ, KONICA MINOLTA). Histomorphometry of bone formation in the stained sections was performed by pseudo-coloring pixels representing formed bone (B) and remaining material (M) in a region of interest (ROI, with surrounding soft tissues outside the implants excluded) using Photoshop (Adobe Photoshop Elements 2.0). Bone formation was calculated as follow:

*B% = B/ (ROI-M)*100*

2.2.7 Statistical analysis

Multiple comparisons were performed with one-way ANOVA using Turkey comparisons (Osteoclast size determination with Kruskal-Wallis test) and *p* values smaller than 0.05 were considered statistically significant. Data are expressed and represent the mean ± standard deviation of five (four for in vivo samples) replicates. Asterisks were marked in Figs. 3-6, if significance differences were found.

2.3 Results

2.3.1 X-rays diffraction analysis (XRD)

The crystalline phases of the obtained TCPs with various zinc concentrations were examined with powder XRD (Fig. 1). New peaks were seen at the 2θ position of 31.8° and 32.4° on the patterns of TZ15 and TZ45. Such peaks increased in intensity with the rising of zinc content, and indicate increasing presence of hydroxyapatite (HA) phase (according to standard PDF 09-0432). No crystalline phases other than β-TCP and HA were detected.

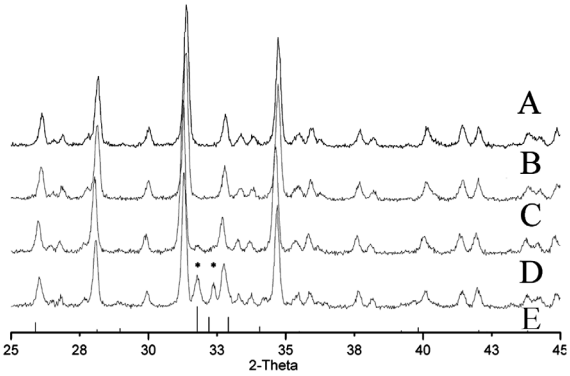

Figure 1. XRD patterns of Zn-TCP: TZ00 (A), TZ05 (B), TZ15(C), TZ45 (D) and HA (E), apatite phase presented in TZ15 and TZ45

2.3.2 Scanning electron microscopy analysis (SEM)

The surface morphology of the samples was observed at SEM. It was seen that the surface of the granules had micropores (Fig. 2) and the grains shrinked in size with increasing zinc content. Statistics showed a decreasing trend of grain size and pore size with increasing zinc content (Fig. 3D). TZ15 has significantly smaller grain size than TZ00 ($p<1*10^{-4}$) while significantly smaller grains ($p<1*10^{-7}$) and pores ($p<1*10^{-5}$) were seen in TZ45 as compared to all other materials.

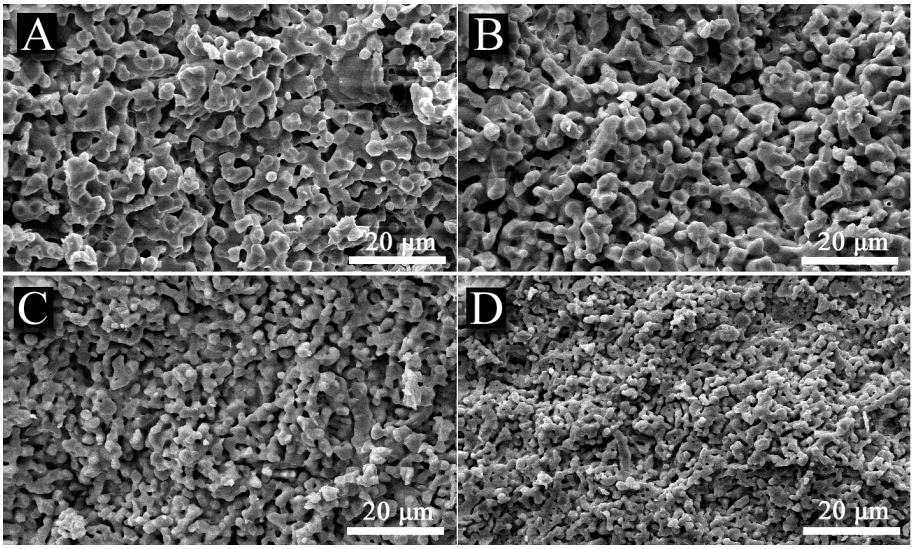

Figure 2. SEM images of TZ00(A), TZ05(B), TZ15(C), TZ45(D), the grain size and micropore size decreased with the increasing zinc content.

2.3.3 Ion release

After four days immersion, Zinc ions were released in significantly higher contents from TZ45 with significant difference than other samples (p<0.001, Fig. 3C) while the Ca^{2+} (Fig. 3A) and PO_4^{3-} (Fig. 3B) concentration in the medium was similar (p>0.05).

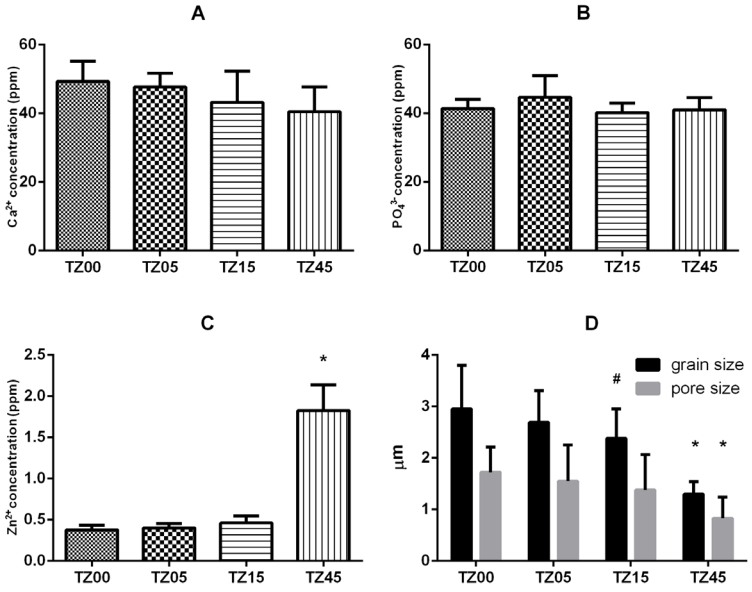

Figure 3. Ion concentration in culture medium after 4 days immersion of Zn-TCP discs: Ca^{2+} (A), PO_4^{3-} (B) and Zn^{2+} (C); D: a summary of grain size and pore size of Zn-TCP (*=significantly different than other samples; #= significantly different as compare to TZoo); the value of Zn^{2+} is not zero for TZoo, which might be due to instrumental errors of AAS.

2.3.4 Human bone marrow stem cells (hBMCs) culture

An increasing number of hBMCs cells were seen on all ceramic discs overtime. However, hBMSC on TZ45 discs showed higher proliferation than others at day 7 (Fig. 4A, p<0.02), indicating a positive effect of zinc on hBMSC proliferation. After 14 days the DNA production was similar on all TCP discs, which may due to full cell confluence on the disc surfaces.

Osteogenic differentiation of hMSCs indicated by the value of ALP/DNA was not different with the zinc content in TCP at day 4 and day 7, while at day 14, the

ALP/DNA value increased with zinc content with a significantly higher osteogenic differentiation on TZ45 as compared to TZ00 (p<0.02) (Fig. 4B).

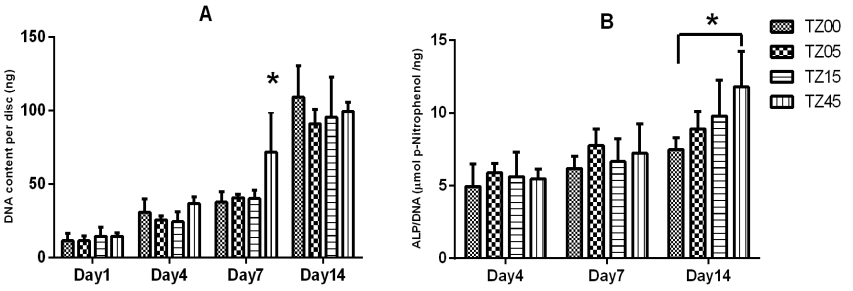

Figure 4. hBMSc cultured on Zn-TCP discs. A: cell proliferation of hBMSC on Zn-TCP discs as shown with DNA production; B: osteogenic differentiation of hBMSC on Zn-TCP discs as shown with the ALP/DNA ratio (After 14 days culture, the difference of hBMSC proliferation was not significant but the TZ45 showed higher ALP expression than TZoo with significant difference, *= p<0.05).

2.3.5 Murine macrophage RAW264.7 culture

DNA data did not show a different proliferation of RAW264.7 cells on TZ00, TZ05 and TZ15, conversely the proliferation was significantly enhanced on TZ45 (p<0.001, Fig. 5A). In addition, RAW264.7 cells on TZ45 produced significantly more TRAP than those on discs with lower zinc content (p<0.01, Fig. 5D) while no differences were seen among TZ00, TZ05 and TZ15.

When cells were cultured on zinc-free TCP, the zinc supplemented to the medium did not influence the proliferation of RAW264.7 until its concentration reached 18 ppm (p<0.001, Fig. 5B). Cells cultured with supplement of 1.8 ppm zinc expressed higher TRAP than other groups (p<0.001, Fig. 5E).

When RAW264.7 cells were cultured on plastic (culture dishes) with supplement of zinc in the culture medium, the proliferation increased gradually along with the zinc supplement. Groups with zinc-containing medium had higher DNA production than the group with zinc-free medium (p<10^{-5}, Fig. 5C) and a concentration of 18ppm zinc induced more proliferation than the group with 0.18 ppm zinc (p<0.01, Fig. 5C), indicating that zinc up to 18 ppm might promote the proliferation of RAW264.7. However, TRAP activity was dramatically inhibited when the zinc concentration was as high as 18 ppm (p<10^{-8}, Fig. 5F), while it was stimulated by lower concentration (i.e. 0.18 ppm and 1.8 ppm) (p<0.03, Fig. 5F).

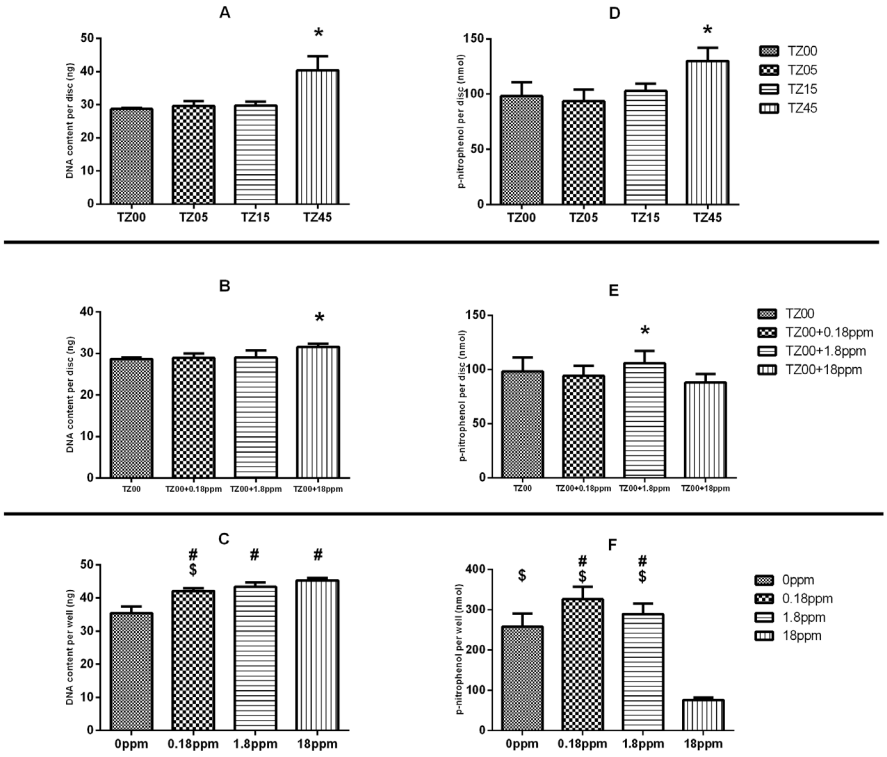

Figure 5. The proliferation (A, B, C) and TRAP expression (D, E, F) of murine macrophage RAW264.7 cultured in three different models: on Zn-TCP discs (A, D); on zinc-free discs with different zinc supplement in medium (B, E); on plastic culture plates with different zinc supplement in medium (C, F). (*=significantly different than other samples; #= significantly different as compare to 0 ppm; $=significantly different as compare to 18 ppm)

When RAW264.7 cells were cultured on plastic with zinc supplement in the culture medium, the fusion of cells into multiple nuclear giant cells (MNGC) was observed with zinc lower than 18 ppm (Fig. 6A). The size of these MNGC was bigger with 1.8 ppm zinc as compared to zinc-free control, indicating that zinc promotes the fusion of mononuclear cells to MNGC. However, fusion did not occur in presence of 18 ppm zinc (Fig. 6A), indicating excessive zinc suppresses the fusion.

The morphological variation of MNGC with zinc content was also observed with RAW264.7 cells on Zn-TCP or zinc free TCP supplemented with zinc in culture medium. The size of MNGC on Zn-TCP discs are bigger than those cultured on

TZ00 (p<0.02, Fig. 6B), while the biggest MNGC were seen on TZ45 (p<10^{-8}, Fig. 6B), showing that the fusion of mononuclear cells to MNGC is promoted with the increase of zinc content in TCP. When zinc is supplemented in medium, the MNGC size on zinc-free TCP was gradually increased until a zinc concentration of 1.8 ppm (p<0.002, Fig. 6C). A suppressing effect was observed thereafter with 18 ppm zinc (p<10^{-4}, Fig. 6C), corroborating what concluded earlier.

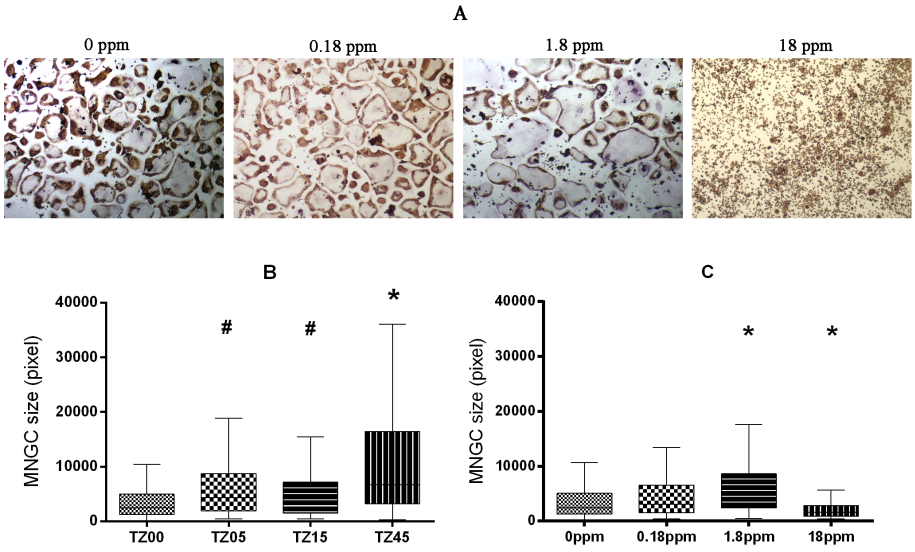

Figure 6. A: TRAP staining light microscopy images of RAW264.7 cells cultured on plastic culture plates supplemented with zinc-free medium, 0.18 ppm zinc, 1.8 ppm zinc and 18 ppm zinc; B: MNGC size on Zn-TCP discs; C: MNGC size on zinc-free TCP discs (*= significantly different as compare to other samples, #=significantly different as compare to the first sample)

2.3.6 Intramuscular bone formation

Histological overview after 12 weeks implantation in canine muscle showed different bone forming abilities of Zn-TCP with a trend following zinc content (Fig. 7A-D). In fact, bone volume increased significantly with zinc content (p<0.02, Table 1).

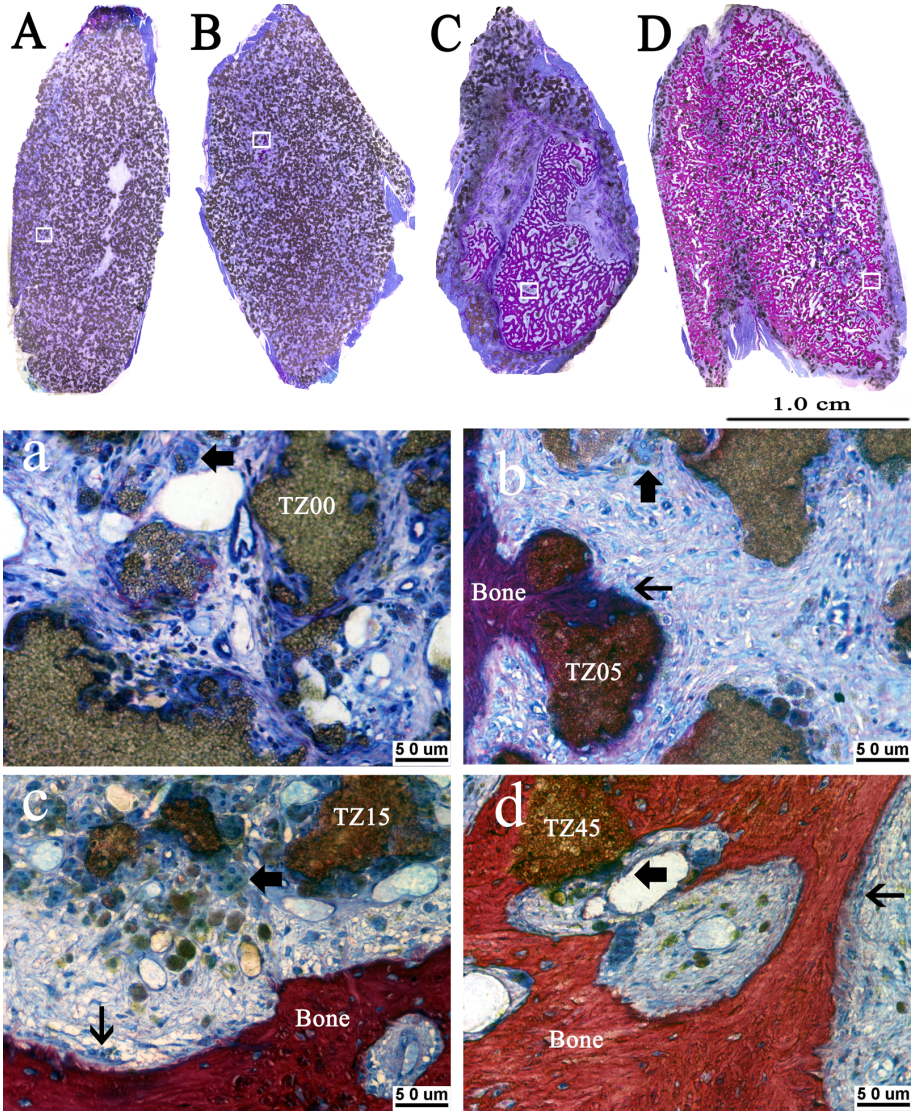

Figure 7. Top: Histology overviews after 12 weeks intramuscular implantation in canines (A: TZ00, B: TZ05, C: TZ15, D: TZ45); Bottom: the squares in A-D observed with light microscopy (a: TZ00, b: TZ05, c: TZ15, d: TZ45), showing osteoblasts (thin arrow) were secreting osteoid while multinuclear giant cells (thick arrow) were resorbing the material and bone.

Table 1. A summary of ectopic bone formation in intramuscular implants

Samples	TZ00	TZ05	TZ15	TZ45
Implants	4	4	4	4
Bone incidence	0/4	1/4	4/4	4/4
Bone formation (B%)	0±0	0.1±0.2	20.1±21.9	51.8±11.8

Detailed histological observations showed no inflammation adjacent to implants while fibroblasts and blood vessel were evident in soft tissue matrix. Bone was directly bond to TCP granules and bridges of mature bone were formed between granules. Osteoblasts were observed on the surface of bone matrix, while multinuclear giant cells were found around the resorption areas on TCP (Fig. 7a-d).

Calcein deposition was observed in bone formed in TZ45 implants (Fig. 8B) but not that in TZ15 implants (Fig. 8A) , indicating the bone formation started in TZ45 between 6 and 9 weeks, earlier than in TZ15. Xylenol Orange deposition was observed on bone tissue in TZ15 and TZ45 implants, indicating that bone was continuously forming after 9 weeks in both materials.

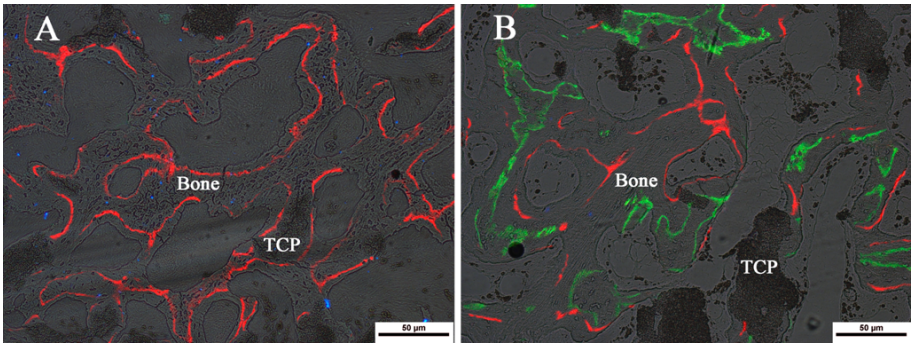

Figure 8. Microscopy images of TZ15 (A) and TZ45 (B) obtained by overlapping the fluorescent and transmitted light images taken in the same position. Bone formation started in TZ45 between 6 and 9 weeks after the implantation (calcein, green) and after 9 weeks (xylenol orange, red), while it appeared in TZ15 only after 9 weeks (xylenol orange, red)

2.4 Discussion

Zn-TCP induced ectopic bone formation in canine muscle related to the concentration of zinc they contained; however, TCP containing no zinc formed no bone (Table 1, Fig. 7). In addition to the observation that increased zinc content in TCP augmented ectopic bone formation in terms of bone incidence and volume, higher zinc content also appeared to accelerate the bone formation process based on fluorescent bone labeling (Fig. 8). These in vivo data suggest that the addition of zinc may be a useful strategy to render a non-inductive TCP osteoinductive.

We speculate that the observed bone formation was due to zinc release from the ceramics after implantation, which was shown to occur passively in physiologic condition (Fig. 3C). Moreover, in vivo, numerous multinuclear giant cells with internalized ceramic particles in close proximity to material resorption areas could be observed in histological sections and may have also facilitated zinc release (Fig. 7a-d). Thus, elevated zinc concentration in the implant microenvironment may occur by both hydrolytic and cell-mediated material degradation resulting in ectopic bone formation.

In agreement with this hypothesis, we found that Zn-TCP positively influenced osteogenic differentiation of hBMCs (Fig. 4), also presumably due to elevated zinc in the medium. These findings are in line with the finding of Ito *et al*., who observed that both rat and human bone marrow stromal cells (BMSc) cultured on zinc-containing BCP differentiated into osteoblast-like cells more than cells on zinc-free ceramics [135]. Elevated zinc released in the medium would potentially play an important role in cell differentiation since it has been reported that supplementing zinc in the medium significantly increases the osteogenic differentiation of both rat and human BMSc [198]. Thus, it is possible that blood/bone marrow stem cells homing to the implantation site due to the inflammatory foreign body reaction may have infiltrated the materials and then differentiated into osteoblasts due to elevated zinc released by the ceramics.

Zn has also been reported to promote the proliferation of other mineralizing cells in addition to stimulating osteogenic differentiation of stem cells. For instance, osteoblast precursor MC3T3-E1 was found to have higher proliferation and ALP expression on zinc-containing ceramics than those without [75,126]. Osteoblast-like line MG63, as well as osteoblasts, had improved adhesion and proliferation in presence of zinc [39,74]. In view of all of these findings, we speculate that Zn-TCP may first trigger osteogenic differentiation of stem cells and then stimulate the proliferation of their mineralizing osteoblast progeny. It follows that with more osteogenic cells at the site, more bone could be formed heterotopically resulting in

large bone mass (Fig. 7C-D). This assumption is demonstrated by our observation that with the increase of zinc content, bone formed earlier and its incidence increased (Table 1) enveloping the granules.

Because bone formation and metabolism are tightly coupled processes, it is also important to consider that Zn may also play a role in osteoclastogenesis. Using the cell line RAW264.7 cultured with RANKL as an in vitro model of osteoclastogenesis, the proliferation and TRAP activity of RAW264.7 cultured on TZ45 was significantly higher than those cultured on zinc-free TCP (Fig. 5A, D). Additionally, increasing zinc content augmented osteoclast size presumably due to higher cell fusion (Fig. 6B). Taken together, we surmised that elevated zinc content can promoted both osteoclast formation and activity. In order to address the confounding influence of the smaller surface microstructure of Zn-TCP accompanying increasing zinc concentrations, cells were cultured on tissue culture plastic and zinc-free TCP discs in the presence of RANKL but various concentrations of zinc doped into the culture medium. In both models, the proliferation, TRAP activity and osteoclast size was dependent on zinc concentration. For instance, the proliferation was slightly increased with zinc concentration in both models (Fig. 5B, C). TRAP activity was also increased with zinc concentration but was attenuated at an excessive concentration (18 ppm, Fig. 5E, F). Corresponding with this, osteoclast size increased with zinc content up until an excessive concentration (18 ppm) whereupon mononuclear cells no longer fused (Fig. 6A). These results suggest that when the factor of surface microstructure is removed, zinc concentration can still regulate the differentiation of monocyte/macrophages into osteoclasts. Furthermore, because the highest concentration of zinc released from the synthesized Zn-TCP was found to be 1.8 ppm (TZ45, Fig. 3C) after 4 days culture and this concentration also elicited similar effects when doped into medium containing Zn-free TCP, it is probable that osteoclast formation and activity was modulated by zinc content rather than differences in surface microstructure.

As TRAP activity and giant cell fusion are hallmarks of osteoclastogenic differentiation of mononuclear precursors, our results indicate that zinc may regulate the osteoclastogenic differentiation of macrophages and osteoclastic precursors. However, this effect may either be a stimulation or suppression, depending on the zinc concentration in the environment. The results presented herein are partly consistent with a finding from an RAW264.7 study in zinc-containing medium [73], which indicated a zinc concentration between 10 μM and 250 μM (i.e. 0.65 ppm and 16.25 ppm) as main cause of osteoclastogenesis suppression. Furthermore, zinc has been reported to inhibit resorption activity of rat osteoclasts [76]. Holloway *et al*. noticed that treatment with zinc concentration lower than 10^{-4} mol/L (6.5 ppm) had no

effect on osteoclast activity, while higher zinc amounts increased the number of TRAP-positive cells. Interestingly, it was also seen that osteoclast bone resorption was dramatically suppressed by high zinc contents [78].

Although zinc release from the ceramics reached a bioactive level after four days in vitro, the situation is more complex in vivo and zinc levels in the implant tissue were not measured. The circulation of body fluids certainly would influence the local ion concentration near the implants, likely dispersing the elevated ions. Still, it stands to reason that ions released in the core of the implants would be more shielded by the circulation, where the body fluid flow is obstructed. Thus we assume that the zinc concentration in the middle of the implant could reach an effective level during the implantation time to modulate osteogenesis.

Beside ion release, differences in chemistry and surface microstructure may have also played a role in the bone formation. The chemical composition varied as shown in XRD, where apatite phase formation was provoked by the presence of zinc in TCP (Fig. 1). The influence of calcium phosphate chemistry on osteogenic differentiation, osteoblast behavior and bone forming ability is reported in various studies with respect to the HA/TCP ratio [213–215]. However, many findings are controversial. Moreover, HA and TCP are physicochemically different and thus the HA/TCP content ratio leads to many other differences like calcium and phosphate ion release rate and surface topography, though these sub-factors were not studied. Thus it is difficult to determine whether such factors are responsible for improved bone forming ability.

We observed that the grain and pore size of TCP decreased with zinc addition (Fig. 2). This difference in surface topography between Zn-TCP might be the reason of the difference in the size of MNGC between TZ45 and the zinc-free control with 1.8 ppm zinc supplement although they experienced equivalent zinc release (Fig. 6), since surface topography (i.e. surface roughness) alone can have influence on cells behaviors of osteoclast [116,216,217]. Not limit to osteoclasts, various cells were sensitive to surface topographical cue regarding cell behaviours of attachment, adhesion, spreading, migration, proliferation and differentiation[218]. For instance, surface topography was able to directly trigger or enhance osteogenic differentiation of hBMSC and MG63 cells [219–221]. It is therefore difficult to attribute the various bone formation in Zn-TCP implants only to the release of zinc, since the different surface topography may have play roles in bone formation as well.

It is important to note that the trace element-substituted ceramic is not a simple overlay of trace element and the ceramic. Many physicochemical properties of the ceramic, such as the chemistry and surface topography can be changed because of ion substitution. Thus, it is a complex issue to directly link the effect of ions to the

biological response [166]. We have shown that using zinc-containing tricalcium phosphate ceramic as a model, incorporating trace elements in bone mineral has the potential to induce bone formation. However, the mechanism behind this phenomenon is still not fully understood. Carefully designed materials that contain only one variable parameter would be useful in more clearly explaining the role of ions, or other materials' factors in osteoinduction [120].

2.5 Conclusion

Zn-TCP enhanced osteogenic differentiation of hBMSC and regulated osteoclastic differentiation of monocyte/macrophages in vitro. Incorporation of high zinc content in TCP led to osteoinductive materials capable of forming abundant de novo bone in the muscle. The in vivo responses may be correlated with the release of zinc as supported by our in vitro cellular results. However, other factors such as the chemical composition and surface topography of TCP, which are modified by the zinc addition, may also have played roles in this intriguing phenomenon.

Acknowledgements

The authors acknowledge University of Twente and Sichuan University for their help in getting the data that have been used in this manuscript.

Chapter 3

Influence of fluoride in poly(D,L-lactide)/apatite composites on bone formation

Influence of fluoride in poly(D,L-lactide)/apatite composites on bone formation

Luo X[1], Barbieri D[1], Passanisi G[1], Yuan H[1,2,3,*], de Bruijn JD[1,2,4]

1 Xpand Biotechnology BV, Prof.Bronkhorstlaan 10, Bld 48, 3723MB Bilthoven, The Netherlands

2 MIRA Institute, University of Twente, Drienerlolaan 5, 7522 NB Enschede, The Netherlands

3 College of Physical Science and Technology, Sichuan University, Wangjiang Road 29, 610064, Chengdu, China

4 School of Engineering and Materials Science, Queen Mary University of London, Mile End Rd, London E1 4NS, UK

Abstract

The influence of fluoride in poly(D,L-lactide)/apatite composites on ectopic bone formation was evaluated in sheep. Nano-apatite powders with different replacement levels of OH groups by fluoride (F) (0 % (F0), 50 % (F50), 100 % (F100) and excessive (F200)) were co-extruded with poly(D,L-lactide) at a weight ratio of 1:1. Fluoride release from the composites (CF0, CF50, CF100 and CF200) was evaluated in vitro and bone formation was assessed after intramuscular implantation in sheep. After 24 weeks in simulated physiological solution, CF0 and CF50 showed negligible fluoride release, while it was considerable from the CF100 and CF200 composites. Histology showed that the incidence of de-novo bone formation decreased in implants with increasing fluoride content indicating a negative influence of fluoride on ectopic bone formation. Furthermore, a significant decrease in resorption of the high fluoride-content composites and a reduction in the number of multinucleated giant cells were seen. These results show that instead of promoting, the presence of fluoride in poly(D,L-lactide)/apatite composites appeared to suppresses their resorption and osteoinductive potential in non-osseous sites.

Keywords: Fluoride; composites; osteoinduction; multinucleated giant cells; resorption

Published in Journal of biomedical materials research. Part B, Applied biomaterials 2015, 103(4), 841-52

3.1 Introduction

Bone is a complex nano–matrix system consisting of an organic framework of mainly type-I collagen fibrils in which small inorganic prism–shaped carbonated hydroxyapatite crystals (2–50 nm) are evenly embedded [222–224]. Because of their chemical similarity to bone mineral, calcium phosphate ceramics are considered the most promising materials for bone replacement [82]. They have been demonstrated to be non-toxic, biocompatible and osteoconductive. A sub-group of these materials has been reported to have osteoinductive properties [99,225], which can be defined as the ability to generate heterotopic bone formation following implantation in non-osseous sites [226]. We have previously reported that the bone regenerative properties of an osteoinductive, submicrostructured calcium phosphate ceramic is equal to that of autograft when implanted in a critical-sized bone defect [109]. However, due to their brittleness, the use of pure calcium phosphate ceramics is largely limited to non-load bearing sites. To overcome this drawback, polymer/calcium phosphates composites have been developed. For example, Verheyen *et al*. reported that the addition of 50 wt% hydroxyapatite to a poly(L-lactide) can generate a mechanically strong osteoconductive graft [227], while recent studies on polylactide/apatite composites have shown that they can also be osteoinductive [104,105,107]. The amount of bone induction observed with such polylactide/apatite composites was however limited as compared to that found in osteoinductive calcium phosphate ceramics [104,105,107,109,228].

Inspired by the fact that bone mineral contains trace elements with various effects on metabolism (e.g. silicon, zinc, fluoride, strontium and magnesium) [37,41,51,229,230], the introduction of trace elements in synthetic bioceramics to improve their biological performance has been studied for decades. Among the numerous trace elements in bone, fluoride (F) has been reported to stimulate the proliferation and osteogenic differentiation of osteoblastic cells in vitro [64–70]. When fluoride was introduced in osseous sites in vivo, beneficial effects on bone metabolism were seen in terms of increased osteoblast number [231] and bone formation [155–157,231–233]. Fluoride therapy has also been used to reduce osteoporotic symptoms [35,234,235]. These findings suggest an anabolic role of fluoride in bone formation and therefore introducing fluoride in polylactide/apatite composites might improve their bone forming ability.

To examine this, we used an osteoinductive model based on poly(D,L-lactide)/apatite composite where fluoride was introduced in the form of fluoride-containing nano-apatite. It is hypothesized that the introduction of fluoride in the composites will result in fluoride release, ultimately improving bone formation. To test this assumption, we synthesized nano-apatite particles with four fluoridation levels where the OH groups

were (partially) replaced by F, incorporated them in poly(D,L-lactide) with a weight ratio of 1:1 to obtain four composites having different fluoride contents. After characterizing their degradation and ion release profiles, the resulting composites were implanted in a heterotopic sheep model to study the possible role of fluoride in inductive bone formation.

3.2 Materials and methods

3.2.1 Hydroxyapatite and fluoride-substituted apatite synthesis

Pure hydroxyapatite (F0) powder was synthesized as previously described[105]. In brief, by adding aqueous solution (concentration = 63.12 g/L, 12.5 mL/min) of $(NH_4)_2HPO_4$ (Fluka, Germany) to aqueous solution (concentration = 117.5 g/L) of $Ca(NO_3)_2{\cdot}4H_2O$ (Sigma, Germany) under continuous stirring rate of 500±10 rpm and temperature of 80±5 °C. The pH was kept above 10 by adding ammonia solution (Fluka, ~25% NH_3) at 17.5 mL/min to the reaction vessel. For fluoride-substituted apatite, calculated amounts of NH4F (Sigma) were added to ammonia solution to obtain apatite with 50 % (atomic ratio) (F50), 100 % (F100) and excessive (F200) fluoridation. For excessive substitution, double amount of NH4F needed for F100 was added. After all solutions were completely added together, the suspension was kept at 80±5 °C and stirred for two further hours. The precipitates were aged overnight, washed with distilled water until the complete removal of ammonia and repeatedly suspended in acetone (Fluka) to dehydrate. Then all apatite powders were vacuum-filtered and dried at 80±5 °C.

3.2.2 Preparation of poly(D,L-lactide)/apatite composites

Obtained apatite powders were sieved with 212 µm mesh and extruded at the weight ratio of 1:1 with poly(D,L-lactide) (PDL45, Purac Biomaterials BV, Netherlands) to obtain composites of CF0, CF50, CF100 and CF200. The extrusion was carried out using a vertical conic twin-screws extruder (RD11-H-1009-025-4, Artecs; top screw diameter: 10 mm; bottom screw diameter: 4.15 mm; screw thread: 8 mm; screw length: 108 mm) at 195±1 °C, screw speed 100±1 rpm for 5.0±0.5 min[104]. The extruded stripes were then grinded (ZM100, Advantec, Japan) and sieved to obtain granules with size range of 0.5-1.0 mm. Granules were ultrasonically cleaned afterwards with distilled water for 15±1 min at room temperature and dried at 37±1 °C.

3.2.3 Sodium hydroxide treatment and sterilization

Prior to all characterization and experiments, surface treatment with sodium hydroxide was applied on clean composite granules to remove surface polymer layer and enhance the apatite exposure. In brief, granules were soaked in NaOH (Merck,

Germany) solution (concentration = 0.75 mol/L) at the ratio of 0.2 cm^3 granules per mL solution for 5.0±0.5 min under shaking conditions and room temperature. The treated granules were then rinsed with distilled water and dried at 37±1 °C. Afterwards, all specimens were sterilized with ethylene oxide (concentration = 450–700 mg/L, followed by washes with nitrogen / air and a 7-day aeration, IsoTron Nederland BV, the Netherlands) and used for all experiments described in this study.

3.2.4 Characterization of apatite and composites

To verify the effective fluoride content in each fluoride-substituted apatite, 0.20 ±0.01 g of each powder were dissolved in 5 mL hydrochloric acid (1 mol/L, Merck) to completely release fluoride. The fluoride concentration in acid was then measured using an ion-meter (Orion 4 stars, Thermo Scientific, USA) equipped with a fluoride-selective electrode (F-SE, 9609BNWP, Thermo Scientific). The fluoride content in apatite was then calculated and represented according to the formula of $Ca_5(PO_4)_3OH_{1-x}F_x$ (not applicable for F200) and the final content of fluoride in composites was considered half of that in apatite by weight. Chemical analysis of the obtained apatite powders was conducted before and after sintering at 1100 °C for 200 min (Nabertherm C19, Nabertherm, Lilienthal, Germany) using X-ray diffractometer (XRD, MiniFlex II, Rigaku, Japan) with Cu Kα radiation (λ = 1.5405 Å, 30 kV, 15 mA) over the 2θ range of 25° – 45°. High resolution electron microscopy images (HR-TEM) of the samples were taken (TEM, FEI Tecnai-200FEG, FEI Europe, Eindhoven, the Netherlands) and fast Fourier transform (FFT) was employed to investigate the interplanar spacing (d-value) of the four apatites along the reflection plane (010). Fourier transform infrared spectrometry (FTIR, Spectrum 1000, Perkin Elmer) was used to characterize the apatite powders, poly(D,L-lactide) and their resulting composites with a typical KBr pellet technique. The surface topography of composite granules before and after surface treatment was analyzed using a scanning electron microscope (SEM, XL 30 ESEM-FEG) to evaluate the enhancement of apatite exposure.

3.2.5 In vitro degradation of apatite powder and composite granules

A simulated physiological solution (SPS) was prepared by dissolving sodium chloride (NaCl, Merck, concentration = 8 g/L), sodium azide (NaN3, Merck, concentration= 0.01 g/L) and 4–(2–hydroxyethyl)–1–iperazineethane–sulfonic acid (HEPES, Sigma, concentration = 11.92 g/L) in distilled water. The pH of the solution was adjusted to 7.3 with NaOH (Merck, concentration = 2 mol/L) at 37 °C. 0.50±0.01 g granules of each composite (six replicates) were carefully weighed and soaked in 200 mL SPS at 37±1 °C for 24 weeks under a 3–week refreshing regime. For powders, 0.25±0.01 g of each apatite powder (in triplicate) was soaked at the same condition used for

composites for 3 weeks and the SPS was refreshed at 1, 7 and 14 days. With the solutions removed at every refreshing time point, the concentrations of calcium and phosphate in the solution were measured by using appropriate biochemical kits (Calcium: QuantiChromTM calcium assay kit, BioAssay Systems, USA; Phosphate: PhosphoWorksTM Colorimetric phosphate assay kit blue color, BioquestInc, USA) and a spectrophotometer (AnthosZenyth 3100, AnthosLabtec Instruments GmbH, Salzburg, Austria) with absorbance filter of 620 nm for both assays. The concentration of fluoride ions in solution was measured using F-SE. At 12 weeks and 24 weeks, 3 replicates of composite granules were removed from SPS, the excess SPS was wiped away and the granules were weighed (Mwet). Afterwards, they were dried at 37±1 °C and carefully weighed (Mdry). The mass loss of the composite was determined as:

$$\text{Mass loss (ML, \%)} = \frac{\text{M0}-\text{Mdry}}{\text{M0}} * 100 \quad (1)$$

where M0 is the exact initial weight of each replicate.

The fluid uptake of the composites was evaluated as:

$$\text{Fluid uptake (FU, \%)} = \frac{\text{Mwet} - \text{Mdry}}{\text{Mdry}} * 100 \quad (2)$$

Afterwards, dried composite granules were sintered at 900 °C for two hours to burn away the polymer phase. The mass of each apatite ashes was weighed (Mash). The changes in the apatite and polymer content in the composite were estimated as:

$$\text{Mass loss of apatite phase (AL, \%)} = \frac{\text{M0}*50\%-\text{Mash}}{\text{M0}*50\%} * 100 \quad (3)$$

$$\text{Mass loss of polymer phase (PL, \%)} = \frac{[\text{M0}*50\%-(\text{Mdry}-\text{Mash})]}{\text{M0}*50\%} * 100 \quad (4)$$

3.2.6 Intramuscular implantation

All surgeries were conducted in Sichuan University, Chengdu, China. Local animal ethics committee guidelines (Regulations for the administration of affairs concerning experimental animals, China, 1988) for the care and use of laboratory animals have been observed. Composite granules were prepared as one cubic centimetre aliquots under a sterile condition in glass vials prior to the implantation. Four two-year-old female small-tail Han sheep with the average body weight of 50 kg were used. After a general anaesthesia by intramuscular injection of xylazine hydrochloride solution (0.1 mL/kg body weight, Vast Moves Guarantees Tech Co. Ltd, China), muscle pouches were created in the paraspinal muscle along the direction of spine by scalpel incision and blunt dissection, then one aliquot was implanted in dorsolateral pockets. The distance between each pocket was about 2~3 cm. The pockets were

then closed with non-resorbable sutures for identification at harvest. Following the surgeries, animals were intramuscularly given benzoxyazole injection solution (0.1 mL/kg body weight, Vast Moves Guarantees Tech Co.Ltd) immediately to terminate the anaesthesia. Penicillin (40 mg/kg body weight) was given for three consecutive days to prevent infection. After operation, animals were allowed full weight bearing and received normal diet. Animals were sacrificed after 24 weeks with an intra-abdominal injection of excessive amount of sodium pentobarbital (Sigma).

3.2.7 Histology and histomorphometry

Explants were fixed with 4 % formaldehyde, embedded in PMMA after gradient ethanol dehydration. Three non-decalcified sections were made across the middle of the explants using a diamond saw microtome (Leica SP-1600, Germany) and stained with 1 % methylene blue (Sigma) and 0.3 % basic fuchsin (Sigma). The histological slides were scanned with a scanner (Dimage Scan Elite5400 II, Konica Minolta, USA). Histomorphometry of bone formation in the stained sections was performed by pseudo-colouring pixels representing formed bone (B) in a region of interest (ROI, with surrounding soft tissues outside the implants excluded) using Photoshop (Adobe Photoshop Elements 2.0). Bone formation (B %) was calculated as:

$$\mathrm{B}\,\% = \frac{\mathrm{B}}{\mathrm{ROI}} * 100 \qquad (5)$$

Histological observation was performed with light microscopy. The number of total granules (P), granules with bulk resorption (i.e. granules with part of their bulk resorbed, R) and multinucleate giant cells (MNGC) in ROI were counted manually under light microscope from the histology sections of each animal with a tally counter. An average of 450 granules was counted in each slide. The resorption (R %) and the average number of MNGC per granule (Nm) were calculated as:

$$\mathrm{R}\,\% = \frac{\mathrm{R}}{\mathrm{P}} * 100 \qquad (6)$$

$$\mathrm{Nm} = \frac{\mathrm{MNGC}}{\mathrm{P}} \qquad (7)$$

3.2.8 Statistical analysis

Statistical analysis was carried out using one-way analysis of means (ANOVA). Differences were considered statistically significant at $p<0.05$. Marks were given on figures if significances were found (a: $p<0.05$; b: $p<0.005$; c: $p<0.0005$)

3.3 Results

3.3.1 Characterization of fluoride-containing apatite

The crystalline phases of the obtained apatites were examined with powder XRD. The patterns of sintered (fig.1b) and not-sintered (fig.1a) fluoride-substituted apatites were similar to that of F0, which is identical to standard hydroxyapatite (PDF#84-1998). When spectra were collected on a narrower 2θ range, it was possible to observe that the fluoride-containing apatite peaks were shifted toward higher 2θ values as compared to F0, with a maximum shift for F100. It should be noted that F200 did not follow such increasing trend but had intermediate shifts indicating a different effect of fluoride in the lattice of apatite (fig.1c). However, the results did not indicate the presence of other phases that may have been provoked by fluoride addition.

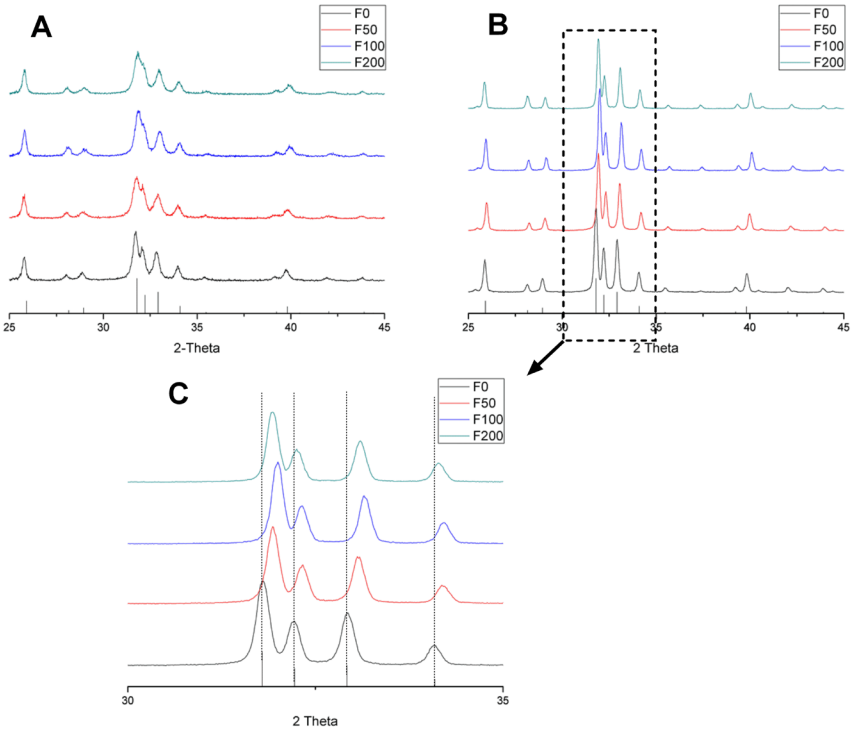

Figure 1. XRD patterns of fluoride-apatite (from bottom to top: Fo, F50, F100, F200): non-sintered (a), sintered (b), the enlargement of b over the 2θ range from 30° to 35° (c). Both non-sintered and sintered Fo showed typical peaks of hydroxyapatite (PDF#84-1998) while peaks of fluoridated apatite were shifted.

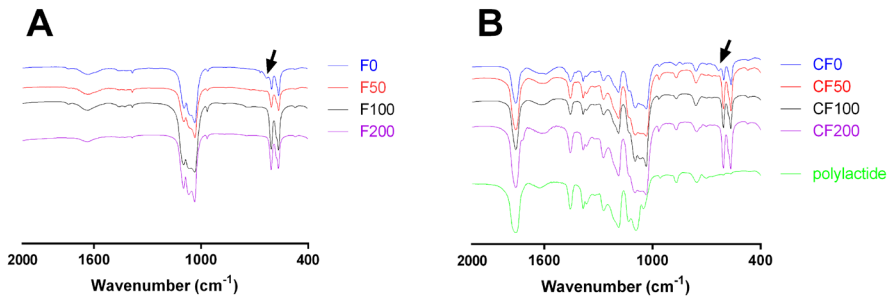

Figure 2. FTIR patterns of fluoride-apatite (a) and their resulting composites (b), the pattern of pure polymer PDL45 was also shown in b to clarify the presence of apatite and polymer in composites; the OH^- vibration at 633 cm^{-1} (pointed by arrow) is observed in Fo and CFo samples, but it is absent in samples with fluoridation indicating the replacement of OH^- by F^-.

The OH vibration at 633 cm^{-1} was observed in FTIR pattern of F0 but disappeared with the increase of fluoride content in the powder (fig.2a).

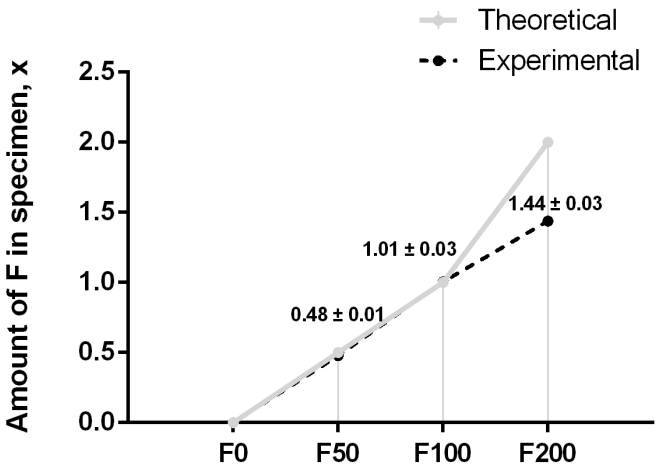

Figure 3. Amount of fluoride in fluoride-containing apatite. Experimental x values are given in the graph and compared with the theoretical ones, which are x = 0 for Fo, x = 0.5 for F50, x = 1.0 for F100 and x = 2.0 for F200. "x" on Y-axis indicates the

stoichiometric quantity of fluorine in the formula $Ca_5(PO_4)_3OH_{1-x}F_x$ (not applicable for F200).

The content of fluoride in apatite ($Ca_5(PO_4)_3(OH)_{1-x}F_x$) was evaluated with F-SE measurements (fig.3). The fluoride content in apatite resulted close to the theoretical stoichiometry for F50 and F100. The fluoride content of F200 was higher than the stoichiometry of F100, but lower than the added amount, indicating that the excessive fluoride could have partly reacted to apatite or had been partly dissolved during the processing. In F0 no fluoride was detected. Based on the obtained "x" values, the mass fraction of fluoride in obtained apatites were 1.81 wt% for F50, 3.81 wt% for F100 and 5.42 wt% for F200. Since the general formula $Ca_5(PO_4)_3(OH)_{1-x}F_x$ is not applicable for F200, the last number is a rough estimation. Naturally, the final fluoride content in composites would be considered as 0 wt% for CF0, 0.91 wt% for CF50, 1.91 wt% for CF100 and 2.71 wt% for CF200.

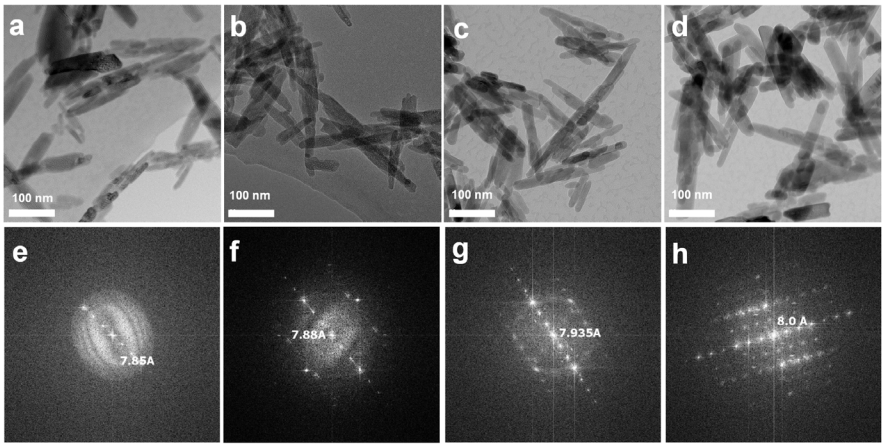

Figure 4. TEM images of F0 (a), F50 (b), F100 (c) and F200 (d). All the apatites are needle-like shaped crystals. FFT transform of TEM images showed an increase of interplanar spacing of fluoride-apatites from 7.85 Å to 8.0 Å along the reflection plane (010): F0 (e), F50 (f), F100 (g) and F200 (h). Scale bar in TEM images: 100 nm

The nanometre size and needle shape of the (fluoride-)apatite particles were confirmed by TEM micrographs, with length ranging between 50 and 200 nm (fig.4a-d). Differences in aspect ratio among the four apatites were not obvious. The interplanar spacing (d-value) obtained from FFT applied to HR-TEM along the plane (010) increased with fluoride substitution level (fig.4e-h), reflecting the changes of lattice structure according to fluoride additions.

3.3.2 Surface geometry of composites

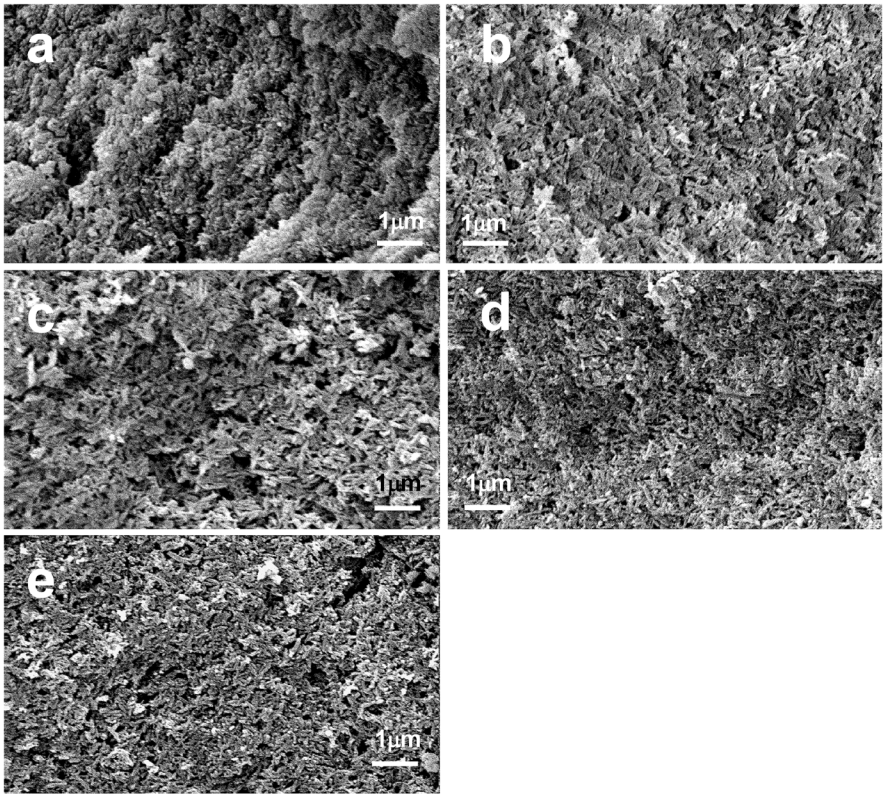

Figure 5. SEM images of composite granules before surface treatment (a, CF0 was took as an example) and after: CF0 (b), CF50 (c), CF100 (d) and CF200 (e); Surface treatment exposed more surface apatite particles. Scale bar: 1 μm

Compared with the spectra of PDL45 polymer, FTIR spectra of composites showed the typical peaks of both apatite and PDL45 (fig.2b), confirming the presence of apatites in polymer matrices. SEM images showed that the surface treatment influenced the surface morphology of composite granules. Comparison between SEM images before (fig.5a) and after surface treatment (fig.5b) showed that apatite particles were less embedded in the surface after treatment. As the composites had same apatite / polymer ratio and were extruded under the same conditions, the surface treatment is expected to give comparable results. Evidently, the exposure of apatite was ubiquitous and visually similar on all materials (fig.5b-e).

3.3.3 Effect of fluoridation on ion-releasing properties of apatite and composites

Possible ion release in SPS from apatites and composites were evaluated. Fluoride released from apatite was obvious only from F200 at short time, i.e. 3 weeks (fig.6e). However, it was possible to detect the fluoride release from fluoride-containing composites after 12 weeks. Fluoride release from CF50 was negligible, while it was considerable for CF100 and CF200 that released significantly larger amounts (fig.6f).

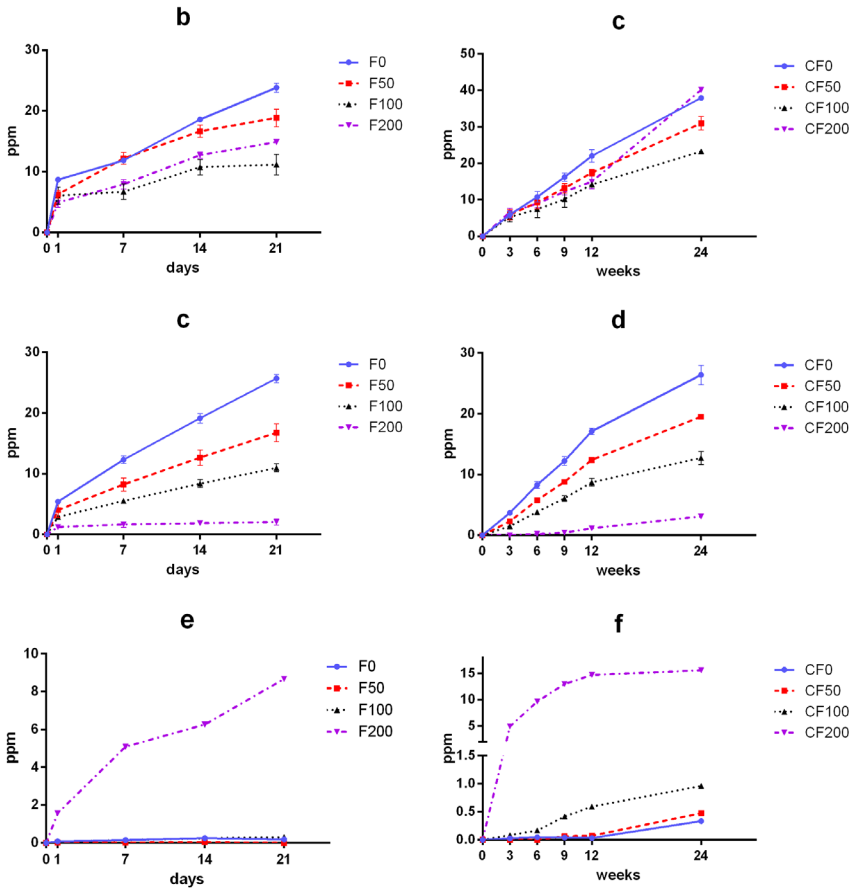

Figure 6. Ion release from apatite (a: Ca^{2+}, c: PO_4^{3-} and e: F^-) and composites (b: Ca^{2+}, d: PO_4^{3-} and f: F^-). Fluoride release was only detectable from apatite with excessive fluoridation, while it was observed from all composites during long term degradation. Fluoridation generally caused a decrease of calcium release except when it was excessive. It also decreased the phosphates release from both apatite and composites.

Apatite and composites showed similar releasing profiles, showing the polymer matrix could allow the release of ions from embedded apatite.

A decreasing trend in the release of calcium from both the apatite powders and the composite granules was seen until the fluoridation level increased to 100 %, indicating that fluoridation reduced the dissolution rate of apatite. Conversely, excessive fluoridation led to larger amounts of calcium release than stoichiometric fluoridation (fig.6a, b). On the other hand, as the fluoridation level increased, phosphate release was reduced both from apatites and composites (fig.6c, d).

It appeared that the amount of ion release was less for the composites than the apatite powders at week 3. This is presumably because most apatite particles in composites were embedded in the polymer matrix and thus less exposed to the fluids. However, apatite and composites showed similar releasing profiles, indicating that embedding apatite in polymer matrix hindered but did not block the release of ions.

3.3.4 Effect of fluoridation on degradation behaviour of composites

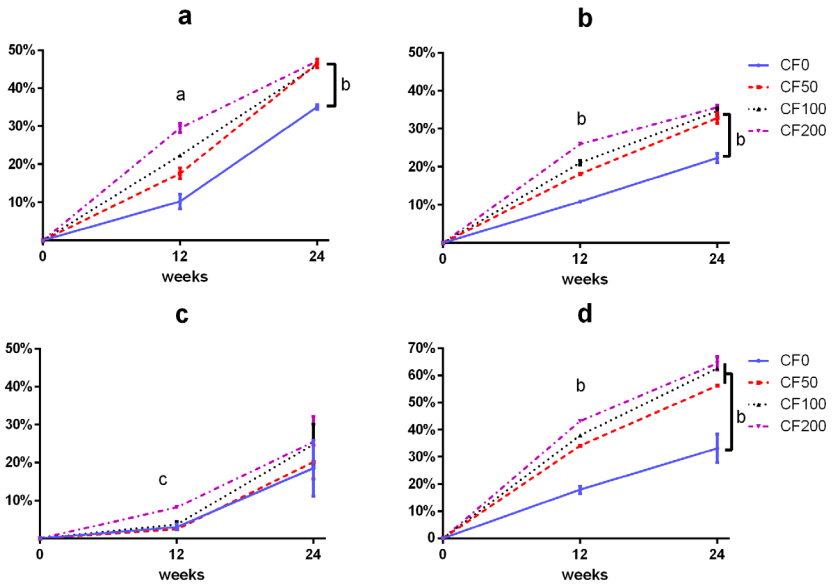

Figure 7. Degradation behaviour regarding fluid uptake (a) and mass loss (b). Loss of apatite phase (c) and polymer phase (d) after 12-week and 24-week degradation. (Marks in figures: a: $p<0.05$; b: $p<0.005$; c: $p<0.0005$)

After 12 weeks in vitro degradation, the mass loss and fluid uptake showed a correlation with the fluoride content in composites: both significantly increased with

increasing fluoride content in apatite (fig.7a, b). After 24 weeks, the mass loss and fluid uptake of fluoride-containing composites were still higher than that of CF0, but the difference among fluoride-containing composites was not significant (fig.7a, b). Burning test showed that after 12 weeks degradation in all composites more polymer phase was lost (fig.7d) than the apatite phase (fig.7c) and so it was after 24 weeks. In particular, with the introduction of fluoride, the loss of polymer phase was significantly increased (fig.7d), while the loss of apatite phase was only significantly higher for CF200 than other composites (fig.7c). After 24 weeks, the loss of apatite phase of all four composites showed a increasing trend with fluoridation level but the differences were not significant (fig.7c) whereas fluoride-containing composites lost more polymer phase than CF0 (fig.7d), suggesting a faster hydrolysis of polylactide during time when fluoride was introduced.

3.3.5 Effect of fluoridation on the in vivo performance of composites after intramuscular implantation

The incidence of heterotopic bone formation in implants decreased with the increasing fluoride content in the composites. Bone was seen in all four CF0 implants and mineralized bone with embedded osteocytes were seen at sites where MNGC were present (fig.8a, b, fig.9a, b). In two out of four CF50 specimens, small amounts of bone formed on degraded granules with nearby MNGC (fig.8c, d). In one out of four CF100 samples, sporadic bone was observed inside a degraded channel in the material (fig.8e, f) while no bone formed in any CF200 implants (fig.8g, h, fig.9c, d). Histomorphometry showed that B % = 1.111 ± 1.643 % for CF0, 0.080 ± 0.113 % for CF50, 0.004 ± 0.007 % for CF100 and 0% for CF200 (fig.9e). Although a decreasing trend of bone formation was observed, the difference was not statistically significant.

Many MNGC were seen at resorbed sites in CF0 composite (fig.9a, b) and their number decreased with increasing fluoridation levels (fig.9f). Significant differences in the amount of MNGC were detected between CF0 and fluoride-containing composites (fig.9f). The number of resorbed composite granules decreased significantly with the fluoridation level except between CF100 and CF200 (fig.9g). A clear correlation between the number of MNGC and the resorption rate was indicated by computer Pearson correlation (R^2 = 0.9972). Additionally, most CF200 granules were surrounded by fibrous tissue only and in some cases lymphocytes or granulocytes were seen indicating an inflammatory response (fig.8h).

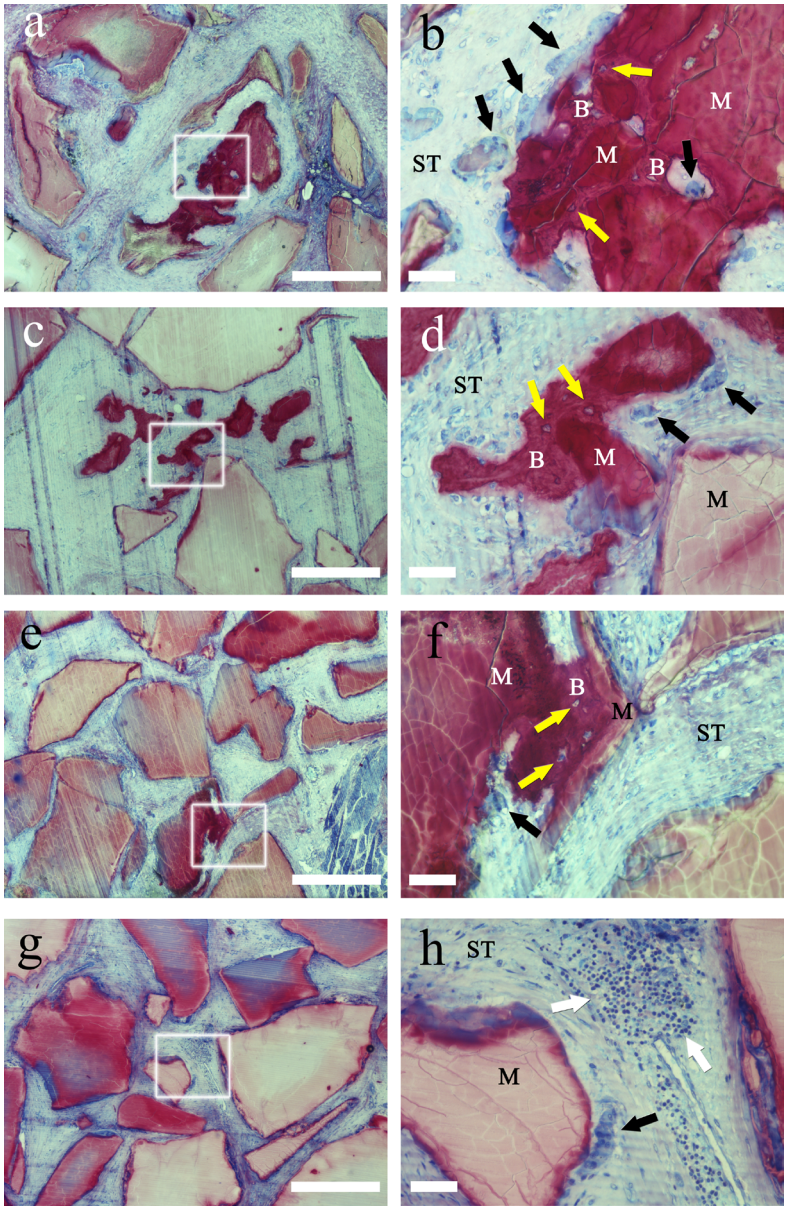

Figure 8. Histological observations of composites containing different fluoride-apatite after 24-weeks intramuscular implantation in sheep: CF0 (a, b), CF50 (c, d), CF100 (e, f) and CF200 (g, h). Each image in the right column represents the enlargement of the inset white square in the left image. M: material; B: bone; ST: soft tissue; black arrow: MNGC; white arrow: lymphocytes or granulocytes; yellow arrow: osteocytes; Scale bar: 500 μm in a, c, e, g, 50 μm in b, d, f, h

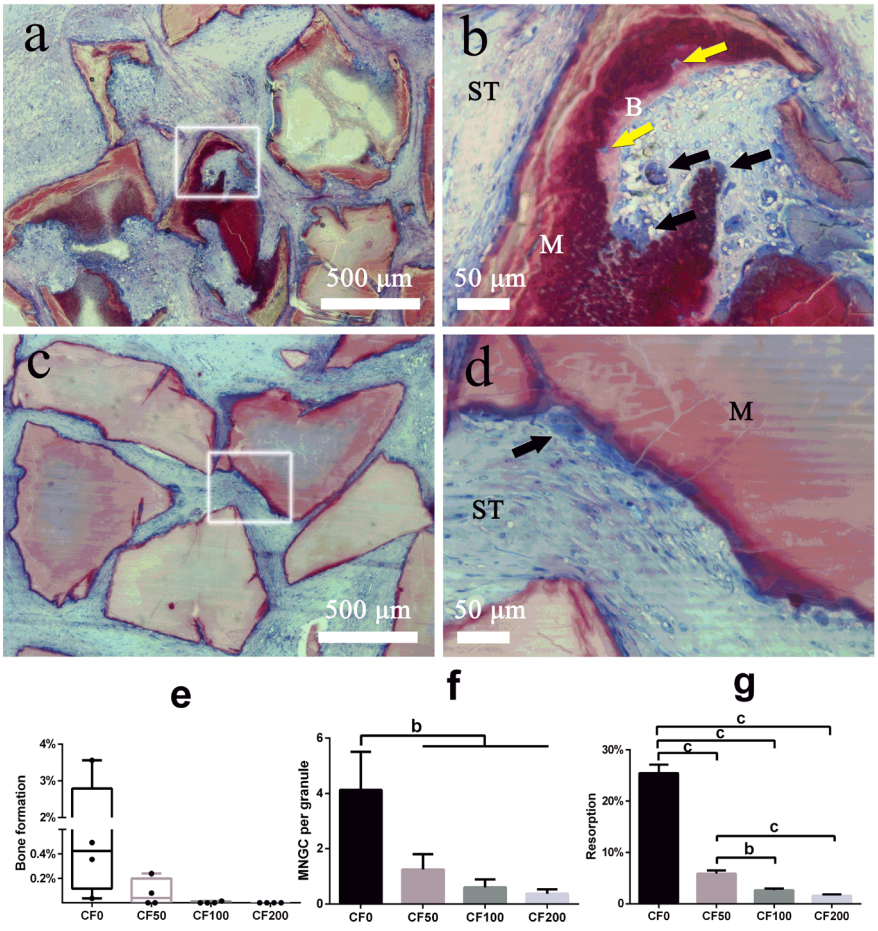

Figure 9. Cell mediated resorption on composite granules: CF0 (a, b), CF200 (c, d). b and d represents the enlargement of the inset white square in a and c. Many MNGC presented in CF0 and bulk resorption of granules was observed. CF200 was not resorbed and few MNGC were seen. M: material; B: bone; ST: soft tissue; black arrow: MNGC; yellow arrow: osteocytes; Scale bar: 500µm in a, c, 50µm in b, d. e: Quantitative bone formation in materials after 24 weeks implantation in box plots (mean and all points). Each dot represented the B % of the implants in one animal. f: Average number of MNGC per composite granule. g: Resorption of composite granules. Computer Pearson correlation showed a clear correlation (R^2 = 0.9972) between the number of MNGC and the resorption. (Marks in figures: b: p<0.005; c: p<0.0005)

3.4 Discussion

The introduction of fluoride in poly(D,L-lactide)/apatite composites influenced the ion releasing property and degradation behaviour of composites in vitro. Heterotopic bone formation, although with different incidence, occurred in all composite implants except CF200 after 24-week intramuscular implantation. The bone formation potential of composites as well as their in vivo resorbability were inhibited by the presence of fluoride whereas CF200 induced also an inflammatory reaction (fig.8g, h). These results suggest that introducing fluoride in composites may have a negative influence on the osteoinductive potential of composites.

Kim *et al.* showed a dose-dependent fluoride release when F was introduced into hydroxyapatite by thermal reaction [69]. In our study, fluoride release was obvious from CF100 and CF200, most significantly from the latter (fig.6f). The fluoride release from CF50 was indiscernible from that of CF0 with the ion electrode, which may be measurable using a more sensitive method such as ion chromatography [154]. Thus, the effect of fluoride release on the biological responses cannot be excluded from these two materials since a difference of F concentration as low as 1 μM (i.e. 0.017 ppm) is enough to elicit a biological response of cells (e.g. macrophages) [236]. Fluoridation decreased calcium and phosphate release until stoichiometric substitution. This result matches with those from other studies [67,69,154] indicating that fluoridation decreases the solubility of apatite. Conversely, when fluoridation became excessive, it resulted in scanty phosphate release but higher calcium release. This twist suggests that an excess of fluoride may alter the chemical stability of apatite. One explanation may be that fluoride has partially replaced the phosphate group in apatite in the form of monofluorophosphate (PO_3F^{2-}) and therefore causes an incongruent dissolution of apatite which can sharply reduce the release of phosphate [237,238].

Fluoridation also affected the degradation behaviour of the composites in simulated physiological environment. Fluid uptake of composites increased with fluoridation after 12 weeks (fig.7a), indicating that the presence of fluoride might increase the water affinity of the resulting composites. Higher fluid penetration can result in faster hydrolysis of the polymer matrix and, in turn, lead to increasing loss of the polymer content in the composites (fig.7d). Furthermore, the hydrolysis of polylactide may have produced degradation products with carboxylic acid end-groups causing a decrease of pH in the surrounding environment, which may have accelerated the self-catalysed hydrolysis of polymer phase [239]. CF200 had higher apatite loss than the other composites (fig.7c) confirming the altered chemical stability of apatite with excessive fluoride addition. As the overlay of both phases, the mass loss of

composites during the degradation increased with fluoride content (fig.7b). After 24 weeks, fluoride-containing composites still had higher fluid uptake and mass loss than CF0, but the difference between them disappeared (fig.7a, b). This latter effect might be attributed to their similar polymer loss of more than 50% (fig.7d), which might reduce the difference in fluid uptake and induce the drop out of apatite particles as evidenced by the large deviation of apatite loss after 24 weeks (fig7.c). All together, these results suggest that the degradation of polymer phase, which is presumably due to hydrolysis, plays an important role in the degradation of poly(D,L-lactide)/apatite composites in vitro. It is worth stressing that the in vitro experiment was conducted in SPS, a simple simulated physiological solution that contains no calcium and phosphate ions, for the purpose of studying fluoride's potential effects on the spontaneous ion release and degradation behaviours of the composites. For general investigations of the degradation behaviours of materials in vivo, simulated body fluid solution (SBF) is suggested since it provides more realistic simulation of the in vivo environment [240]. Nevertheless, it is worth pointing out that the real situation in vivo is complex (e.g. cell-mediated resorption could be involved as well).

A resorbable bone graft substitute can be resorbed by osteoclast and subsequently replaced by newly formed bone [175], thus the resorbability of an implanted material is important to determine its in vivo fate. Our results showed that fluoridation suppresses the resorption of the composites in vivo. Histomorphometry showed a clear correlation between the amount of MNGC and the number of granules with bulk resorption (fig.9f, g) indicating that cell-mediated resorption, but not the degradation of the material itself (i.e. the dissolution of calcium phosphates or polymer hydrolysis), is the driving force of biodegradation of these composites. Although immunostaining was not performed in this study to identify these resorbing cells, other studies showed that multinucleated resorbing cells have typical osteoclastic features, e.g. positive for TRAP and cathepsin K, and could resorb calcium phosphate ceramics [228,241–243] indicating their similarity with osteoclasts. The resorption of composites (fig.9a, b) may lead to the dissolution of exposed calcium phosphate, release of ions [174,175], more porous architecture for fluid penetration and the acceleration of polymer's hydrolysis. As a result, bulk resorption of the implant could be triggered. However, when fluoride was introduced, it generated apatite physically tolerant to dissolution in acidic environment [244] and thus more resistant to cell-mediated resorption. As a result, both the number of MNGC and granule resorption decreased with increasing fluoridation level (fig.9f, g), indicating fluoride's suppressive effect on cell-mediated resorption.

It was shown that osteoclast-like MNGC appeared on calcium phosphate ceramics prior to inductive bone formation [241–243], indicating a possible important role of

osteoclast-like MNGC in early stage of inductive bone formation. Interestingly, there are growing evidences showing that osteoclast-like cells can secrete unique coupling factors, e.g. CTHRC1, interacting with osteoprogenitors and bone cells, thus playing a role in osteogenesis [212,245,246]. In support of this, most osteoclast-like MNGC were observed on newly formed bone and the nearby granules in composites having higher osteoinductive potential (i.e. CF0). On the contrary, granules containing higher fluoridation levels were surrounded by fewer MNGC (fig.9f) with less resorption (fig.9g) and lower (or no) bone incidence (i.e. CF100 and CF200), suggesting that fluoridation might suppress the formation of osteoclast-like cells leading to less protein secretion, less osteogenesis and finally causing the failure of inductive bone formation.

It is worth taking into consideration that the in vivo responses could differ from individual to individual [100], i.e. the volume of ectopic bone formation is not related to the implanted materials only but also to the characteristics of each laboratory animal. Although animals used in this study were of the same species, gender, age and similar body weight, the bone volume varied between different animals causing the difference in bone volume not statistically significant. However, a decreasing trend of bone incidence was observed among animals, indicating the inhibited osteoinductivity of fluoride-containing composites. Our results show that the introduction of fluoride can largely change the dissolution properties and the resorbability of poly(D,L-lactide)/apatite composites and subsequently influence their osteoinductive potential. However, unexpectedly, an enhanced inductive bone formation was not observed here. Differently from other studies showing increased bone formation by fluoride at osseous site [155–157,231–233], here the materials were implanted intramuscularly where different mechanisms (e.g. the differentiation of stem cells) of bone formation may be involved [120].

3.5 Conclusions

The introduction of fluoride in poly(D,L-lactide)/apatite composites affected their ion-releasing property and the degradation behaviour in vitro. When implanted at non-osseous sites, the presence of fluoride suppressed the number of resorbing cells as well as the resorption of composites and decreased their osteoinductive potential.

Acknowledgements

The authors acknowledge financial support from the European Commission (Integrated Infrastructure Initiative 026019 ESSTEEM) in TEM imaging and Dr. Xu from Delft University of Technology for his contribution in TEM characterization. The authors would like to thank Purac Biomaterials BV (Gorinchem, the Netherlands) for

kindly providing the polymers and Prof.Grijpma from the University of Twente to allow the use of the extruder. The authors also acknowledge Msc.Zhang for his help in ion release analysis. The authors would like to acknowledge Biomedical Materials Program (BMM bone-IP), the Netherlands Institute for Regenerative Medicine (NIRM) and Rapid Prototyping of Custom-Made Bone-Forming Tissue Engineering Constructs (RAPIDOS Project) for their financial support in this study.

Chapter 4

The impact of polymer matrix composition on the ion release and osteoinductivity of Sr-containing apatite/polylactide composites

The impact of polymer matrix composition on the ion release and osteoinductivity of Sr-containing apatite/polylactide composites

Xiaoman Luo [a,b], Davide Barbieri [a], Yunfei Zhang [c], Yonggang Yan [d], Huipin Yuan [a,b,d,*], Joost D. Bruijn [a,b,e]

[a] Xpand Biotechnology BV, Prof. Bronkhorstlaan 10, Bld 48, 3723MB Bilthoven, The Netherlands

[b] MIRA Institute, University of Twente, Drienerlolaan 5, 7522 NB Enschede, The Netherlands

[c] Chongqing Academy of Metrology and Quality Inspection, Yangliu North Road No.1, Yubei District, 401123, Chongqing, China

[d] College of Physical Science and Technology, Sichuan University, Wangjiang Road 29, 610064, Chengdu, China

[e] School of Engineering and Materials Science, Queen Mary University of London, Mile End Rd, London E1 4NS, UK

Abstract: In this study, we investigated the impact of polymer matrix composition on the ion release properties and osteoinductivity of strontium-substituted apatite/polylactide composites. Nano-sized apatite with 0 to 50 at% strontium substitution (Sr0, Sr0.5, Sr5 and Sr50) was synthesized using a wet precipitation method. Eight composites were obtained by introducing the four strontium-substituted apatites into two different polylactide matrices: PDL04 (Poly(DL-lactide), with an inherent viscosity midpoint of 0.4 dl/g) and PLDL7060 (Poly(L, DL-lactide), with an inherent viscosity midpoint of 6.0 dl/g). The release of strontium, calcium and phosphate ions in SPS was higher from PDL04-based composites than PLDL7060-based composites after a 3-week immersion in simulated physiological solution (SPS) with a dose-dependent strontium release from both groups. After a 12-week intramuscular implantation in canines, inductive bone formation was observed in PDL04-based composites but not in PLDL7060-based composites. In addition, the incidence of bone formation was higher in Sr50/PDL04 as compared to other strontium containing composites. These results indicate that polymer matrix composition impacts the release of calcium, phosphate and strontium ions, which in turn affects the bone forming ability of apatite/polylactide composites.

Keywords: Strontium, apatite, polylactide, composites, ion release, osteoinduction

The contents in this chapter will be submitted for publication.

4.1 Introduction

When bone defects cannot be healed by the body (a critical size defect), the implantation of a bone graft is required to aid in the repair [247]. Autograft is the "gold standard" in this case but has several drawbacks such as the requirement for an extra operative harvesting procedure and limited availability. The search for alternative bone graft substitutes has recently revealed a series of attractive inorganic, calcium phosphate based materials with bone inducing properties [109]. These materials are equivalent in bone repair to autograft [100,109] and have the ability to induce bone formation in both heterotopic and orthotopic sites. The physico-chemical, ion release and surface structural properties have been postulated to play a role in the bone inductive potential of these materials [120].

It has been reported that calcium and phosphate ions can stimulate osteogenic differentiation of mesenchymal stem cells (MSCs) [57] and enhance the biomineralization of collagen [61]. It has also been shown that the release of calcium and phosphate ions from a ceramic material can lead to super-saturation of the ions in the surrounding body fluid, leading to (re)precipitation of biological apatite and subsequent bone matrix apposition [248–250]. Since some of these materials have been shown to induce bone formation at ectopic sites [98,99,251,252], a role of calcium and phosphate release in osteoinduction is suggested.

Synthetic polymers such as polylactide are attractive candidates for the development of composites for biomedical applications due to their biocompatibility and widespread clinical use [253,254]. When calcium phosphates are introduced into polylactide, calcium and phosphate ion release can be influenced by varying the weight ratio of calcium phosphate in the composite [105]. Several studies have reported that (nano)apatite/polylactide composites can be made osteoinductive if they contain more than 40 wt% of apatite [105,107]. In addition, we have recently shown that the osteoinductivity of nano-apatite/polylactide composites is suppressed by reducing the calcium phosphate dissolution rate through fluoride substitution [255]. These data suggest that the release of inorganic ions such as calcium and phosphate can affect the bone forming ability of apatite/polylactide composites.

Next to the effect of calcium and phosphate ions on MSCs, strontium has also been shown to enhance the osteogenic differentiation of MSCs [145,199,256]. Strontium can replace calcium ions in calcium phosphate materials and be released upon dissolution [144]. Therefore, strontium-substituted apatite holds the potential to further improve the bone forming ability of (nano)apatite/polylactide composites [127,142,148]. Next to the inorganic filler component, it is likely that the polymer composition will also influence composite degradation and ion release.

In this study, we synthesized a series of strontium-substituted apatite powders and introduced them into two polylactide matrices with different molecular compositions to investigate the impact of polymer matrix composition on bone formation of

strontium-containing composites. The first polymer, i.e. PDL04, is composed of D,L-lactide with an inherent viscosity midpoint of 0.4 dl/g (designed for drug delivery applications) whereas PLDL7060 is a copolymer of L-lactide and D,L-lactide in a 70/30 molar ratio and an inherent viscosity midpoint of 6.0 dl/g (designed for medical device applications). The release of calcium, phosphate and strontium ions from the resulting composites was evaluated by immersing them in simulated physiological solution (SPS). Afterwards, the intramuscular bone forming ability of the composites was evaluated in a canine osteoinduction model.

4.2 Materials and methods

4.2.1 Synthesis and characterization of strontium-containing apatite

Apatite (i.e. Sr0) powder was synthesized by adding an aqueous solution (concentration 63.12 g/L, 12.5 mL/min) of $(NH_4)_2HPO_4$ (Fluka, Germany) to an aqueous solution (concentration 117.5 g/L) of $Ca(NO_3)_2{\cdot}4H_2O$ (Sigma) under continuous stirring rate of 500±10 rpm and temperature of 80 ± 5°C. The pH was kept above 10 by adding ammonia solution (Fluka, ~25 % NH3, 17.5 mL/min) to the reaction vessel. For Sr-doped apatite, specific amounts of $Ca(NO_3)_2{\cdot}4H_2O$ (Sigma) were replaced by $Sr(NO_3)_2$ (Sigma) to obtain apatite powders with 0.5 % (i.e. Sr0.5), 5 % (i.e. Sr5) and 50 % (i.e. Sr50) atomic ratio of strontium substitution. After all solutions were completely added to the reaction vessels, the suspensions were kept at 80±5°C with stirring at 500±10 rpm for two hours. Afterwards, the precipitates were aged overnight, rinsed with distilled water until the complete removal of ammonia and repeatedly suspended in acetone (Fluka) to dehydrate. Then the powders were vacuum-filtered and dried at 60 ± 5 °C for 48 hours. Afterwards, their morphology was evaluated by scanning electron microscopy (SEM).

Chemical analysis of the obtained apatite powders was conducted with an X-ray diffractometer (XRD, MiniFlex II, Rigaku) using Cu Kα radiation (λ = 1.5405 Å, 30 kV, 15 mA) over the 2θ range of 25° – 45°. Unit cell parameters and crystallite size were calculated from XRD data using the software Jade (v6.5.26, Materials Data Inc., Livermore, CA, USA). Using an energy dispersive X-ray spectroscopy (EDX, FEI Tecnai-200FEG, FEI Europe, Eindhoven, the Netherlands), the experimental strontium substitution level in each apatite was estimated and compared with the theoretical values based on the formula $Ca_{(10-x)}Sr_x(PO_4)_6(OH)_2$ where x=0 for Sr0, x=0.05 for Sr0.5, x=0. 5 for Sr5 and x=5 for Sr50.

4.2.2 Preparation and characterization of PDL04- and PLDL7060-based composites

The powders previously obtained were sieved with 212 µm mesh and extruded at the weight ratio of 1:1 with 70 mol.% L-lactide/ 30mol.% D,L-lactide copolymer (PLDL7060, IV midpoint 6.0 dL/g, Purac Biomaterials BV, Gorinchem, The Netherlands) and poly(DL-lactide) (PDL04, IV midpoint 0.4 dL/g, Purac Biomaterials BV, The Netherlands) to obtain two groups of composites respectively. The extrusion

was carried out using a mini vertical conic twin-screw extruder (RD11-H-1009-025-4, DSM Research BV, Geleen. The Netherlands) with the screw speed of 100 ± 1 rpm for a mixing time of 5 ± 0.5 min at the extrusion temperature of 205 ± 1 °C for PLDL7060-based group and 130 ± 1°C for PDL04-based group. The obtained composite stripes were then grinded (ZM100, Advantec, Japan) and sieved to obtain granules with size range of 0.5-1 mm. Afterwards the granules were ultrasonically cleaned in distilled water for 15 ± 1 min at room temperature and dried at 37 ± 1°C. All specimens were sterilized with ethylene oxide (concentration 450–700 mg/L, followed by washes with nitrogen / air and seven-day aeration; IsoTron Nederland BV, the Netherlands) and used for all the experiments described in this study.

Fourier transform infrared spectrometry (FTIR, Spectrum 1000, Perkin Elmer, Waltham, MA, USA) was used to chemically characterize the composites using a typical KBr pellet technique, while SEM was performed to evaluate their surface topography. To evaluate the possible changes of polymer matrices during extrusion, the viscosity molecular weight of the polymers before and after the extrusion was measured. In brief, the extruded polymers were extracted from composites by dissolving the composites' granules in chloroform (Sigma, Germany) and vacuum filtering with glass funnels (ROBU, Germany; borosilicate 3.3 with glass filter having porosity #5) and PTFE membrane filter (Toyo Roshi Kaisha, Advantec, Japan; pore size 0.1 µm) followed by solvent evaporation under room temperature. Afterwards the extracted and original polymers were dissolved respectively in chloroform (Sigma) at the concentration of 0.1 g/dL and their relative viscosity (η) was measured using an Ubbelohde viscometer (0C, PSL-Rheoteck, Burnham on Crouch, United Kingdom) at 25 ± 0.1°C. The viscosity molecular weight (Mη) of polymer was calculated according to Mark-Houwink equation as follows:

$\eta = t_p/t_0$,

$M\eta = \exp [(\ln(\ln\eta/c) - \ln(K))/\alpha]$

where t_p and t_0 are the flow time (sec) of polymer solution and pure chloroform through the viscometer respectively, c is the polymer concentration in chloroform, K and α are the polymer-related Mark-Houwink constants. For PLDL60, $K = 2.0*10^{-4}$ dL/g and α = 0.73; for PDL04, $K = 1.8*10^{-4}$ dL/g and α = 0.72 as indicated by the supplier [257].

4.2.3 Fluid uptake and ion release from the two series of composites

Simulated physiological solution (SPS) was prepared as previously described [255]. 50 ± 0.5 mg sterile granules of each composite were weighed and soaked in 20 ± 1 mL SPS in glass jars (in triplicates) at 37 ± 1°C with shaking speed of 70 ± 5 rpm. After three weeks, the granules were removed from SPS and their wet weight was measured (m_{wet}). Afterwards they were vacuum-dried at room temperature until their weight was stable and then were weighed (m_{dry}). The fluid uptake of the composites was determined as:

Fluid uptake % = 100 x (m_{wet} – m_{dry})/m_{dry}

The concentration of calcium and phosphate ions released in SPS was measured using biochemical kits (Calcium: QuantiChromTM calcium assay kit, BioAssay Systems, USA; Phosphate: PhosphoWorksTM colorimetric phosphate assay kit blue color, BioquestInc, USA) and a spectrophotometer (AnthosZenyth 3100, AnthosLabtec Instruments GmbH, Salzburg, Austria) with absorbance filter of 620 nm for both assays. The concentration of strontium ions released in SPS was measured using inductively coupled plasma atomic emission spectroscopy (ICP-AES, DV7000, Perkin Elmer, USA) at the emission peaks of 407.771 nm and 421.552 nm.

4.2.4 Animal study

The implantation was conducted following local animal ethics committee guidelines (Regulations for the administration of affairs concerning experimental animals, China, 1988) for the care and use of laboratory animals. Eight adult male mongrel dogs (average body weight 12.5 kg) were used. After a general anaesthesia by abdominal injection of sodium pentobarbital (30 mg/kg body weight, Sigma), pouches were created in the longissimus muscle along the direction of the spine by scalpel incision and blunt dissection. One cubic centimetre of granules of each composite was implanted in a muscle pouch following a random order and the pouches were closed with non-resorbable sutures for identification at harvest. Following surgery, penicillin (100,000 IU/kg body weight) was given by intramuscular injection for three consecutive days to prevent infection. After surgery, animals were allowed full weight bearing and received a normal diet. Animals were sacrificed 12 weeks after surgery by a celiac injection of excessive sodium pentobarbital (Sigma).

4.2.5 Histology and Histomorphometry

The implants were harvested with surrounding soft tissues and fixed in 4% formaldehyde and embedded in PMMA after gradient ethanol dehydration. The explants were sectioned sequentially from one side to the other using a diamond saw microtome (Leica SP-1600, Germany) and stained with 1% methylene blue (Sigma) and 0.3% basic fuchsin (Sigma). The tissue response and potential bone formation was inspected with light microscopy. The histological slides were scanned with a scanner (DIMAGE Scan Elite5400II, KONICA MINOLTA).

4.2.6 Statistical analysis

Statistical analysis was carried out using one-way analysis of variance (ANOVA) with Tukey's test. Differences were considered statistically significant at $p < 0.05$ and marked with asterisks.

4.3 Results

4.3.1 Physicochemical properties of strontium-substituted apatite

Table 1: Summary of physicochemical parameters of obtained apatite

Notation	Intended chemical formula	Theoretical molar ratio of Sr substitution to Ca	Experimental molar ratio of Sr substitution to Ca	Crystallite size (Å)	Cell parameters a=b (Å)	Cell parameters c (Å)
Sr0	$Ca_{10}(PO_4)_6(OH)_2$	0%	0.10±0.17%	487±4	9.414±0.004	6.884±0.004
Sr0.5	$Ca_{9.95}Sr_{0.05}(PO_4)_6(OH)_2$	0.5%	0.43±0.09%	489±7	9.413±0.005	6.880±0.004
Sr5	$Ca_{9.5}Sr_{0.5}(PO_4)_6(OH)_2$	5%	6.15±0.26%	491±5	9.419±0.003	6.891±0.002
Sr50	$Ca_5Sr_5(PO_4)_6(OH)_2$	50%	53.33±1.19%	197±6	9.531±0.009	7.259±0.002

The experimental strontium substitution levels in the four apatite powders were calculated from EDX data. As shown in Table 1, the apatite powders had varying strontium content, which was close to that of the theoretical values.

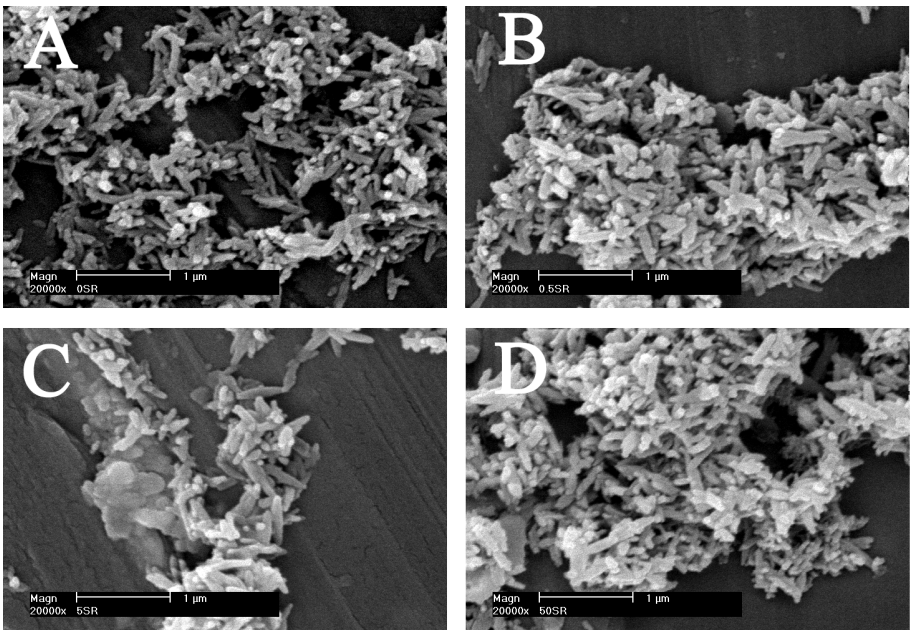

Figure 1. SEM images of apatites showing the obtained apatites are dispersed needle-like particles with a length shorter than 1µm. The morphology of all four apatites is similar, regardless with their Sr content. Scale bar: 1 µm

Scanning electron microscopy showed that the introduction of strontium did not provoke significant morphological changes to the apatite particles. The apatite was needle-shaped with a needle length shorter than 1μm (Fig. 1).

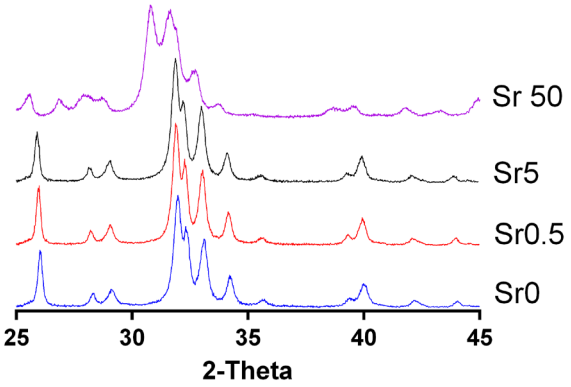

Figure 2. XRD patterns of the four apatites. Sr0, Sr0.5 and Sr5 showed patterns similar to HA while the diffraction peaks were broader and shifted towards lower 2θ values for Sr50

XRD pattern showed that the strontium-free apatite is typical HA (PDF#84-1998), and not much differences were seen for Sr0.5 and Sr5. With regard to Sr50, the diffraction peaks were broader and shifted towards lower 2θ values (Fig. 2). The 0.5% strontium-substituted apatite did not show obvious changes to the lattice parameters while the 5% and 50% strontium substitutions caused significant (p<0.001) extensions of the lattice parameters in both the a- and c-axes (Table 1). In addition, the crystallite size of Sr50 was dramatically reduced indicating an interrupted crystal growth in apatite with the Ca^{2+} replaced by the larger Sr^{2+}.

4.3.2 Physicochemical properties of strontium-containing apatite/polylactide composites

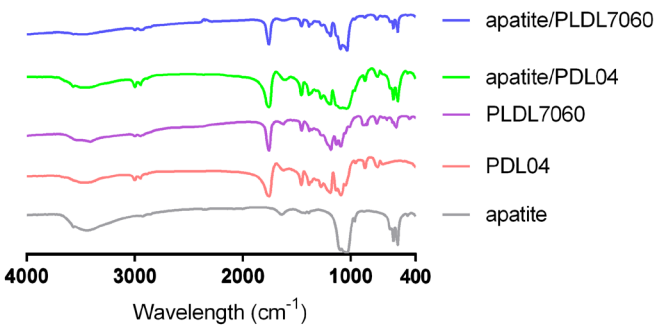

Figure 3. FTIR spectra for apatite, the two polymers (PLDL7060 and PDL04) and the resulting composites (apatite/PLDL7060 and apatite/PDL04). Only the two Sr-free composites were shown as the example of each group.

By comparing FTIR spectra of the apatite, the polymers and composites, it was observed that the vibrational bands of the composites included those of apatite (around 600 cm^{-1}) and those of polylactide (around 1100 and 1800 cm^{-1}), showing the successful introduction of apatite into the polymer matrices (Fig. 3).

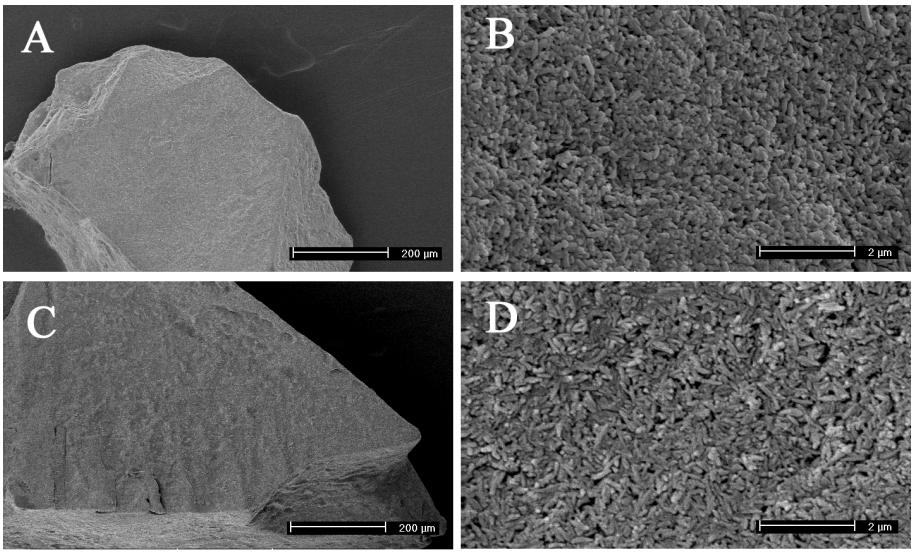

Figure 4. SEM images showing the surface morphology of apatite/PDL04 (A-B) and apatite/PLDL7060 (C-D). Scale bars: 200 µm (A, C), and 2 µm (B, D)

SEM evaluation of the composite granules showed that the apatite particles were uniformly distributed on the surface with a random orientation. A similar surface morphology was seen among all strontium-containing composites (Fig. 4).

A decrease in viscosity molecular weight was seen for both polylactides after extrusion with apatite. Particularly, PLDL7060 showed a dramatic reduction (>95%) in its viscosity molecular weight whereas PDL04 lost about 30%. The final viscosity molecular weights of the polymer phases in the PLDL7060 composites were slightly higher but comparable to that of the PDL04 group (Table 2).

Table 2. The viscosity molecular weight of the two polylactide used in the experiments

Polylactide	As supplied Mη (kDa)	Extruded with apatite Mη (kDa)
PDL04	57.0±1.3	41.4±1.4
PLDL7060	1512.3±3.8	51.9±1.4

4.3.3 Fluid uptake of the composites

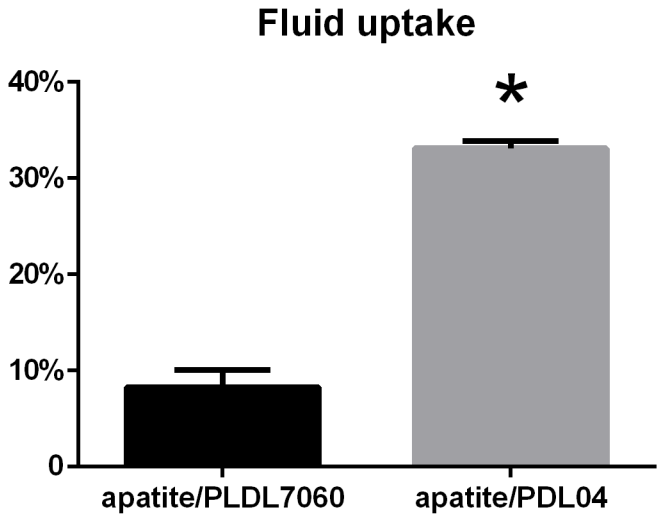

Figure 5. The fluid uptake of the two composites after 3-week immersion in SPS. *: $p<0.001$

After 3-weeks of immersion in SPS, the PDL04-based composites showed a significantly higher fluid uptake as compared to the PLDL7060-based composites (Fig. 5), which suggest a higher water affinity of PDL04.

4.3.4 Ion release from the composites

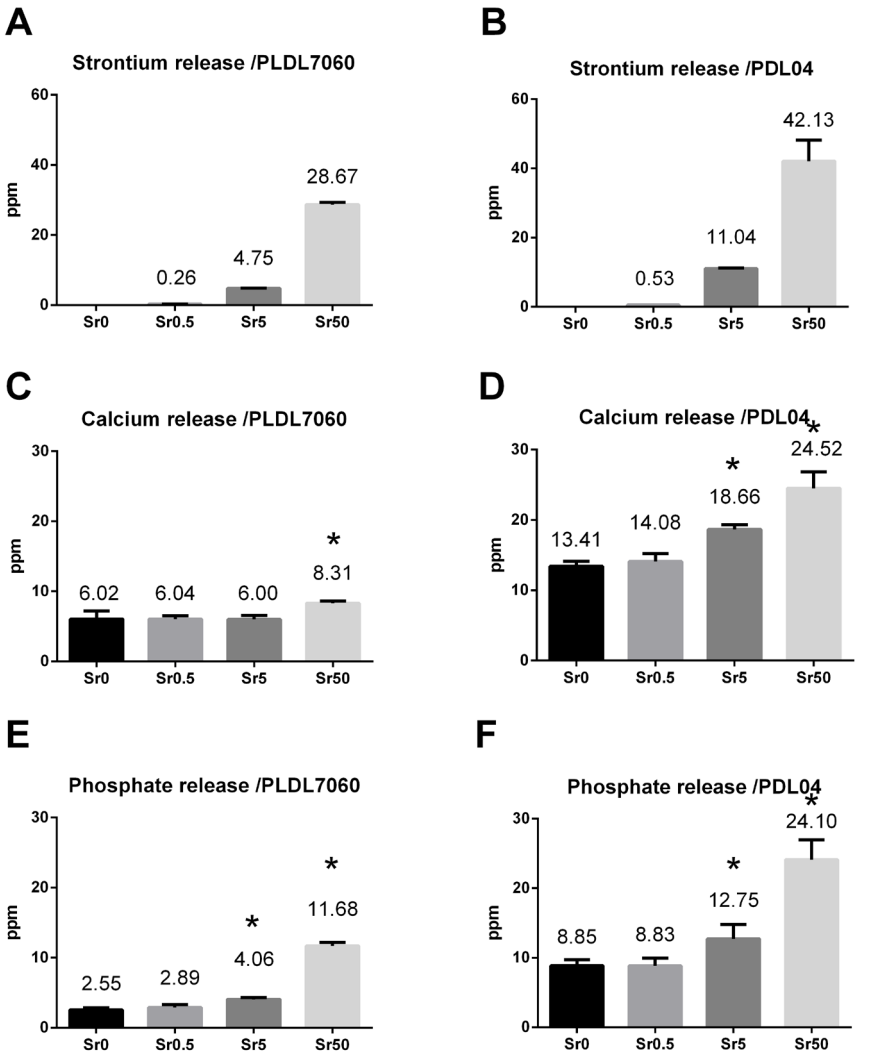

Figure 6. Ion release from PLDL7060-based (A, C, E) and PDL04-based (B, D, F) composites after 3-week immersion in SPS. The release of strontium (A, B), calcium (C, D) and phosphate ions (E, F) increased with the strontium substitution in apatite. The release of all the ions was lower from PLDL7060 group than PDL04 group. The strontium releases in each group were all significantly different with each other (A, B). * in C-F: $p<0.01$

The release of strontium ions from both composite groups significantly increased with their strontium content, while higher amounts were released from PDL04-based composites (Fig. 6A-B). In PLDL7060 based composites, the release of calcium was similar when the substitution of strontium in apatite was lower than 5%. The 50% strontium-substituted composites resulted in significantly higher calcium release (Fig. 6C, $p<0.05$). In contrast, the release of calcium ions from PDL04-based composites clearly increased with strontium content (Fig. 6D). Phosphate ion release increased along with the strontium content in both groups (Fig. 6E-F, $p<0.05$). Overall, the release of all ions was significantly higher from PDL04-based composites as compared to their PLDL7060-based counterparts, indicating that PDL04 allowed a higher dissolution of the embedded apatite than PLDL7060.

4.3.5 In vivo experiments

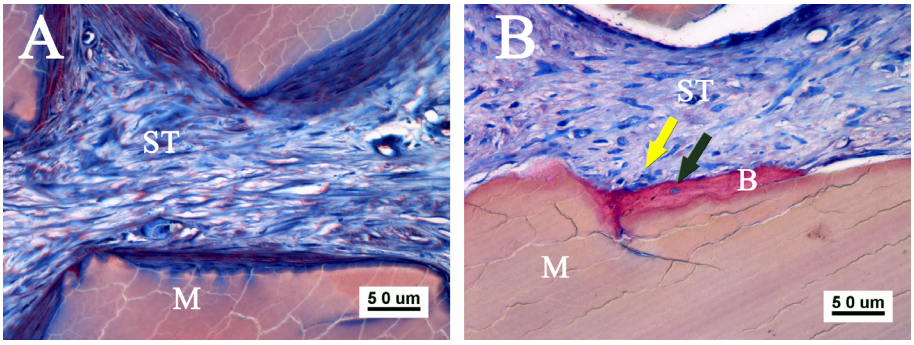

Figure 7. Histology images (non-decalcified, 1% methylene blue and 0.3% basic fuchsin staining) of 50Sr/PLDL7060 (A) and 50Sr/PDL04 (B) explants harvested from muscle longissimus of canines after 12 weeks. M, composite material; B, bone; ST, soft tissue; yellow arrow, osteoblast; black arrow, osteocyte

Table 3. The incidence of de novo bone in composite implants

Polymer \ Apatite	0Sr	0.5Sr	5Sr	50Sr
PLDL7060	0/8	0/8	0/8	0/8
PDL04	1/8	1/8	1/8	4/8

Histological observations showed no inflammation adjacent to the implants, while the composite granules had hardly resorbed in either group (Fig. 7). Bone was not formed in any of the PLDL7060-based composites, regardless of their strontium content (Fig. 7A). In contrast, de novo bone was observed among PDL04-based composites. Osteoblasts were seen secreting bone matrix, together with osteocytes located within mineralised bone (Fig. 7B). In addition, the incidence of de novo bone

formation was highest with the 50Sr/PDL04 composite (Table 3). The absolute amount of bone was however very limited in all PDL04-based implants (<1%), regardless of their strontium content.

4.4 Discussion

The release of calcium, phosphate and strontium ions from strontium-substituted nano-apatite/polylactide composites differed with the chosen polylactide matrix. PDL04 showed a higher degree of ion release and led to osteoinductive composites while having lower ion release composites of PLDL7060 did not show any bone formation. A dose dependent release of strontium was seen in both polylactide matrices, the combination of PDL04 with the highest degree of strontium-substituted apatite, i.e. 50Sr/PDL04, showed the highest incidence of de novo bone formation (Table 3).

The introduction of strontium in apatite altered various physicochemical parameters such as crystallite size and lattice parameters (Table 1 and Fig. 2). In particular, the extensions in both the a- and c-axes and crystallite size were significant when strontium had replaced half of the calcium ions (i.e. Sr50). This may be explained by the larger ionic radius of Sr^{2+} (1.13 Å) compared to Ca^{2+} (0.99Å), which could have perturbed the hindrance equilibriums in the apatite lattice [258]. In accordance to the decreased two-theta value and broader diffraction peaks in the XRD pattern (Fig. 2), the incorporation of strontium expanded the crystal lattice of apatite leading to a decreased stability and enhanced dissolution rate [153,179,259–261]. Consequently, strontium substitution did not only enhance strontium release (Fig. 6A-B), but also that of calcium (Fig. 6C-D) and phosphate (Fig. 6E-F), regardless of the polymeric matrix.

The composites with higher fluid uptake (i.e PDL04-based composites showed significantly higher ion release profiles (Fig. 5 and Fig. 6) suggesting a stronger fluid infiltration in the PDL04 matrix, which may have allowed a higher dissolution of the embedded apatite. Although the two polymers used in this study shared the same molecular formula $(C_6H_8O_4)_n$, they differed in their composition and viscosity molecular weight (Table 2). Due to the higher molar ratio of L-lactide units in PLDL7060, its chains may have contained some blocks of L-lactide, which could have formed semi-crystalline regions in the structure and this decreased its water absorption capacity [262]. In contrast, PDL04 is completely amorphous due to disordered polymer chains, indicating its high hydrophilicity [263]. Another parameter that might have influenced the water absorption of the two polylactide is their molecular weight. A decrease of the molecular weight during extrusion is observed for both PLDL7060 and PDL45, more pronounced for the latter (Table 2). This is in line with literatures, where it was suggested that both the thermal degradation of the polymer and frictional effects between the polymer and apatite particles during extrusion may have contributed to the rupture of polymer chains [185]. Further, PLDL7060 might have experienced a greater thermal degradation because of the

higher processing temperature (i.e. 205 °C). Nevertheless, the viscosity molecular weight of extruded PLDL7060 was still higher than that of PDL04, indicating that PLDL7060 has longer polymer chains. This might result in higher degree of twine around other chains thus the entangled network of macromolecules would become less mobile [104,264]. This may have contributed to the lower dissolution rate of the embedded apatite in PLDL7060 as well since the polymer matrix would be less prone to absorb water [265]. As a result, the release of strontium, calcium and phosphate was higher from PDL04-based composites than from PDL7060 (Fig.6).

The observed differences in bone forming incidence of the composite granules may have been the result of their different strontium, calcium and phosphate ion release profiles (Table 3, Fig. 6). Among the three ions, Sr^{2+} has been shown to enhance the osteogenic differentiation of mesenchymal stem cells and enhance in vivo bone formation [199]. We observed that the highest strontium-releasing composite, Sr50/PDL04, also showed the highest bone incidence. However, the observed bone induction cannot be solely attributed to strontium release as Sr50/PLDL7060 failed to induce bone formation, while it released considerable and similar amounts of strontium to the inductive composites (e.g. Sr5/PDL04 and Sr50/PDL04) (Fig. 6A-B, Table 3). It is therefore necessary to also consider the role of calcium and phosphate release in bone induction. Sr50/PDL04 released not only the highest amount of strontium ions but also the highest amount of calcium and phosphate ions. Both could therefore have affected osteogenic differentiation and bone mineral deposition [57,61,266]. Furthermore, in one out of eight implants the bone was triggered without strontium (Table 3). Taken together, it appears that the release of strontium from the materials cannot guarantee the formation of de novo bone and sufficient release of calcium and phosphate ions appears necessary for bone induction to occur. These results suggest that strontium may not be the essential osteogenic trigger in the current model and that calcium and phosphate release may also play an important role.

In particular, the role of calcium ions may be stressed as the composite, i.e. Sr50/PLDL7060, which released comparable or even higher amount of strontium and phosphate ions but less calcium as compared to the inductive composites (i.e. Sr0/PDL04 and Sr5/PDL04), is not osteoinductive at all (Fig. 6C-F). Aina *et al.* reported that the Sr-substituted HA increased the proliferation of osteoblast cells and enhanced cell differentiation but Sr ions alone at the concentrations released by Sr-HA (1.21–3.24 ppm) could not [141]. To further address the effect of ion release on bone formation at a cellular level, in vitro cell experiments should be performed in future studies.

The bone incidence and bone volume observed in the apatite/polylactide composite implants are lower than those previously reported by Barbieri *et al.* [105] and Hasegawa *et al.* [107]. In these studies, the composites were manufactured using either a solvent way or by co-precipitation, giving a porous structure to the implants,

which may have favoured cell attachment and ion accumulation [267]. Nonetheless, the current data suggest the potential of strontium-substituted apatite to enhance the bone forming ability of apatite/polylactide composites, while the selection of the polymer phase is of crucial importance.

4.5 Conclusions

After 12-week intramuscular implantation in canines, inductive bone formation was observed in PDL04-based apatite/polylactide composites but not in PLDL7060-based composites. In addition, the incidence of bone formation was higher in Sr50/PDL04 as compared to other strontium containing composites. These results indicate that polymer matrix composition impacts the release of calcium, phosphate and strontium ions, which in turn affects the bone forming ability of apatite/polylactide composites.

Acknowledgements

The authors would like to thank Purac Biomaterials BV (Gorinchem, the Netherlands) for kindly providing the polymers. The authors would like to acknowledge Biomedical Materials Program (BMM bone-IP), the Netherlands Institute for Regenerative Medicine (NIRM) and Rapid Prototyping of Custom-Made Bone-Forming Tissue Engineering Constructs (RAPIDOS Project, Ref. NMP-2013-EU-China 604517) for their financial support in this study.

Chapter 5

Strontium-containing apatite/poly-lactide composites favouring osteogenic differentiation and in vivo bone formation

Strontium-containing apatite/poly-lactide composites favouring osteogenic differentiation and in vivo bone formation

Xiaoman Luo [a,b], Davide Barbieri [a], Yunfei Zhang [c], Yonggang Yan [d], Joost D. Bruijn [a,b,e], Huipin Yuan [a,b,d,]*

[a] Xpand Biotechnology BV, Prof. Bronkhorstlaan 10, Bld 48, 3723MB Bilthoven, The Netherlands

[b] MIRA Institute, University of Twente, Drienerlolaan 5, 7522 NB Enschede, The Netherlands

[c] Chongqing Academy of Metrology and Quality Inspection, Yangliu North Road No.1, Yubei District, 401123, Chongqing, China

[d] College of Physical Science and Technology, Sichuan University, Wangjiang Road 29, 610064, Chengdu, China

[e] School of Engineering and Materials Science, Queen Mary University of London, Mile End Rd, London E1 4NS, UK

Abstract: Strontium was shown to enhance bone growth however its oral administration may lead to severe side effects. The application of strontium in orthopaedic biomaterials may therefore be an alternative to achieve targeted and sustained strontium treatment to the surgery site in aid of bone growth locally. In this study, strontium-containing composites were prepared by introducing various levels of strontium into amorphous apatite and extruding the obtained apatite powders into polylactide in a weight ratio of 1:1. Strontium substitution increased apatite dissolution and enhanced the degradation behaviour of the resulting composites. Sustained and dose-dependent strontium release from the composites was observed for up to 24 weeks in simulated physiological solution, indicating that strontium release can be tuned by its substitution level in the embedded apatite. Strontium-containing composites enhanced the osteogenic differentiation of murine mesenchymal stromal cells in vitro in a dose-dependent fashion. After heterotopic implantation with the combination of rhBMP-2, bone formation on strontium-containing composites was enhanced. These results suggest that strontium-releasing composites provide a local ion-rich (i.e. Sr^{2+} as well as Ca^{2+} and PO_4^{3-}) environment that favours osteogenic differentiation and in vivo bone formation.

Keywords: Strontium, composite, controlled release, osteogensis, in vivo.

Published in ACS Biomaterials Science & Engineering 2015, 1(2), 85-93

5.1 Introduction

Bone tissue is continuously being remodelled through a dynamic balance between osteoclastic bone resorption and osteoblastic bone formation. In diseases such as osteoporosis, this balance is shifted towards resorption. It has been reported that strontium (Sr), one of the trace elements present in bone, has a dual effect on bone metabolism by stimulating osteogenesis and inhibiting osteoclast resorption [40,79]. Strontium ranelate is therefore used clinically in osteoporotic patients to reduce bone fracture risks [202,268–271]. Its daily oral administration [269–271], however, has adverse side effects, leading to cardiovascular events, skin reactions and acute renal failure [272–279], and its usage was rigidly restricted by European Medicines Agency in 2014 [280,281].

Due to the aging of population, orthopaedic biomaterials will be used mainly in osteoporotic and elder patients with lower osteogenesis [153]. As this negatively influences their bone healing processes of the defect, additional stimulus such as strontium could be considered to facilitate the recovery of bone defect [282]. However, it is worth keeping in mind that the systemic side effect of strontium needs to be avoided. Hence implants that can provide in situ administration of strontium may be an alternative way to achieve a targeted treatment to the surgery site without inducing systemic effects, once the materials meet two criteria: (1) it could provide a continuous release of Sr^{2+}; (2) the concentration of released Sr^{2+} is sufficient to provoke local bone regeneration. To get such materials, the quantity of Sr and the release profile must therefore be controlled.

Due to the chemical similarities between Sr and Ca [161], Sr^{2+} can replace Ca^{2+} in calcium phosphate ceramics (e.g. tricalcium phosphate (TCP) [131,147], biphasic calcium phosphate (BCP) [283] and hydroxyapatite (HA) [153]) and subsequently be released when these materials dissolve in aqueous solutions [131,153]. As the Sr substitution of Ca can be obtained in a range varying from 0 to 100 mol % [53], which increases the solubility of the doped apatite [43], a sustained Sr release could be feasible.

Here, we synthesized composites of Sr-containing apatite and polylactide to create mechanically durable materials [104,185] that allow dissolution of the embedded apatite [185] and thus Sr release. We hypothesize that these composite materials could affect osteogenic differentiation and bone formation in vitro and in vivo. To test this, four apatites with different Sr substitution levels were synthesized and introduced in a polylactide matrix. After physicochemical characterization, Sr release was evaluated and its effect on osteogenic differentiation of murine mesenchymal stromal cells (mMSCs) was determined in vitro. To finely emerge the potential

enhancement of bone formation around implants and avoid the interfere from the spontaneous reparation of the host bone at the implantation site, we built a bony environment ectopically in rabbits, using recombinant human bone morphogenetic protein-2 (rhBMP-2). Composites loaded with equal amount of rhBMP-2 were heterotopically implanted in dorsal muscle of rabbit to assess the effects of Sr on the bone metabolism.

5.2 Materials and methods

5.2.1 Apatite and Sr-doped apatite synthesis

Pure apatite (i.e. Sr0) powder was synthesized by adding aqueous solution (concentration 63.12 g/L, 12.5 mL/min) of $(NH_4)_2HPO_4$ (Fluka, Germany) to aqueous solution (concentration 117.5 g/L) of $Ca(NO_3)_2{\cdot}4H_2O$ (Sigma) under continuous stirring rate of 500 ± 10 rpm and temperature of 80 ± 5 °C. The pH was kept above 10 by adding ammonia solution (Fluka, ~25 % NH_3, 17.5 mL/min) to the reaction vessel. For Sr-doped apatite, calculated amount of $Ca(NO_3)_2{\cdot}4H_2O$ (Sigma) was replaced with $Sr(NO_3)_2$ (Sigma) to obtain apatite with 0.5 % (atomic ratio) (i.e. Sr0.5), 5 % (i.e. Sr5) and 50 % (i.e. Sr50) Sr substitution. After all solutions were completely added together, the suspensions were kept at 80 ± 5 °C with stirring for further two hours. The precipitates were aged overnight, washed with distilled water until the complete removal of ammonia and suspended in acetone (Fluka) repeatedly to dehydrate. Then the powders were vacuum-filtered and dried at 60 ± 5 °C for 48 hours.

5.2.2 Preparation of apatite/polylactide composites

The powders previously obtained were sieved with 212 μm mesh and extruded at the weight ratio of 1:1 with poly(D,L-lactide) (PDL04, IV midpoint 0.4 dL/g, Purac Biomaterials BV, The Netherland) respectively to obtain four composites of CT (control, PDL04 with Sr0), SrL (PDL04 with Sr0.5), SrM (PDL04 with Sr5) and SrH (PDL04 with Sr50). The extrusion was carried out using a Micro Rheology twin screw compounder (HAAKE™ MiniLab II, Thermo Scientific™) at 130 ± 1 °C with screw speed set at 100 ± 1 rpm for 5.0 ± 0.5 min. The extruded stripes were then grinded (ZM100, Advantec, Japan) and sieved to obtain granules with size range of 0.5-1 mm. Afterwards the granules were ultrasonically cleaned in distilled water for 15 ± 1 min at room temperature and dried at 37 ± 1 °C. All specimens were sterilized with ethylene oxide (concentration = 450–700 mg/L, followed by washes with nitrogen / air and a 7-day aeration, IsoTron Nederland BV, the Netherlands) and used for all the experiments described in this study.

5.2.3 Characterization of apatite and composites

Chemical analysis of the obtained apatite powders was conducted using X-ray diffractometer (XRD, MiniFlex II, Rigaku) using Cu Kα radiation (λ = 1.5405 Å, 30 kV, 15 mA) over the 2θ range of 25° – 45°. Unit cell parameters and crystallite sizes were calculated from XRD data using the software Jade (v6.5.26, Materials Data Inc., Livermore, CA, USA). High resolution transmission electron microscopy (HR-TEM, FEI Tecnai-200FEG, FEI Europe, Eindhoven, the Netherlands) and fast Fourier transform (FFT) was employed to investigate the morphology of apatite particles and the interplanar spacing (d-value) of the four apatites along the reflection plane (010). Using an energy dispersive X-ray spectroscopy (EDX) equipped on the HR-TEM, The experimental Sr substitution in obtained apatite was evaluated and compared with the theoretical values, which were calculated basing on the formula of $Ca_{(5-x)}Sr_x(PO_4)_3OH$ where x=0 for Sr0, x=0.025 for Sr0.5, x=0.25 for Sr5 and x=2.5 for Sr50. Fourier transform infrared spectrometry (FTIR, Spectrum 1000, Perkin Elmer) was used to characterize the apatite powders, poly(D,L-lactide) and their resulting composites with a typical KBr pellet technique. The morphology of composites was analyzed using a scanning electron microscope (SEM, XL 30 ESEM-FEG) to evaluate the microstructure of composites.

5.2.4 In vitro degradation of composite granules

Simulated physiological solution (SPS) was prepared by dissolving sodium chloride (NaCl, Merck, concentration = 8 g/L), sodium azide (NaN_3, Merck, concentration= 0.01 g/L) and 4–(2–hydroxyethyl)–1–iperazineethane–sulfonic acid (HEPES, Sigma, concentration = 11.92 g/L) in distilled water. The pH of the solution was adjusted to 7.3 with NaOH solution (Merck) at 37 °C. Amounts of 0.05 ± 0.001 g (M_0) granules of each composite (in triplicate) were weighed and soaked in 20 mL SPS at 37 ± 1 °C. The SPS was refreshed after 1, 3, 6, 9 and 12 weeks. At every refreshing time point, the concentration of calcium and phosphate ions in SPS was measured by using appropriate biochemical kits (QuantiChromTM calcium assay kit, BioAssay Systems, USA; PhosphoWorksTM Colorimetric phosphate assay kit blue colour, BioquestInc, USA) and a spectrophotometer (Anthos Zenyth 3100, AnthosLabtec Instruments GmbH, Salzburg, Austria) with an absorbance filter of 620 nm for both assays. The concentration of Sr^{2+} released in SPS was measured using inductively coupled plasma atomic emission spectroscopy (ICP-AES, DV7000, Perkin Elmer, USA) at the emission peaks of 407.771 nm and 421.552 nm. After 1, 3, 6, 9, 12 and 24 weeks, composite granules were removed from SPS, the excess SPS was wiped away gently with filter paper. Afterwards, they were dried at 37 ± 1 °C, weighed (M_{dry}) and compared with the initial weight (M_0). The mass loss of the composite (ML%) was

determined as: ML% = 100*(M_0-M_{dry})/M_0. Afterwards, dried composite granules of each sample were sintered at 900 °C for two hours to burn away the polymer phase. The mass of the remaining apatite ash was weighed (M_{ash}). The changes of the mass loss of apatite phase (AL%) and the mass loss of polymer phase (PL%) in the composite were estimated as: AL% = 100*(M_0*0.5-M_{ash})/(M_0*0.5); PL% = 100*[M_0*0.5-(M_{dry}-M_{ash})]/(M_0*0.5)

5.2.5 Murine mesenchymal stromal cells culture

Murine mesenchymal stromal cells (mMSCs, D1 ORL UVA, ATCC® Number: CRL-12424) were purchased (ATCC, Manassas, VA, USA). After thawing from liquid nitrogen, cells were expanded in culture flasks (Greiner Bio-one) with growth medium composed of Dulbecco's Modified Eagle Medium (DMEM, catalog 41965, Gibco) supplemented with 10 % fetal bovine serum (FBS, catalog 10270, Invitrogen), 100 IU mL^{-1} Penicillin, 100 µg mL^{-1} Streptomycin (catalog 11558876, Invitrogen, UK) and 1mM sodium pyruvate (Sigma, catalog D2650) under a humidified atmosphere of 5 % CO_2 at 37 °C. The medium was refreshed twice a week until cells reached 70~80% confluence. Then cells were harvested with 0.25 % trypsin (catalog 11570626, Invitrogen). Then 5 * 10^3 cells were cultured on 50 mg granules (n=5 per material for each time point) with 200 µL growth medium per well in 96-well plate (Ref 655101, Greiner Bio-one) for up to 21 days. The medium was refreshed twice a week until day 14 and afterwards every two days. Samples were harvested after 1, 4, 7, 14 and 21 days for SEM observation and bioassay.

5.2.6 Proliferation assay of mMSCs

At every harvest time point, cells were rinsed once with 37 °C phosphate buffered saline (PBS) and then frozen at -80 °C for 24 hours. Afterwards they were thawed, 150 µL CyQuant lysis buffer were added to each well and shook at 400 rpm for five min to obtain the cell lysate. The proliferation of mMSCs was measured using a CyQuant cell proliferation assay kit (Invitrogen) following the manufacturer's instructions. Briefly, GR reagent was diluted 400 times in CyQuant lysis buffer. Then 100 µL diluted reagent was mixed with 100 µL cell lysate and further incubated in dark at room temperature for five min. Then the fluorescent analysis was performed at wavelength of 480 nm for excitation and 520 nm for emission using a spectrophotometer (Anthos Zenyth 3100).

5.2.7 Osteoblastic differentiation of mMSCs

Alkaline phosphatase (ALP) activity was evaluated using AttoPhos® AP fluorescent substrate system (catalog S1000, Promega) and presented as the amount of 2-[2-benzothiazoyl]-6-hydroxybenzothiazole (BBT) produced during the reaction. The

same cell lysate prepared for DNA assay was used. Briefly, 10 µL cell lysate was added to 90 µL substrate reagent and incubated for 15 min in dark at room temperature. The fluorescence signal was then collected at 450 nm for excitation and 580 nm for emission using a spectrophotometer (Anthos Zenyth 3100).

5.2.8 Intramuscular implantation

All surgeries were conducted in Sichuan University. Local animal ethics committee guidelines (Regulations for the administration of affairs concerning experimental animals, China, 1988) for the care and use of laboratory animals have been observed. Composite granules of each material were prepared in one cubic centimetre aliquots under sterile conditions and loaded with 300 µL demineralized water containing 10 µg rhBMP-2 (Reborn, Shanghai). The adsorption of the protein was allowed for one hour in stillness. Granules were then dried in sterile fume hood for 48 hours at room temperature. 1 CC aliquots were then kept in sterile glass vials respectively. Five 6-month old female New Zealand white rabbits (body weight 3.5 ± 0.2 kg) were used. After a general anaesthesia by the injection of sodium pentobarbital (30 mg/Kg body weight, Sigma) in the marginal ear vein, muscle pouches were created in the paraspinal muscle along the direction of the spine by scalpel incision and blunt dissection. The distance between each pocket was about 1~2 cm. The composite aliquot was transferred into an open-head 2 mL syringe for the ease of handling. The open side of the syringe was inserted in the pocket and the granules were pushed out gently. The pockets were then closed with non-resorbable sutures for identification at harvest. Following the surgeries, penicillin (100000 IU/kg body weight) was given for three consecutive days to prevent infection. After operation, animals were allowed full weight bearing and received normal diet. They were sacrificed 4 weeks later with a marginal ear vein injection of excessive amount of sodium pentobarbital (Sigma).

5.2.9 Histology and histomorphometry

Explants were fixed with 4 % formaldehyde and embedded in PMMA after gradient ethanol dehydration. Non-decalcified sections were made sequentially (i.e. section thickness ≈ 15 µm and step-size ≈ 280 µm which is the thickness of the blade) for each explants from one side to the other using a diamond saw microtome (Leica SP-1600, Germany) and stained with 1 % methylene blue (Sigma) and 0.3 % basic fuchsin (Sigma). About 15 slides were obtained from each explant. Histological observation was performed with light microscopy. All slides were scanned with a scanner (Dimage Scan Elite5400 II, Konica Minolta, USA). Histomorphometry was performed on each slide by pseudo-colouring pixels representing formed bone (B) in available space, i.e. the space between composite granules (M) in the region of

interest (ROI, with surrounding soft tissues outside the implants excluded) using Photoshop (Adobe Photoshop Elements 2.0). The pixels of B, M and ROI of each slide were stacked together to have an overall estimation of each explant. Bone formation (B %) was calculated as: B%= 100*∑B/ (∑ROI-∑M). Area of materials (M %) was calculated as: M%= 100*∑M/∑ROI

5.2.10 Statistical analysis

Statistical analysis was carried out using one-way analysis of variance (ANOVA) with Tukey's test. Differences were considered statistically significant at $p<0.05$ and marked with asterisks.

5.3 Results

5.3.1 Characterization of Sr-doped apatites and composites

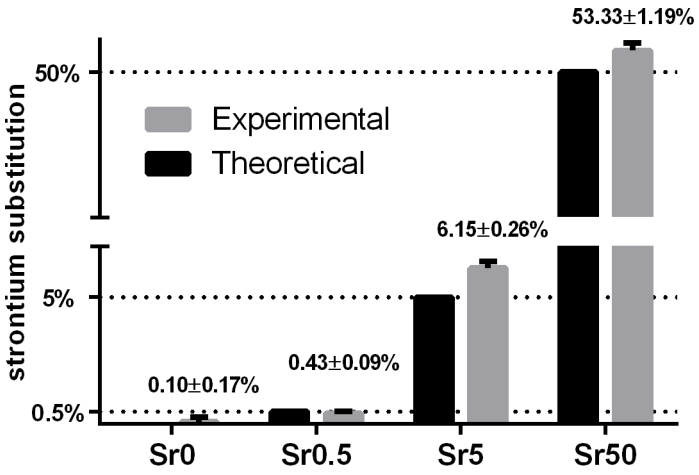

Figure 1. The content of strontium in obtained apatites. EDX data confirmed the obtained apatites had Sr substitution similar to the theoretical values.

EDX results verified the Sr substitution in apatite and the values were shown to be close to the theoretical expectation (fig.1).

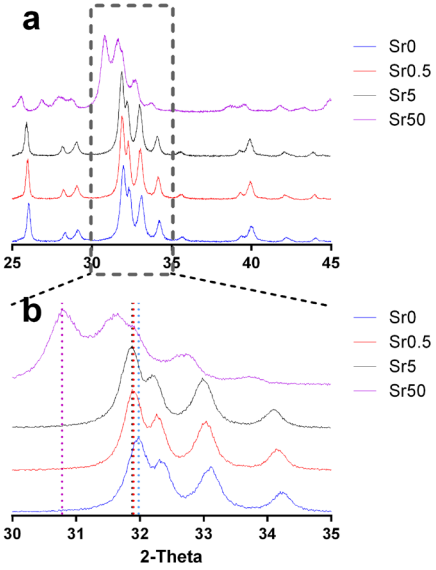

Figure 2. XRD patterns of obtained strontium-containing apatite (**a**), the enlargement of **a** over a narrower 2θ range from 30° to 35° (**b**). The spectra shifted towards lower 2θ values with the substitution of strontium (from bottom to top: Sr0, Sr0.5, Sr5, Sr50.) The diffraction peaks of 50Sr were also broader.

XRD pattern of pure apatite was identical to standard HA (PDF#84-1998) while increasing shifts towards lower 2θ values with the substitution of Sr were noticed when spectra were collected on a narrower 2θ range (fig.2b). The diffraction peaks of 50Sr were also broader, indicating a lower degree of crystallinity when the larger Sr^{2+} (radius = 0.118 nm) replaced half of Ca^{2+} (radius = 0.100 nm) [38].

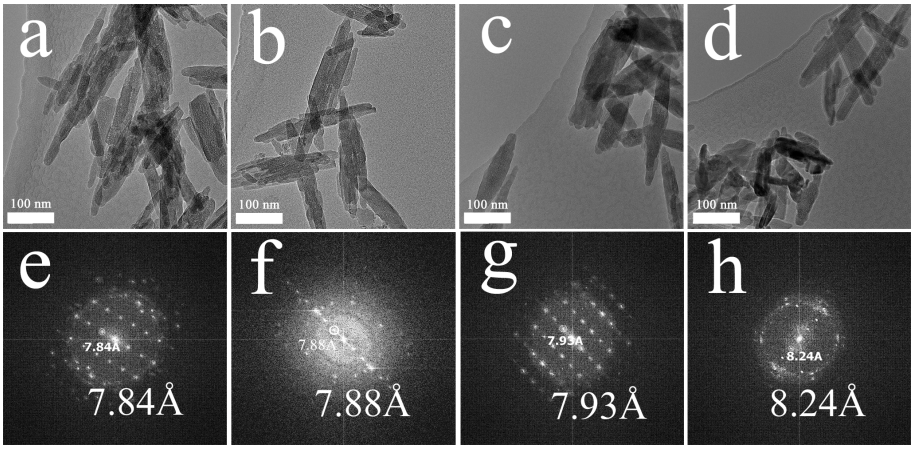

Figure 3. TEM images of Sr0 (**a**), Sr0.5 (**b**), Sr5 (**c**) and Sr50 (**d**). All the particles were nano-sized and had needle-like shape. Particles of 50Sr were relatively shorter in length. The interplanar spacing obtained from FFT applied to HR-TEM along the plane (010) increased with strontium substitution (**e**~**h**).

The morphology of apatite powders was visualized by TEM, and all particles were nano-sized and had needle-like shape (fig.3a-d). Particularly, particles of 50Sr were relatively shorter in length as compared to the others (fig.3d). The interplanar spacing (d-value) obtained from FFT applied to HR-TEM along the plane (010) increased with Sr substitution (fig.3e-h), reflecting the expansion of lattice structure during the substitution. This was corroborated by the decreased two-theta value of Sr-substituted apatite in XRD of the (010) plane (fig.2).

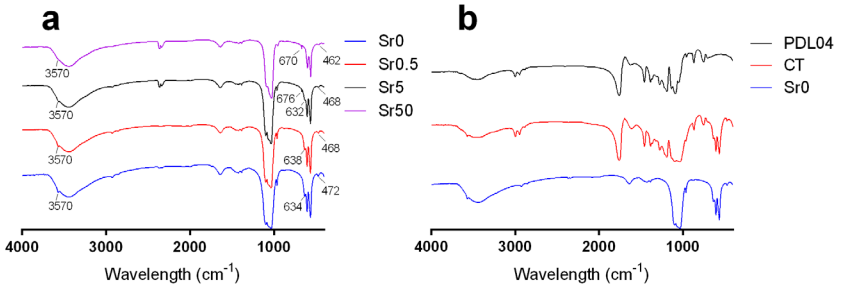

Figure 4. FTIR patterns of strontium-containing apatite (**a**) and the resulting composites (**b**, CT was taken as an example). The pattern of pure polymer PDL04 was also shown in **b** to clarify the presence of apatite and polymer in the composite.

Figure 4a shows the FTIR spectra of apatite powders, which had similar phosphate group modes near 1000-1100 cm^{-1}. The intensity of O-H band (near 634 cm^{-1} and 3570 cm^{-1}) decreased with the Sr content, indicating the alteration in the bonding strength of O-H during substitution [283]. A tiny peak appeared around 670 cm^{-1} with the Sr content indicating their trace possession of carbonate ion [284]. The bands around 470 cm^{-1} became obscure in 50Sr, which can be ascribed to potential alternation of PO_4^{3+} groups when the substitution of Sr reached 40 % [141]. The FTIR spectra of composites (CT was taken as an example) included the vibrational bands of both apatite and polymer (fig.4b), confirming the successful preparation of composites.

SEM images showed that the surface of the granules of all four composite had similar morphology, in particular it was generally flat at the cellular scale (i.e. >10 μm) (fig.5a-d). When the morphology was examined at a sub-micro scale, embedded apatite particles were exposed on the surface of the granules with random orientations (fig.5e-h). This qualitatively shows the homogenous distribution of apatite in the polymer matrix, and demonstrates the comparable surface morphology of all composites.

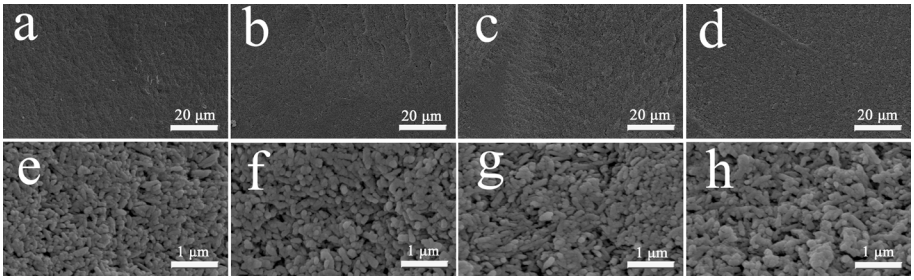

Figure 5. SEM images of CT (**a**, **e**), SrL (**b**, **f**), SrM (**c**, **g**) and SrH (**d**, **h**); the surface morphology of composite was similar on both micro- and sub-micro scale. Apatite particles were observed with random orientation on the surface of composite granules.

5.3.2 Ion release and degradation behaviour of composite granules

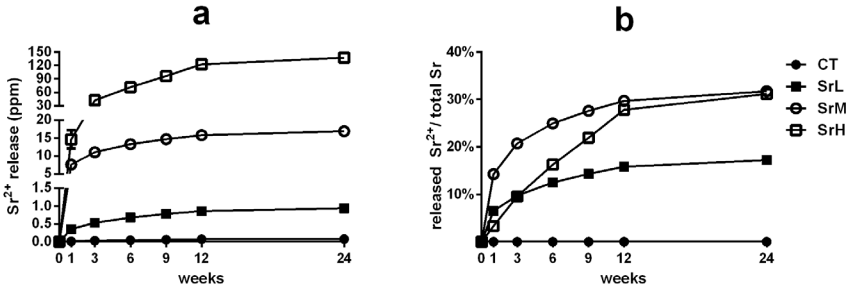

Figure 6. a: Strontium release profiles from strontium-containing composites. The amount of strontium release was dose-dependent according to their content in embedded apatite and differed from each other during 24 weeks. Note that the y-axis of the graph is cleaved to exhibit all profiles visibly. **b:** The total percentage of strontium released from the composites. The releasing rate of strontium changed from parabolic to almost linear for SrH composite.

The amount of Sr release increased dose-dependently according to the Sr content in the embedded apatite (fig.6a). Furthermore, the proportional release rate was elevated by the Sr content, e.g. SrL released nearly 10 % of its Sr content during the first 3 weeks while SrM released more than 20 % (fig.6b). The release rate of SrL and SrM then decreased gradually, slower for the latter. When the substitution level reached 50 %, the releasing rate became almost linear for the first 12 weeks (fig.6b), numerically about 10 mg per week, which is about 2.3 % of total Sr in SrH. Both the amount of calcium and phosphate release from the composites gradually increased

with the Sr content (fig.7a, b), indicating that the substitution of Sr^{2+} towards Ca^{2+} up-regulated the solubility of apatite. The periodic refreshment was not continued after 12 weeks and the releasing rate from all sample decreased.

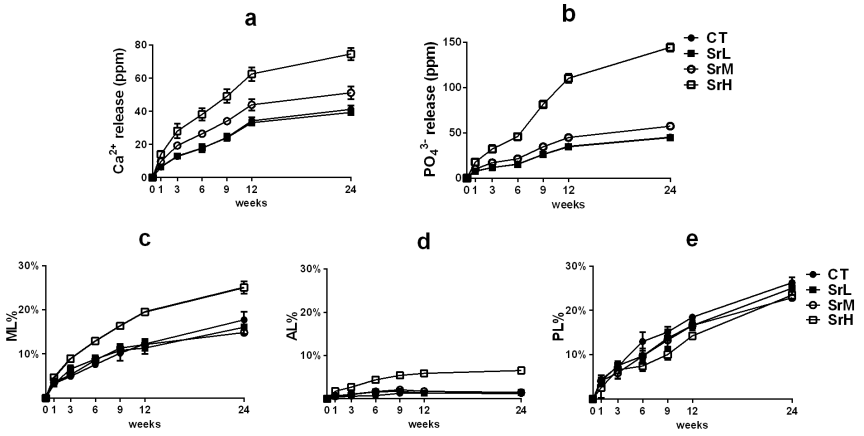

Figure 7. Calcium and phosphate release from strontium-containing composites (**a**: Ca^{2+} and **b**: PO_4^{3-}) and the mass loss of composites (**c**: total mass loss, **d**: apatite phase loss and **e**: polymer phase loss). The strontium substitution gradually increased calcium and phosphate release from the composites, indicating an up-regulated solubility of strontium-substituted apatite. Polymer phases in all composites followed similar degradation profile but SrH had faster apatite dissolution than other composites, leading its higher total mass loss.

Mass loss was observed one week after the composite granules were immersed in SPS (fig.7c). However, only SrH had higher mass loss than the rest. When the two phases of composites were considered separately, it was seen that the polymeric phase in all composites degraded similarly (fig.7e), while SrH had much higher apatite phase loss than others (fig.7d).

5.3.3 In vitro cell culture experiments

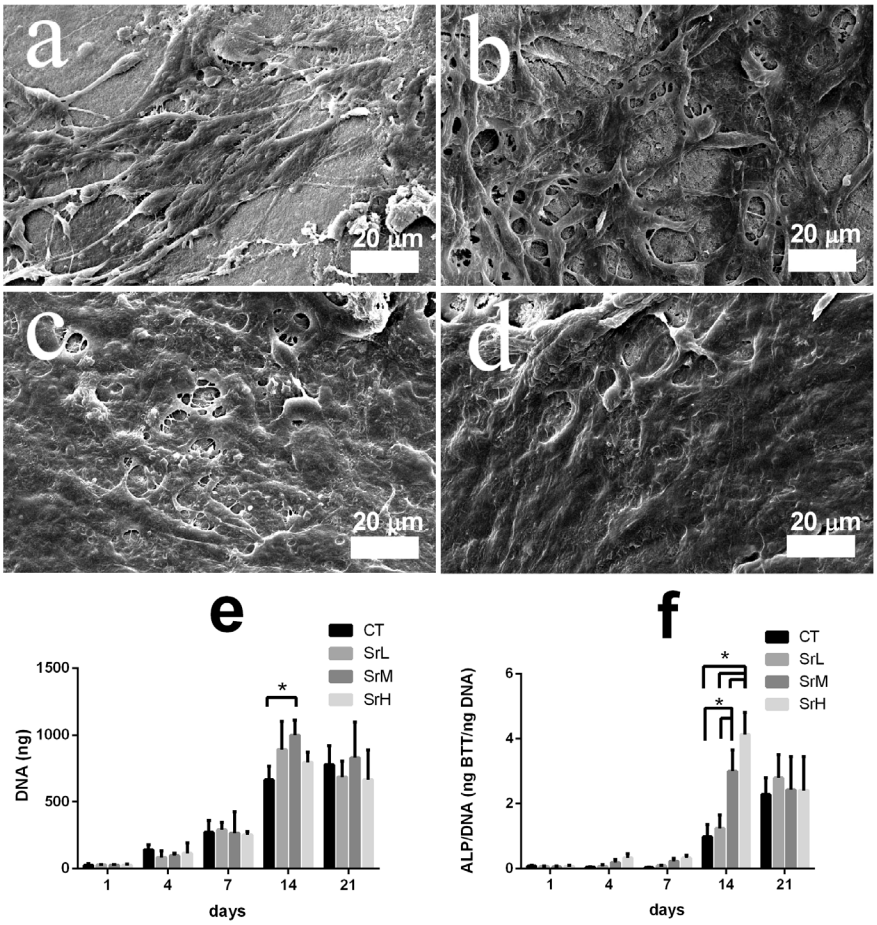

Figure 8. mMSCs cultured on strontium-containing composites. The morphology of mMSCs on CT (**a**), SrL (**b**), SrM (**c**) and SrH (**d**) after a 14-day culture; **e**: cell proliferation of mMSCs on strontium-containing composites as shown with DNA production; **f**: osteogenic differentiation of mMSCs on strontium-containing composites as shown with the ALP/DNA ratio. At 14 days, the proliferation of mMSCs on SrM was higher than that on CT (p<0.01) while mMSCs on SrM and SrH had higher osteogenic differentiation than those on samples with less Sr content (p<0.02). One-way ANOVA with Tukey's test was used for the statistics analysis.

mMSCs on all composite granules had fibroblast-like shape (fig.8a-d) and formed layer colonies after confluence, showing the adhesion and spreading of mMSCs on composite granules. The proliferation of mMSCs on the different composites had similar trends until day 7. By day 14, cell proliferation peaked and was significantly higher on SrM than Sr-free composite (fig.8e, $p<0.01$). Afterwards, proliferation declined, indicating that the cells had reached confluence. Although no osteogenic inducers, i.e. ascorbic acid, dexamethasone, and β-glycerophosphate, were employed in this study, a correlation between the Sr content and ALP/DNA value was observed after 14 days of culture (fig.8f). Particularly, mMSCs on SrM and SrH showed higher osteogenic differentiation than those on samples with less Sr content ($p<0.02$), indicating the potential of Sr in promoting the osteogenesis of stem cells.

5.3.4 In vivo experiments

Evidential bulk degradation or cell-mediated resorption of implants was not observed from histological observation (fig.9). It was then quantitatively confirmed by means of M %, showing that the granules occupied around 60 % of the implants through all section slides, with no significant differences between Sr-containing composites and Sr-free control, indicating a similar (or no) resorption of all composites after four-week implantation (fig.10a). Histological observations showed no inflammation adjacent to the implants. Bone was formed on the surface of the granules, where bone forming osteoblasts were seen on site and osteocytes were embedded in the bone matrix (fig.9). Histomorphometry data showed an increasing trend of bone formation with the increase of Sr content in composites, where significant difference was observed between SrH and CT ($p<0.05$, fig.10b).

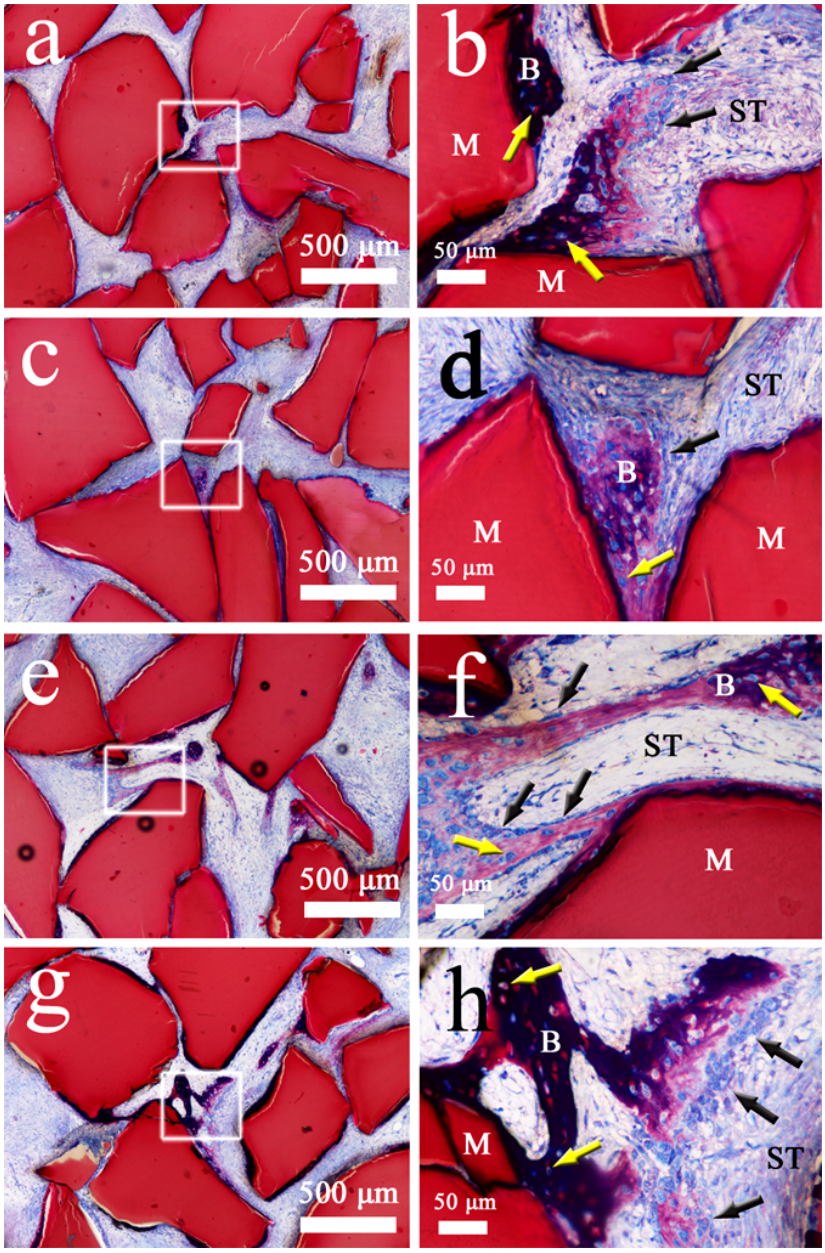

Figure 9. Histological observations of strontium-containing composites after 4-week intramuscular implantation in rabbit: CT (a, b), SrL (c, d), SrM (e, f) and SrH (g, h). Each image in the right column represents the enlargement of the inset white square in the left image. M: material; B: bone; ST: soft tissue; black arrow: osteoblast; yellow arrow: osteocytes.

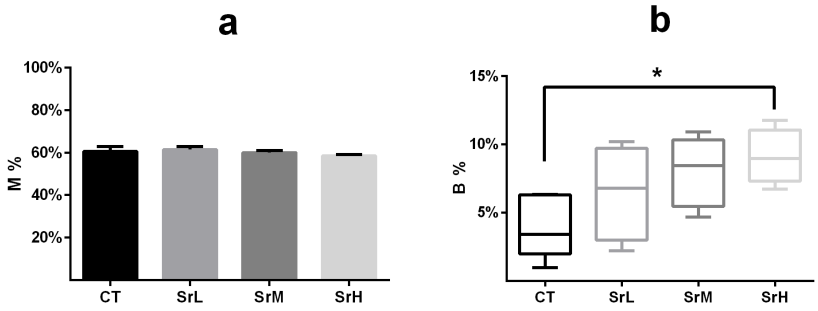

Figure 10. Area of composite materials in implants after 4 weeks (**a**) was similar for all implants. An increasing trend of bone formation along with the Sr content was observed where significantly more bone was formed in SrH as compared to CT (**b**, $p<0.05$) indicating the addition of strontium in composites created a local environment that might favour bone formation. One-way ANOVA with Tukey's test was used for the statistics analysis.

5.4 Discussion

The results of this study show that Sr-rich composites provide sustained strontium release and enhance osteogenic differentiation of murine MSCs in vitro. The introduction of Sr also lead to enhancement of bone formation in the ectopic model investigated in this study. The overall bone formation is modest, which might be attributed to the relatively short time for bone formation (4 weeks), the relatively low BMP-2 dose used and the low osteogenic capacity of the animal model (rabbits) [215,251]. However, increasing Sr content led to more bone formation, where SrH composite outperformed CT by at least 40 % ($p<0.05$, fig.10b). Since equal amounts of rhBMP-2 were used, the observed increase in bone volume in Sr-containing composites may be attributed to Sr doping in composites. Although most likely Sr-containing composites may not give rise to inductive bone formation in ectopic sites of rabbits according to literature [285,286], the lack of implants without rhBMP-2 in this study could not exclude the possible osteoinductive potential of strontium. Therefore, including such group without rhBMP-2 may further address the possible synergic effects of rhBMP-2 and strontium in bone formation, thus it would be an orientation of future studies.

It was observed that the release of Sr from the composites was dose-dependent, which significantly increased according to the Sr content in the embedded apatites (fig.6a). However, the proportional release rate was not consistent from SrL and SrM,

where a burst release was observed in the first week, followed by a gradual decrease over time (fig.6b). This decrease was ameliorated by the increase of Sr content in apatite (fig.6b). As a combined effect of Sr content and apatite dissolution rate, the sustained release profile of SrH was approximately linear for 12 weeks under intermittent medium refreshments (fig.6b). This indicates that, by adjusting the substitution level of Sr in embedded apatite, a desired consistent and stable release profile of Sr can be obtained [79,152,287]. This release is expected to last longer than 24 weeks as 65 % of Sr still remained in the composites at 24 weeks (fig.6b).

The dissolution of Sr-containing apatite is expected to create a local Sr-rich environment that may favour osteogenesis. Naturally, higher osteogenic differentiation would lead to greater population of cells with osteoblastic phenotype and thus to more secretion of bone [256]. Our results showed that mMSCs on composites with higher Sr content had significantly higher osteogenic differentiation, without the addition of osteogenic inducers, indicating that material-induced osteogenesis occurred (fig.8f). It has been reported that the implantation of Sr-containing materials promotes bone repair in both normal [140,151] and ovariectomized animals [122,148,149], which indicates the potential of this strategy in enhancing bone fracture healing [81]. In addition to its positive effect to bone formation, sufficient Sr release may also preserve bone mass by inhibiting osteoclastic resorption [40,79], especially after a longer period of implantation (e.g. > 8 weeks) [288–291]. This effect was not conclusively shown in this study as no multinucleated giant cells were observed microscopically.

Other factors such as the release of Ca^{2+} and PO_4^{3-}, may also have played a role in the observed in vitro and in vivo effects [81]. During Sr-substitution, Ca^{2+} in apatite were partially replaced by Sr^{2+} and their content decreased accordingly. However, the enhanced solubility of Sr-containing apatite led to higher release of Ca^{2+} and PO_4^{3-} (fig.7a,b), which are known to regulate osteoblastic differentiation and activity in vitro [56–58,292]. It was suggested that the substitution of Ca^{2+} by Sr^{2+} causes a lattice expansion due to the larger atomic radius of Sr^{2+} thus alters the solubility of strontium-substituted apatite [179,260]. This is supported by the observation of expanded diffraction peaks and interplanar spacing (figure 2 and 3) and is in accordance with many previous studies [153,179,259,260] . Here the release of Sr^{2+}, Ca^{2+} and PO_4^{3-} are interrelated, making it difficult to ascribe the biological up-regulation to Sr only [166]. However, given the fact that the calcium and phosphate concentration in extracellular fluid is tightly maintained at a constant level [293,294], the effect of spontaneous calcium and phosphate release from implants might be of less impact than Sr on local bone metabolism.

5.5 Conclusions

Composites that can provide long-term dose-dependent and sustained Sr release profile were obtained by adjusting the substitution level of Sr in the apatite embedded in the polymeric matrix. The addition of Sr in composites enhanced osteogenic differentiation of mMSCs in vitro and promoted in vivo bone metabolism in the created bony site.

ACKNOWLEDGMENT

The authors acknowledge financial support from the European Commission (Integrated Infrastructure Initiative ESSTEEM, Ref. 026019 ESTEEM) and Dr. Xu from Delft University of Technology for his contribution in TEM characterization. The authors would like to thank Purac Biomaterials BV (Gorinchem, the Netherlands) for kindly providing the polymers, and acknowledge Biomedical Materials Program (BMM bone-IP), the Netherlands Institute for Regenerative Medicine (NIRM) and Rapid Prototyping of Custom-Made Bone-Forming Tissue Engineering Constructs (RAPIDOS Project, Ref. NMP-2013-EU-China 604517) for their financial support.

Chapter 6

Strontium-containing apatite/polylactide composites enhance bone formation in osteopenic rabbits

Strontium-containing apatite/polylactide composites enhance bone formation in osteopenic rabbits

*Xiaoman Luo [a,b], Davide Barbieri [a], Rongquan Duan [b], Huipin Yuan [a,b,c] *, Joost D. Bruijn [a,b,d]*

[a] Xpand Biotechnology BV, Prof. Bronkhorstlaan 10, Bld 48, 3723MB Bilthoven, The Netherlands

[b] MIRA Institute, University of Twente, Drienerlolaan 5, 7522 NB Enschede, The Netherlands

[c] College of Physical Science and Technology, Sichuan University, Wangjiang Road 29, 610064, Chengdu, China

[d] School of Engineering and Materials Science, Queen Mary University of London, Mile End Rd, London E1 4NS, UK

Abstract: Strontium (Sr) has been shown to favour bone formation and is used clinically to treat osteoporosis. We have previously reported that Sr addition in apatite/polylactide composites could enhance the BMP-induced bone formation around implants at ectopic site in healthy animals. In this study we aimed to investigate the effectiveness of Sr addition on the local bone formation in osteoporosis. Apatite/polylactide composite granules with different Sr content were loaded with equal amount of rhBMP-2 and implanted intramuscularly in healthy rabbits (Con) and rabbits that received bilateral ovariectomy and daily injection of glucocorticoid (OP) for 12 weeks. The potential effect of Sr on the final volume of BMP-induced bone in both groups was investigated histologically and histomorphometrically. The de novo bone formed in OP implants was significantly less than in Con group when the implants contained no Sr, indicating that the BMP-induced osteogenesis was impaired in OP animals. Sr substitution as low as 0.5 mol% in apatite increased the bone volume in OP implants to levels comparable to that in the Con group, indicating a positive effect of Sr addition on the local bone formation in OP animals. In addition, more adipose tissue formed in parallel with the appearance of cartilage tissue in OP implants, suggesting that the differentiation potential of stem cell in OP animals may have shifted towards adipogenesis and chondrogenesis. From these results, we conclude that the use of Sr addition to enhance the bone growth surrounding implants in osteoporosis merits further study.

Keywords: strontium, bone formation, osteoporosis, composites, adipocytes, cartilage

Published in Acta Biomaterialia 2015, Vol 26, p331-337.

6.1 Introduction:

Bone is continuously renewed through a balance between osteoblastic bone formation and osteoclastic bone resorption. With aging, this balance leans towards bone resorption leading to a loss of bone mass, i.e. osteopenia, which may eventually develop into osteoporosis and result in a higher fracture risk [295]. It has been reported that the bone healing capacity of osteoporotic patients is less effective as compared to healthy individuals, which might result in poor osteointegration and surgical failure in case implants are placed [153,296,297]. Therefore, it is worthy to consider the use of additional stimulus such as trace elements in orthopaedic implants to facilitate the local growth of bone [282].

Strontium (Sr) has been reported to enhance the osteoblast differentiation and inhibit osteoclast formation and resorption [79,290]. Therefore implants that provide sustained treatment of Sr are expected to locally stimulate the bone growth at the desired site. Among the synthetic biomaterial candidates, calcium phosphates have received most interest for their osteoconductive property and their ability to incorporate Sr in their lattice [153,258,283].

We have previously demonstrated that molten extruded Sr-containing apatite/polylactide composite materials can provide sustained release of Sr for up to 12 weeks [298]. In this strategy, Sr is incorporated into nano-sized apatite particles, which are then embedded in a polylactide matrix. The resulting composites were shown to favour osteogenic differentiation in vitro and upregulate BMP-induced bone formation in an intramuscular implantation model at four weeks [298]. However, the effectiveness of such strategy in osteoporotic individuals is unclear since their bone forming ability may be impaired.

S Castañeda *et al.* and L Baofeng *et al.* have demonstrated an osteoporotic model (OP) in rabbits, in which the bone mass of experimental animals was reduced significantly 3 months posterior to bilateral ovariectomy and daily injection of glucocorticoid [299,300]. To better understand the effectiveness of Sr on bone formation in osteoporotic individuals, we prepared composites with or without different Sr content and loaded them with equal amount of recombinant human bone morphogenetic protein-2 (rhBMP-2). We implanted the rhBMP-2-loaded materials intramuscularly in eight healthy rabbits and induced four of them into the aforementioned OP model. 12 weeks after the surgery, the volume of de novo bone formed on composite implants in healthy rabbits and in OP model was analyzed and compared.

6.2 Materials and methods

6.2.1 Preparation of Sr-containing apatite/polylactide composites

Sr-containing composites were manufactured as previously described [298]. In brief, nano-sized Sr-substituted apatites were synthesised with a wet precipitation method by mixing aqueous solution of $(NH_4)_2HPO_4$ (Fluka, Germany), $Ca(NO_3)_2{\cdot}4H_2O$ (Sigma) and $Sr(NO_3)_2$ (Sigma) under continuous stirring rate of 500 ± 10 rpm and temperature of 80 ± 5 °C. After dehydration and mesh screening, four apatites with Sr substitution of 0% (Sr0), 0.5% (Sr0.5), 5% (Sr5) and 50% (Sr50) were obtained and further extruded with poly(D,L-lactide) (PDL04, IV midpoint 0.4 dL/g, Purac Biomaterials BV, The Netherland) at the weight ratio of 1:1 to obtain composites of CT (control, Sr0/polylactide), SrL (Sr0.5/polylactide), SrM (Sr5/polylactide) and SrH (Sr50/polylactide) respectively. The extrusion was carried out using a HAAKE MiniLab II Micro Compounder (Thermo Fisher Scientific, USA) with the screw speed of 100 ± 1 rpm for a mixing time of 5 ± 0.5 min at the temperature of 130 ± 1 °C. The obtained composite stripes were then grinded (ZM100, Advantec, Japan) and sieved to obtain granules (size: 0.5~1 mm). All granules were sterilized with ethylene oxide followed by washes with nitrogen/air and 7-day aeration (IsoTron Nederland BV, the Netherlands). Composite granules were divided into one cubic centimetre aliquots under sterile conditions and loaded with 300 μL distilled water containing 10 μg rhBMP-2 (Reborn, Shanghai). After one hour static adsorption, granular aliquots were allowed to dry in sterile fume hood for 48 hours at room temperature and kept in sterile glass vials, respectively. The theoretical and experimental content of Sr in the four composite materials is summarized in Table 1 [298].

Table 1: Content of Sr in samples [298]

Sample	Theoretical molar ratio of Sr substitution for Ca in apatite	Actual molar ratio of Sr substitution for Ca in apatite	Actual weight ratio of Sr in Sr-apatite	Actual weight ratio of Sr in final composites
CT	0%	0.10±0.17%	0,00%	0,00%
SrL	0.5%	0.43±0.09%	0,37%	0,19%
SrM	5%	6.15±0.26%	5,22%	2,61%
SrH	50%	53.33±1.19%	37,15%	18,57%

6.2.2 Animal study

All animal care and experimental procedures were conducted with the approval of Sichuan University. Local animal ethics committee guidelines (Regulations for the administration of affairs concerning experimental animals, China, 1988) for the care and use of laboratory animals have been observed. Eight 6-month female New Zealand white rabbits (body weight 3.5 ± 0.2 kg) were obtained from the Chengdu Dossy Experimental Animals Co., Ltd. Rabbits were housed separately in stainless cages in laboratory animal house at 20-25 °C with 50-60% humidity, and a light cycle coincided with daylight hours. They were fed with standard diet, allowed access to tap water ad libitum and had been acclimated under laboratory conditions for 14 days prior to the surgery. Prior to surgery, the eight rabbits were randomly divided into the control group (Con) and the osteoporotic group (OP) with four rabbits each.

The rabbits were fasted for 24 hours prior to surgery and then received general anaesthesia by the injection of sodium pentobarbital (30 mg/Kg body weight, Sigma) in the marginal ear vein. Afterwards, muscle pouches were created in the paraspinal muscle by scalpel incision and blunt dissection along the direction of the spine with a distance of 2~3 cm in between. The composite aliquots (1 cc) were transferred into an open-head syringe and then inserted in the pockets respectively. Each rabbit received one implant of each composite (4 pockets per rabbit). The pockets were then closed with non-resorbable sutures for identification at harvest. The OP model was induced by bilateral ovariectomy and daily injection of methylprednisolone sodium succinate (Sigma) as described by S Castañeda *et al.* and L Baofeng *et al.* [299,300]. In brief, rabbits in OP group received bilateral ovariectomy through a ventral incision while the Con group received sham surgery. During the same surgery, After surgery, all rabbits were given penicillin ($1x10^5$ IU/kg body weight) for three consecutive days for antibiotic prophylaxis. Two weeks after the surgery, the OP group received daily intramuscular injection of methylprednisolone sodium succinate dissolved in 0.9 % benzyl alcohol at the dosage of 1 mg/kg body weight for ten consecutive weeks. The Con group received 0.9 % benzyl alcohol injection. Both groups received standard diet and water and were allowed full weight bearing in their cages. 12 weeks after the surgery, all rabbits were sacrificed with lethal dose of pentobarbital sodium (Sigma).

6.2.3 Histology and histomorphometry

Intramuscular implants were harvested with surrounding soft tissue, fixed in 4 % formaldehyde and embedded in PMMA after gradient ethanol dehydration. The distal femurs were also harvested and processed to verify the loss of bone mass in OP model. Non-decalcified sections were made sequentially for each intramuscular

explant using a diamond saw microtome (Leica SP-1600, Germany) and stained with 1 % methylene blue (Sigma) and 0.3 % basic fuchsin (Sigma). The thickness of each section is about 15 μm with a step size of 280 μm in between, which is the thickness of the blade. About 15 slides were obtained from each explant. Histological observation was then performed under light microscopy. Scans of each slide (Dimage Scan Elite5400 II, Konica Minolta, USA) were used for histomorphometry. After pseudo-colouring, the area of bone (BA), adipocytes (AA) and composite material (MA) as well as total area (TA) were stacked together to have an overall estimation of each explant. De novo bone formation (B%) was calculated as: B%= 100*∑B/ (∑TA-∑MA); adipocyte colony (Ap%) was calculated as: Ap%= 100*∑AA/ (∑TA-∑MA). The distal femurs of both Con and OP group were sectioned longitudinally. Three slides were obtained for each distal femur. The volume of cancellous bone in distal femur (CA) was measured as the average proportional area of cancellous bone in the total distal femur. The thickness of the cortical bone next to the distal femur (Th.Co) was measured as well in histomorphometry.

6.2.4 Statistical analysis

Statistical analysis was carried out using one-way analysis of variance (ANOVA) with Tukey's test. Differences were considered statistically significant at $p<0.05$ and marked with asterisks.

6.3 Results

6.3.1 Osteoporotic model

According to literatures, rabbits reach skeletal maturity around 6 months [301]. Rabbits used in this study are averagely 27 weeks by age prior to surgery, which can be considered skeletally mature. After the bilateral ovariectomy and 10-weeks injection of glucocorticoid, the OP rabbits had fewer trabeculae and a higher porosity in their distal femur as compared to the Con rabbits (Fig. 1A). Histomorphometry showed that the area of cancellous bone in the distal femur of the OP group decreased about 20% as compared to Con animals ($p<0.01$, Fig. 1B), while the thickness of cortical bone in the OP group was 38% lower than the Con group ($p<0.005$, Fig. 1C). This confirms that this treatment resulted in the loss of bone mass in OP model, i.e. ostepenia or osteoporosis.

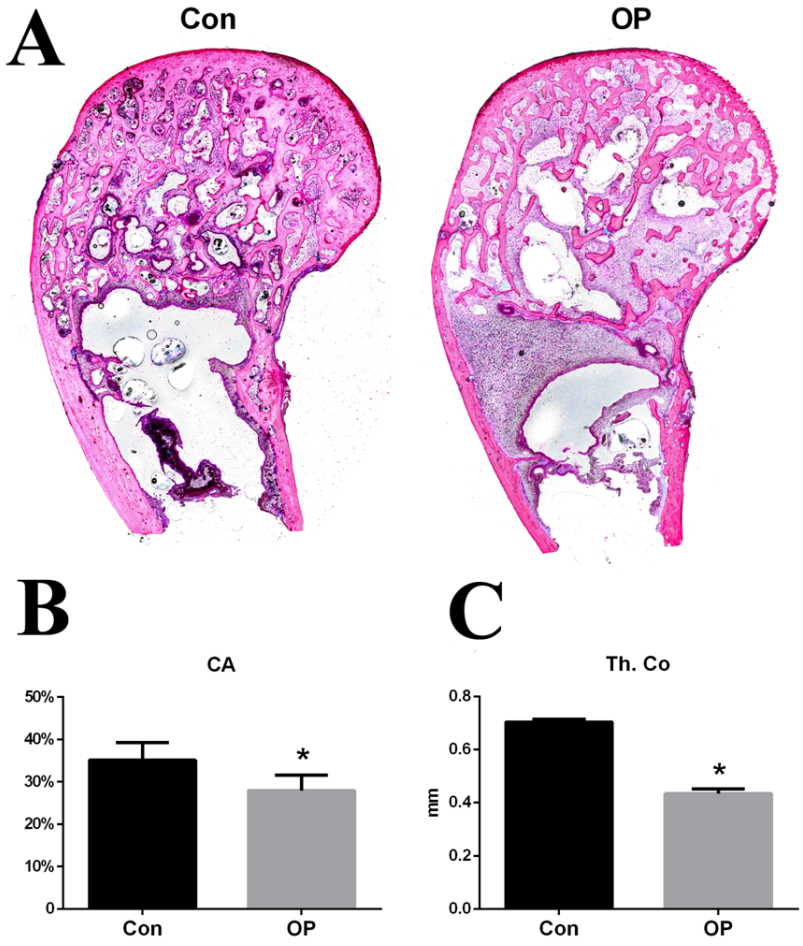

Figure 1. A: Typical overview of distal femur in Con and OP group after 12-week implantation; B: The area of cancellous bone in distal femur; C: the thickness of femur cortical bone in Con and OP group. *: significantly different

6.3.2 Tissue responses in intramuscular implants

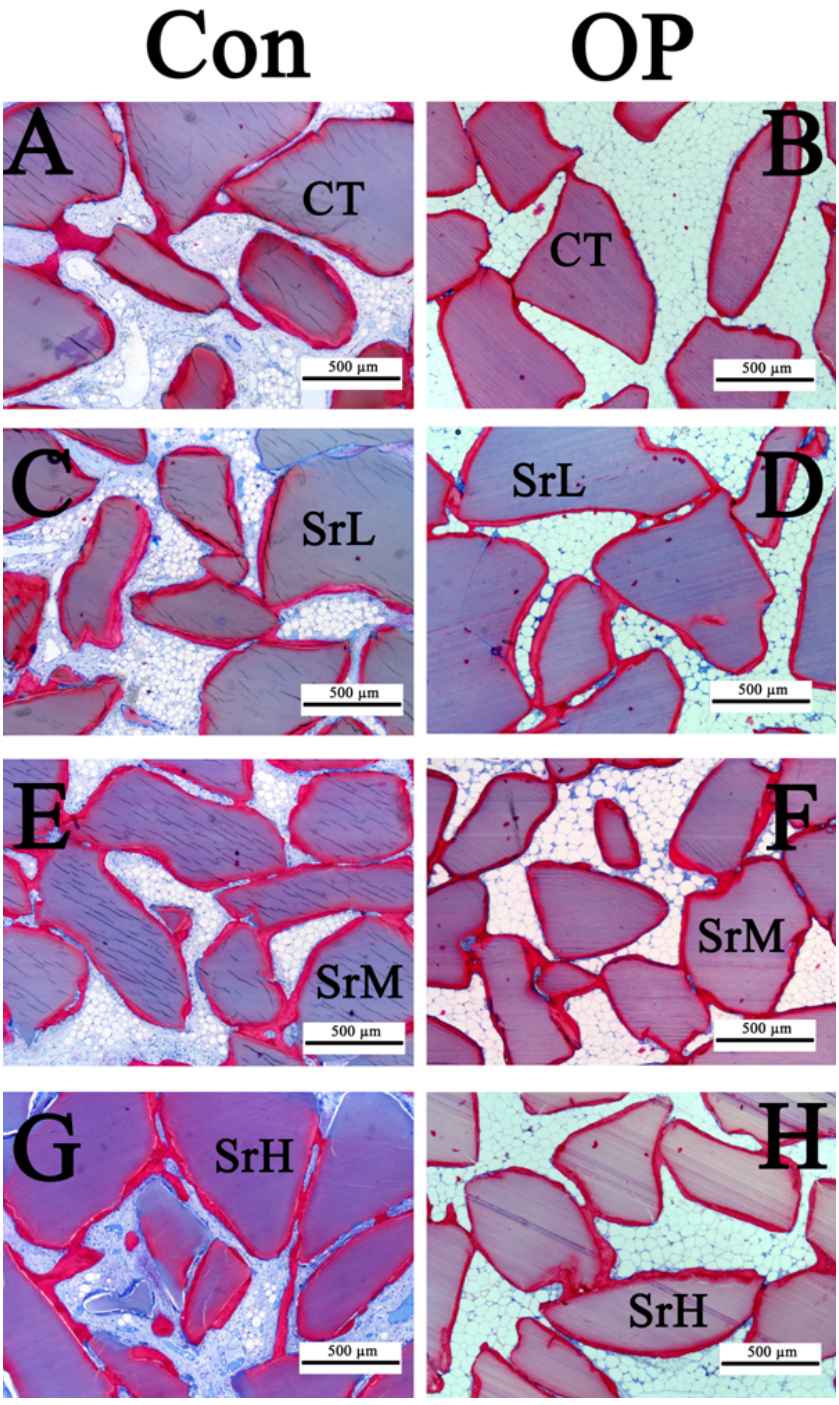
Con
OP
A
CT
500 μm
B
CT
500 μm
C
SrL
500 μm
SrL
D
500 μm
E
SrM
500 μm
F
SrM
500 μm
G
SrH
500 μm
H
SrH
500 μm

Figure 2. Histological observation of implants from Con group (A: CT, C: SrL; E: SrM; G: SrH) and OP group (B: CT, D: SrL; F: SrM; H: SrH). Methylene blue and basic fuchsin staining. Bone (pink-red colour) was formed on composite granules (gray-slate colour). The space between granules was filled with fibrous matrix, which was stained in light blue. Adipocytes (white colour) were observed among fibrous matrix. The thickness of bone layer on CT granules in Op group (B) was thinner as compared to the CT in Con group (A), and was also thinner as compared to Sr-containing implants (D, F, H). Note the massive development of adipocyte colony in all OP implants, which provided the bright background under microscopy.

De novo bone was observed around composite granules in both groups (Fig. 2). The thickness of newly formed bone on CT granules decreased visibly in the OP group as compared to that in Con (Fig. 2A-B). Histomorphometry confirmed that the bone formation in CT implants in the OP group decreased significantly (Fig. 3, $p<0.05$). Bone formation in SrL implants was significantly higher than that of CT implants in the OP group ($p<0.05$, Fig. 3B), and was equivalent to their counterpart in the Con group (Fig. 3A). Higher content of Sr did not further increase the overall amount of bone formation in either the Con or OP groups (Fig. 3) and the average B% did not exceed 10% for all implants.

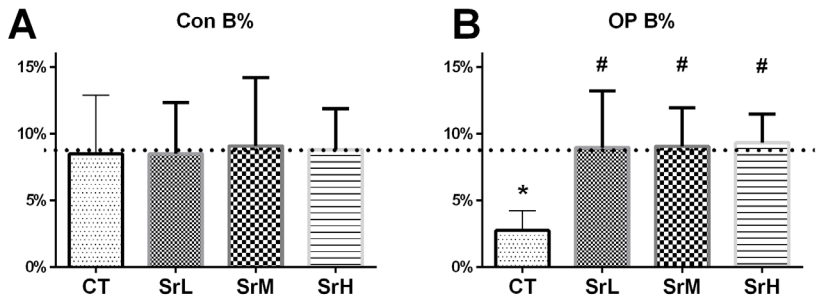

Figure 3. The relative area of bone in intramuscular implants in the Con (A) and OP group (B). Sr significantly enhanced the de novo bone formation in OP implants to the level in Con group, albeit the influence was not dose-dependent in either group. *: significant as compare to the CT in Con group; #: significant as compare to the CT in OP group

Fibrous and adipose tissue appeared in both groups (Fig. 2). The volume of adipose tissue slightly decreased with the Sr content in the Con group but the difference was not statistically significant (Fig. 4A). Notably, significantly more adipose tissue was seen in all OP implants than in the Con group ($p<0.001$, Fig. 4), occupying most of

the available space in implants leading to an obvious reduction of fibrous tissue (Fig. 2). Also fewer areas with active cuboidal osteoblasts secreting osteoid tissue were seen in the OP groups as compared to the control animals (Fig. 5).

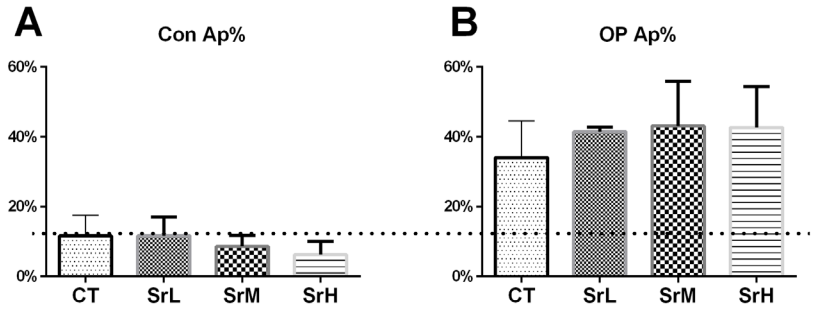

Figure 4. The relative area of adipose tissue in intramuscular implants in the Con (A) and OP group (B). The volume of adipose tissue almost tripled in OP group as compared to Con group.

Interestingly, in all OP groups, cartilage tissue was observed. This cartilage was surrounded by unmineralized and mature bone (Fig. 5). The occurrence of cartilage formation among histological slides is summarized in Table 2. Although the occurrence of cartilage tissue slightly increased with Sr content, this difference was not statistically significant (Table 2). None of the Con animals showed considerable formation of cartilage.

Table 2: Occurrence of cartilage formation among histological slides (number of slides with cartilage/ total slides)

Con					OP				
	CT	SrL	SrM	SrH		CT	SrL	SrM	SrH
Rabbit 1	0/12	0/13	0/13	0/13	Rabbit 5	7/14	9/15	10/15	11/15
Rabbit 2	0/11	0/11	0/10	1/11	Rabbit 6	1/18	2/17	1/18	2/15
Rabbit 3	0/10	0/18	0/17	0/20	Rabbit 7	1/14	2/16	1/17	9/17
Rabbit 4	0/12	0/11	0/12	0/12	Rabbit 8	0/14	0/19	0/12	3/19
Total	0/45	0/53	0/52	1/56	Total	9/60	13/67	12/62	25/66
Percentage of cartilage occurrence	0%	0%	0%	2%	Percentage of cartilage occurrence	15%	19%	19%	38%

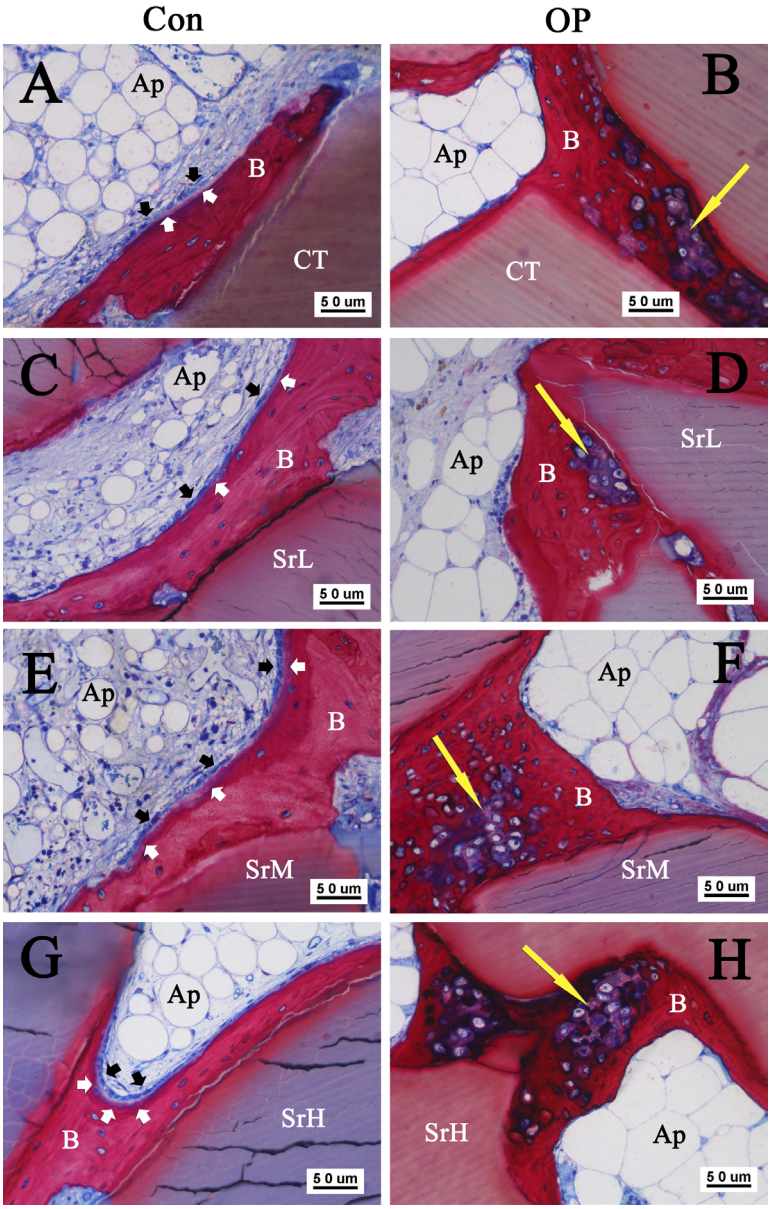

Figure 5. Histological observation of implants in Con (A: CT C: SrL E: SrM, G: SrH) and OP group (B: CT, D: SrL, F: SrM, H: SrH). In Con group, active osteoblasts were observed sitting on osteoid they secreted, whereas much less active bone formation was seen in OP group. The size of adipocytes in OP group was much larger than that in Con. In addition, cartilage appeared in OP implants. B: bone; Ap: adipocytes; black arrow: active osteoblasts, white arrow: osteoid, yellow arrow: cartilage

6.4 Discussion

We showed that the de novo bone formation in the intramuscular implants of the OP group was significantly reduced as compared to that of the Con group, which paralleled with the loss of bone mass in distal femur. This indicates that the bone forming ability of OP group is impaired not only at the bony site, but is also compromised at this ectopic site. The current data is not sufficient to determine whether the impaired bone formation or the active bone resorption is dominant on the fewer bone in CT implants in OP animals due to the lack of experimental data at early time point, while the reduction of bone mass observed at bony site in OP animals (Figure 1) indicated that the intensive bone remodeling in OP animal might have played a major role. Although multiple time points in future experiments are needed to confirm the major function of intensive bone remodeling in OP animals, our current findings showed the profoundly different implant-induced tissue responses in both healthy and OP animals and that the volume of newly formed bone could be impacted by the presence of strontium in implants.

Upon implantation in healthy animals, rhBMP-2 was expected to recruit stem cells to differentiate into osteoblast lineage and secrete bone therein after 2~3 weeks [302,303]. With regard to the BMP-signaling under osteoporotic/osteopenic conditions, it has been shown that the BMP-2 mRNA expression was down-regulated in MSCs derived from OVX mice, indicating the impairment of BMP-2 function in surgical menopause-related osteopenic/osteoporosis [304]. However, Turgeman *et al.* showed that the administration of rhBMP-2 in mice with postmenopausal osteoporosis increased the proliferation and differentiation of MSCs resulting in an increase of trabecular bone volume [305]. Thus, these data suggest that, even though MSCs from osteoporotic conditions might have poorer secretion of BMP-2, they still can actively respond to exogenous BMP-2 leading to osteogenesis.

We have shown in a previous study that the addition of Sr in composite implants enhanced the volume of BMP-induced bone intramuscularly from 5% to about 10% in healthy rabbits at week 4 [298]. When these data are compared with the results in the current study, an increase of bone formation from 5% at 4 weeks to 10% at 12 weeks in strontium-free implants (CT) was observed. However, the bone formation in strontium-containing groups did not increase significantly with the strontium content with time because the final bone volume at week 12 was still about 10% in either healthy or osteoporotic rabbits. This suggests that (1) the presence of strontium accelerated the osteogensis at early stage, which is in line with literatures and also our precious study where strontium ions enhanced the osteogenic differentiation of MSCs [298]; (2) the amount of bone observed in samples in healthy animals and in

Sr-containing samples in OP animals might be the maximal bone volume that can be obtained in the ectopic sites at late stage (e.g. 12 weeks). According to Wolff's law [306], the equilibrium of bone remodeling under such environment lacking of mechanical stimuli will lean to resorption leading to less bone mass. As the result, this may partly conceal the effect of strontium on the final bone mass in the used model at late stage (figure 3A-B).

Nevertheless, Sr addition in composite implants elevated the BMP-induced bone formation in the osteopenic environment to the level of the Con group (Fig. 3), suggesting the potential of Sr addition to reinforce the bone growth around implants in osteopenia. It has been suggested that the anabolic effect of Sr on bone formation is associated with increased osteoblastogenesis of bone marrow stromal cells as well as the anabolic activities of osteoblast precursors [256]. Further, the positive effect of strontium-containing scaffolds on the osteogenic differentiation of MSCs derived from osteoporotic rats has been shown by Lin *et al.* [122] and Boanini *et al*. [152]. Considering the sustained strontium release profile of the obtained composite materials in vitro [298], it is suggested that strontium-containing implants could create an local ion-rich environment that favours the osteogenic differentiation of nearby stem cells as well as bone formation in the osteopenic/osteoporotic environment. However, because the ions surrounding implants may be continuously refreshed by the circulating body fluid, methods have to be created to verify Sr concentrations at the implant site in vivo.

We observed that the area of adipose tissue in intramuscular implants tripled in the OP group along with the decrease of bone formation, as compared to the Con group (Fig. 3, 4). The increase of bone marrow adipogenesis has been reported in aging, diabetic or glucocorticoid therapy-releated osteoporosis paralleled with the inhibition of bone formation [307–311], suggesting that the differentiation potential of mesenchymal stem cells from osteoporotic individuals shifts towards adipogenesis [312–314]. Saidak *et al.* (2002) reported that this tendency can be reversed to osteogenic differentiation by Sr administration [315]. However, we could not confirm this because the adipose tissue in implants did not decrease significantly with Sr content (Fig. 4), while the active osteoblasts were seldom seen in all OP implants regardless of their Sr content (Fig.5). This suggests that Sr's inhibitory effect on adipogenesis might be mild in the ectopic model used in this study. Nevertheless, Sr's inhibitory effect on osteoclastic bone resorption during 12 weeks should be put into consideration as one factor that may have contributed to the higher bone mass in Sr-containing implants [79].

Surprisingly, ectopic cartilage formation appeared in the OP group (Fig. 5) but not in the Con group. This may have influenced the bone formation in the OP rabbits since the population of osteoblast might be perturbed due the selective differentiation of stem cells. Further, it suggested that endochondral ossification was involved in the bone formation in OP group although examinations at early time points are necessary to confirm this. Although the cartilage occurrence was higher in SrH implants (Table 2), we could not show statistical significance in the current study between Sr content and cartilage formation, presumably due to a too small sample pool. More investigations are therefore needed to address whether this phenomenon is associated with the Sr content in implants and how this would influence local bone formation. Taken together, the presence of adipogenesis and chondrogenesis suggest that ovariectomy and glucocorticoid injection have resulted in a different differentiation potential of stem cells in the OP group. To the best of our knowledge, this is the first report showing the osteopenia-associated adipogensis and chondrogenesis at an ectopic site in vivo.

In this study the materials were implanted in muscle, where the bone was induced by rhBMP-2. The advantage of the ectopic model is that the de novo bone could be solely attributed to BMP and implanted materials, rather than to the conductive bone formation from the site of orthopaedic implantation. It is true that the metabolism of bone at ectopic site may differ from orthopaedic site. For example, due to the lack of mechanical loading, the remodelling of bone at ectopic site may largely shift towards bone resorption [306,316]. Nonetheless, studies have shown that the bone forming ability of a biomaterial at ectopic site is related to its performance orthotopically [100,109]. This suggested the clinical relevance of our results although future studies are necessary to confirm the effectiveness of Sr-containing composites at orthopaedic site. Meanwhile, in the current study the materials were implanted at the same time of the initiation of OP model, which focused more on the impact of strontium on bone formation during the development of OP. Considering the possibility that OP may have varied anabolic and anti-resorptive responses at its different stages [317], it would be worthy to include both settings (developing and mature osteoporotic model) in future experiments to further address the performance of strontium-containing implants under different methodologies.

6.5 Conclusions

We have demonstrated that, in a validated osteopenia/osteoporosis model, Sr addition in composite implants increased the rhBMP-2-induced bone formation to a level comparable to healthy animals at an ectopic site.

Acknowledgement

The authors would like to thank Purac Biomaterials BV (Gorinchem, the Netherlands) for kindly providing the polymers. The authors would like to acknowledge Biomedical Materials Program (BMM bone-IP), the Netherlands Institute for Regenerative Medicine (NIRM) and Rapid Prototyping of Custom-Made Bone-Forming Tissue Engineering Constructs (RAPIDOS Project, Ref. NMP-2013-EU-China 604517) for their financial support in this study.

Chapter 7

General Discussion

7. General Discussion

The aim of this thesis is to study the effect of trace element additions on the bone forming ability of synthetic calcium phosphate materials. By incorporating various trace elements into calcium phosphate materials, we expected a release of the doped ion, in this way affecting the cellular responses surrounding the implants and subsequently promote the local osteogenesis. So far the introduction of ions in synthetic materials have been shown to improve their osteoconductivity [122,129,132,135,140,142,148,149,199,318–320], but it is not clear whether osteoinduction may be achieved or whether trace elements may boost the osteoinductivity of the small group of inductive ceramics [42,98,321]. If osteoinduction is obtainable by trace element containing calcium phosphates, it needs to be determined to which extent the inductive bone formation can be attributed to the doped ions. The work in this thesis shows that the introduction of foreign ions can either promote (e.g. Zn and Sr) or suppress (e.g. F) the osteoinductive potential of doped calcium phosphate materials. However, as trace elements do not only affect ion release but can also change physical parameters such as surface geometry, the introduction of trace elements in synthetic materials may function in a much more complicated manner than it may seem. The effect of trace element addition in synthetic materials in terms of their ion release properties, physicochemical parameters and resulting contribution to enhanced bone formation are discussed and summarized in this chapter.

7.1 Do ions play an essential role?

Although improved bone forming ability was seen with certain ion-containing materials, the introduction of foreign ions provoked multiple parameters that were known to play a role in cell-material interactions. It is thus difficult to attribute the improvements to the dopant solely. These parameters include the release of the dopant, the release of calcium [57] and phosphate ions [322] as well as surface geometry [112,118].

Nevertheless, only a few studies considered the roles of these “sub factors” when evaluating the biological performance of ion-containing materials [141] while many studies ignored [135,136,198]. For example, the change of grain size was noticed when introducing zinc into calcium phosphate materials, but this change was not further considered in the resulting biological effect [132,323]. Another example is silicon, which has been suggested to stimulate the biological performance of calcium phosphate ceramics mainly via (1) increasing the dissolution rate, (2) generating an electronegative surface and (3) finer microstructure [121]. However, these changes can also be tuned by other methods, such as sintering or surface modification, and

are thus not uniquely related to Si ions. Criticisms were raised because there is currently no study directly linking the improved biological performance of Si-substituted calcium phosphate materials to Si release [166], not to mention that sometimes the release of Si ions was not confirmed [129].

In this thesis, we studied the effect of Zn, F and Sr addition in synthetic materials with an emphasis on their osteoinductive potential. The results suggest that foreign ion introduction affects both the release of this ion as well as other physical parameters such as the surface geometry and the release of calcium and phosphate ions. Because these "side effects" provoked by the substitution of foreign ions are almost inevitable, there is thus a lack of direct evidence proving the essential role of trace elements in osteoinduction. Furthermore, considering osteoinduction can be triggered without trace elements (Chapter 3 and Chapter 4), while many positive results with trace elements have been obtained at bony sites or with the combination of BMP [128,147,148,318], the current data suggest that the added ions may not be the essential trigger responsible for the observed osteoinduction.

On the other hand, there is no denying that trace elements can affect the cellular fate and bone metabolism. Plenty of in vitro studies have shown that the ions alone are able to influence the proliferation and guild the differentiation of mesenchymal stem cells and osteogenic progenitors [71] [73,199,324–326]. The importance of osteoclastogenesis in de novo bone formation has recently been revealed [118,242,327] and it can be influenced by trace elements as well. In Chapter 2, the supplement of zinc ions in culture medium influenced both the TRAP activity and the osteoclast-like multinuclear giant cells formation of raw264.7 monocyte/macrophages. Our unpublished data show that a high concentration of Sr can also suppress the formation of multinucleated giant cells (figure 1). Therefore, it is reasonable to infer that these trace elements may influence the bone metabolism when these cells were presented (i.e. when osteogenesis is already triggered).

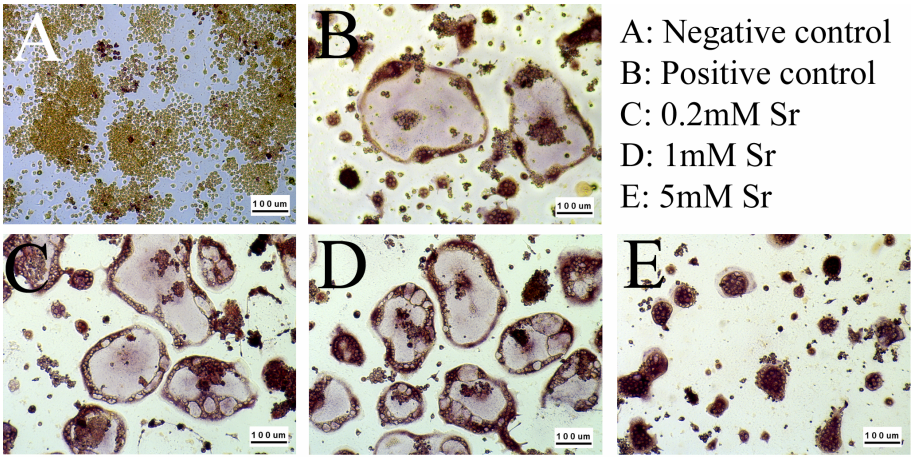

Figure 1. TRAP staining light microscopy images of RAW264.7 cells cultured on plastic plates in the presence of RANKL for 4 days. An image of RAW264.7 cultured without RANKL (A) was shown as the negative control. The addition of strontium chloride in the culture medium was shown to suppress the formation of osteoclast-like cells since the multinucleated giant cells fused from RAW264.7 cells tended to be smaller when exposed to higher concentration of Sr. This effect is most likely due to Sr^{2+} but not Cl^- because the culture medium contains already about 120 mM Cl^- thus the impact of 5 mM $SrCl_2$ on the concentration of Cl^- in the medium would be less than 10% [328]. Furthermore, so far little reports have mentioned the effect of Cl^- on osteoclastogenesis.

In some ion-containing materials, the effect of the doped ions is the only reasonable factor responsible for the unique cellular responses. For instance, Barralet *et al.* showed that the incorporation of copper ions in calcium phosphate scaffolds could enhance the formation of microvessels and wound tissue ingrowth [329]. Silver-doped synthetic materials showed anti-inflammatory activity [330–332]. In chapter 6 of this thesis, we observed increasing chondrogenesis in strontium-containing composites in an osteoporotic model. These data suggest that trace element dopants can indeed play a role in the material-cell interactions because so far no physical cues has been reported to affect the angiogenesis, inflammatory activity or chondrogenesis.

Taken together, the current data suggest that the introduction of trace elements influences the bone forming ability of ion-containing synthetics via both the release of the doped ion and other physicochemical parameters that are changed by the introduction of ions. In such combined effects, the role of physicochemical changes might be equally important than the role of the doped ion itself.

7.2 The role of Ion release from trace element-containing materials

Throughout the experimental chapters of this thesis, it was consistently observed that the release of ions does not increase proportionally with the amount of trace element addition. This indicates that the stability of foreign ions in the lattice changes with the substitution level. We have shown that this change depends on the kind of element inserted. Because the foreign ions cannot fit in the crystal structure of CaP materials perfectly as compared to the ion they replace, the introduction of foreign ions in calcium phosphate-based materials is commonly paralleled with either the extension or the condensation of the lattice leading to changes of chemical stability. In the case of Zn- and Sr-containing calcium phosphates, their chemical stability decreases leading to the increase of dissolution rate while the fluoridation leads to the reverse direction.

The alteration in solubility changes not only the release of the doped ion, but also tailors the release of Ca^{2+} and PO_4^{3-} regarding the yields of substitution. Both ions have been reported to influence osteogenic differentiation of stem cells as well as bone formation [57,322]. This means in a context of calcium phosphate-based materials, the effect of trace element doping is always mixed with the potential influence of Ca^{2+} and PO_4^{3-}. Practically this is not a problem since an environment rich in Ca^{2+} and PO_4^{3-} may favour the osteogenesis. But scientifically it becomes difficult to analyse the effect of trace elements in a single factor model.

In case of composites, the situation is more complicated since the release of doped ion is not only related to the dissolution rate of organic filler but is also depended on the feature of polymer matrix. This shows the possibility to regulate the intensity and duration of ion release by selecting different polymers as the matrix. A general conclusion is that a polymer with lower molecular weight and higher fluid uptake capacity would allow higher degree of filler dissolution leading to higher ion release. Additionally, the degradability of polymer matrix may also impact the release of ions as the hydrolysis degradation of matrix would lead to a reduction of the crystallinity and molecular weight [188].

The concentrations of ion release needed to induce cellular activities have been studied mainly using in vitro models [79,333,334]. However, the ion release might be tightly affected by the in vivo environment because the mechanical loading and the circulation of body fluid may dramatically differ with the location of implants. For example, an ion-containing implant in muscles might have completely different release profile than those implanted in the jaw or condyle. Considering the possible cellular resorption, the ion release profile in vivo might be very complicated and yet difficult to monitor. Because of this difficulty, many studies tried to correlate the

optimal in vivo response directly to the content of ions in synthetic materials without knowing the required concentration for biological responses [129,132].

Besides their effect on the ion release properties of synthetic materials, we have also observed physicochemical changes along with the introduction of foreign ions, which will be discussed in the next section.

7.3 Physicochemical changes provoked by ion substitution and their potential roles

The introduction of trace element in synthetic calcium phosphate materials can provoke physicochemical changes such as an increase in HA content (Chapter 2) and water affinity (Chapter 3) as well as the alteration of surface microstructures [141,323] and apatite crystal aspect ratio [258]. An essential reason behind is that the atom of trace elements has different atomic radius and electromagnetic forces as compared to the ion they replace and the insert of foreign ions may interrupt the growth of the crystal structure and water affinity [43].

The role of surface microstructure in guiding the differentiation fate of mesenchymal stem cells and osteoclastogenesis has been recently revealed. Zhang and co-workers showed that the size of the surface microstructure is a crucial parameter that is sufficient to induce osteogenic differentiation of mesenchymal stem cells [112]. Further, Davison *et al.* showed that surface architecture can be tuned to control osteoclastogenesis and resorption activity [118,119]. Although the biological mechanism behind is still under debate, these data show that the surface geometry of synthetic calcium phosphates is a controllable cue that may lead to inductive bone formation.

The interaction between cells and physical parameters such as surface microstructure has often not been well considered in previous studies and this could be a major reason for many controversial results [132,135,136,140,198]. When the role of physical cues is ignored, it is possible that materials with multiple variances were compared and the results were probably interfered by the varied physicochemical properties.

In this regard, better designed materials with fewer physiological differences would be helpful to distinguish the role of doped ions in ion-containing synthetics. In Chapter 3~6, we proposed composite models to diminish the difference on surface microstructure by introducing the trace element into amorphous apatite particles and further embedding such particles in polymer matrices. By using the same kind of matrix, composites with similar topography but different release of trace elements were obtained. However, due to the inherent correlation between the chemical

stability and lattice structures, these series of ion-containing composites still differed in their calcium and phosphate release. The current data suggested that there may not be ideal counterparts with only one parameter varied and the role of these sub factors (e.g. the surface microstructure) should always be considered when evaluating the role of ions in trace element-containing materials.

7.4 The role of animal models

The biological differences between animal models may be an additional parameter when evaluating the effect of trace elements. In this thesis, canine, ovine and rabbits were employed but rodent and primates models are also often used in osteoinduction research [104,167,215,242,285,335]. These models showed significantly different osteoinductive potential [243,251,285]. Ripamonti showed that the amount of de novo bone formation in hydroxyapatite specimens implanted in baboons was higher than that in rabbits and canines [285]. Our unpublished data also showed that even the most powerful calcium phosphate that can induce substantial ectopic bone in canine and ovine, but failed to induce any bone in rabbit. To better understand the reason at a cellular level, Akiyama and co-workers showed that the osteoclastogenesis prior to inductive bone formation on hydroxyapatite implants was different between canines and rats [243]. These data suggest that the material-induced cellular response in different species may follow a different biological mechanism. Following the same logic, the effect of ions may also differ among species. Little data is available and future studies concerning these issues may be helpful to define the animal model best fit for showing clinical relevance.

7.5 Future perspectives

- **The detection of ions in vivo**

To date most release profiles of ion-containing materials are studied in vitro in physiological solutions such as PBS, SBF or culture medium under periodic refreshment [65,329,336]. However, it is not clear to which extent the available concentration at the implant site is related to the release profile obtained in vitro. Due to the continuous body fluid circulation and the difficulty of in vivo ion detection, little is known about the biological concentration at the interface or surrounding area of implants.

So far, atomic absorption spectroscopy (AAS) or inductively coupled plasma (ICP) have been employed to detect the ion concentration in urine [318], plasma [337,290,270,338] and bone mineral [290]. However, few methods could locally monitor the release of ions at the implant site. It has been shown that the mass distribution of various elements in the selected area on thin histological sections

could be visualized by using Time-of-Flight Secondary Ion Mass Spectrometry (TOF-SIMS) [149]. Similar results can be obtained by using the high lateral resolution of energy dispersive X-ray microanalysis combined with scanning transmission electron microscopy [339], X-ray fluorescence [340,341] and Energy-dispersive X-ray spectroscopy (EDXS) [342]. These methods could visualize the concentration of ions in the area of interest, but can only be done after the harvest and histological processing. This means the result is not live and may be modified due to the complex processing. To sum up, so far there are few methods to expediently monitor the ion concentration at the implant site, and all in vitro evidences can only be indirect as long as the methodology of in vivo detection is not advanced. The ideal tools for the measurement of local ion concentration should most likely be micro-sensors that can be implanted along with ion-containing materials, which is currently a thorny point. Although implantable micro-sensors that can provide continuous measurement in vivo have been described [343–345], so far they can only measure organic molecules such as glucose and insulin but not inorganic ions. Progress in such field could result in powerful tools to determine the optimal content of trace element additions in substituted biomaterials.

- **Ion-containing materials in non-osseous fields**

Because of the popularity of calcium phosphates in orthopaedic field, it has been proposed to also use them as drug delivery vehicles in other fields [81]. Antibiotics, growth factors and bisphosphonate have been considered so far [346,347], meanwhile increasing interests are directed towards trace element-loaded calcium phosphates. Dozens of trace elements are shown to affect tissue responses and their effect can very much vary depending on their particular roles on cell fate and function. This provides vast potential to use vary trace elements additions to meet diverse demands in clinic. The application of trace elements is thus not limited to bone, but also in other fields such as instructing vascularisation [318,329,348–350] and anti-infection [331,351,352]. For example, the antimicrobial silver (Ag) could suppress inflammatory responses [330,353,354] and the doping of Ag in calcium phosphates has shown to reduce the risk of implant-associated infections [331,351,352,355]. It is known that on the one hand inflammatory response is important for the recruitment of osteoprogenitors and activation of osteogenic cytokine secretion [356–358], while on the other hand, excessive inflammation as well as severe infection after implantation should be avoided. The use of Ag in bone regeneration materials might diminish the infection and control excessive inflammatory reactions thus to ensure a proper tissue response. Another example is the use of copper (Cu) in tissue engineering for early vascular establishment in scaffolds, which is one of the biggest challenges in tissue engineering field [359].

Due to the lack of blood vessels in the scaffolds, insufficient angiogenesis will result in a lack of oxygen and nutrition supply resulting in poor survival of seeded cells and failure of osteogenesis [360,361]. Cu was shown to promote angiogenesis therefore the incorporation of Cu in tissue engineering scaffolds might lead to better ingrowth of blood vessels thus benefit the efficiency of tissue engineering [329,349].

- **Smart ion releasing material with multiple trace element additions**

Bone contains numerous trace elements and the nature of bone metabolism is complex [362]. This suggested the synthesis of calcium phosphates with multiple element additions [363–365], aiming to obtain synthetic biomaterials with combined improvements. Ideally, a "smart" ion-releasing material should contain various effective elements. The strategy is to provide the desired ions at different period of implantation to meet clinical demands. For example, the implant could provide Ag^{+} shortly after implantation to prevent infection while releasing Cu^{2+} to induce early angiogenesis. Afterwards it is expected to persistently provide Zn^{2+} or Sr^{2+} during bone growth and remodelling to promote the proliferation and osteogenic differentiation of stem cells which may favour the bone formation. However, it has been reported that the use of multiple ions might result in conflicting absorption and interactional accumulation of each ion [337,366]. Thus the possible ion-interactions should be considered when trying to combine the benefits of individual trace elements.

- **From ectopic to orthopaedic**

In this thesis the in vivo studies were all conducted ectopically (i.e. through intramuscular implantation), where mature osteoblasts are not present. Although it is debatable whether the bone formed at ectopic sites possesses the same characteristics than osseous sites, the bone formation was conducted by the same category of cells. At osseous site, bone is secreted by osteoblast phenotype whereas at the ectopic site undifferentiated osteoprogenitor cells (i.e. mesenchymal stromal cells) needs to be induced towards osteogenic lineage, either by the material alone or with the help of BMP-2, to trigger the inductive bone formation. It has been shown that an osteoinductive material possessing significantly better performance of at the ectopic model may also perform better at orthopaedic site as compared to nonosteoinductive materials [100]. This suggests the relevance between the performance of synthetic materials in an ectopic model and their clinical bone forming ability at osseous site. The ectopic model provides an efficient way to screen potential candidates for orthopaedic applications. It is expected that the observed biological improvement by trace element addition would also reproduced at osseous site. In view of the potential effect of trace elements on the bone forming ability of

synthetic calcium phosphate material at the ectopic site, orthopaedic studies are suggested to further elucidate the efficiency of trace elements on the repair of bone.

In summary, the introduction of trace elements in synthetic calcium phosphate materials have shown enormous potential in enhancing their bone forming abilities either directly or indirectly and is also demonstrated in this thesis. The findings presented here would help to better understand the role of doped ions in the resulting biological performance and might provide meaningful information for future researches. In closing, the effect of trace element substitution may vary depending on the element and the selected carrier, ranging from an osteoinductive material that can instructively trigger bone formation to an engineered orthopaedic implant that may provide desired nutritional ions throughout its lifetime.

References

References

[1] Martinón-Torres M. The Archaeology of Alchemy and Chemistry in the Early Modern World: An Afterthought. Archaeol Int 2012;15. doi:10.5334/ai.1508.

[2] Norris JA. The Mineral Exhalation Theory of Metallogenesis in Pre-Modern Mineral Science. Ambix 2006;53:43–65. doi:10.1179/174582306X93183.

[3] More LT. Boyle as Alchemist. J Hist Ideas 1941;2:61. doi:10.2307/2707281.

[4] Partington JR. A Short History of Chemistry. 2nd editio. New York: The Macmillan Company; 1951.

[5] Klein U. Styles of Experimentation and Alchemical Matter Theory in the Scientific Revolution. Metascience 2007;16:247–56. doi:10.1007/s11016-007-9095-8.

[6] Richard Beatty. Phosphorus. New York: Marshall Cavendish Corporation; 2000.

[7] Eagle CT, Sloan J. Marie Anne Paulze Lavoisier: The Mother of Modern Chemistry. Chem Educ 1998;3:1–18. doi:10.1007/s00897980249a.

[8] John Dalton. On the Absorption of Gases by Water and Other Liquids, Memoirs of the Literary and Philosophical Society of Manchester. 2nd Series. 1805.

[9] Kak S. Mendeleev and the Periodic Table of Elements. Hist Philos Phys 2004;4:115–23.

[10] Steigman G. Primordial Nucleosynthesis in the Precision Cosmology Era. Annu Rev Nucl Part Sci 2007;57:463–91. doi:10.1146/annurev.nucl.56.080805.140437.

[11] Lodders K. SOLAR SYSTEM ABUNDANCES AND CONDENSATION TEMPERATURES OF THE ELEMENTS Katharina Lodders 2003:1220–47.

[12] Boothroyd AI. Astronomy. Heavy elements in stars. Science 2006;314:1690–1. doi:10.1126/science.1136842.

[13] Hoyle F, Fowler WA, Burbidge GR, Burbidge EM. Origin of the Elements in Stars. Science 1956;124:611–4. doi:10.1126/science.124.3223.611.

[14] Clarke FW. The data of geochemistry. Washington: Goverment Printing Office; 1908.

[15] ORÓ J. Mechanism of Synthesis of Adenine from Hydrogen Cyanide under Possible Primitive Earth Conditions. Nature 1961;191:1193–4. doi:10.1038/1911193a0.

[16] Miller SL, Urey HC. Organic Compound Synthes on the Primitive Eart: Several questions about the origin of life have been answered, but much remains to be studied. Science (80-) 1959;130:245–51. doi:10.1126/science.130.3370.245.

[17] Cleaves HJ, Chalmers JH, Lazcano A, Miller SL, Bada JL. A reassessment of prebiotic organic synthesis in neutral planetary atmospheres. Orig Life Evol Biosph 2008;38:105–15. doi:10.1007/s11084-007-9120-3.

[18] Legros R, Balmain N, Bonel G. Age-related changes in mineral of rat and bovine cortical bone. Calcif Tissue Int 1987;41:137–44.

[19] Winter WE, Bazydlo LAL, Harris NS. The molecular biology of human iron metabolism. Lab Med 2014;45:92–102.

[20] Christian P, West KP. Interactions between zinc and vitamin A: an update. Am J Clin Nutr 1998;68:435S – 441S.

[21] Zhao X, Yao H, Fan R, Zhang Z, Xu S. Selenium deficiency influences nitric oxide and selenoproteins in pancreas of chickens. Biol Trace Elem Res 2014;161:341–9. doi:10.1007/s12011-014-0139-9.

[22] McCall a S, Cummings CF, Bhave G, Vanacore R, Page-McCaw A, Hudson BG. Bromine is an essential trace element for assembly of collagen IV scaffolds in tissue development and architecture. Cell 2014;157:1380–92. doi:10.1016/j.cell.2014.05.009.

[23] Reichlmayr-Lais AM, Kirchgeßner M. Effects of lead deficiency on lipid metabolism. Z Ernahrungswiss 1986;25:165–70. doi:10.1007/BF02021248.

[24] Mayer DR, Kosmus W, Pogglitsch H, Mayer D, Beyer W. Essential trace elements in humans. Serum arsenic concentrations in hemodialysis patients in comparison to healthy controls. Biol Trace Elem Res 1993;37:27–38. doi:10.1007/BF02789399.

[25] Cohen-Solal M. Strontium overload and toxicity: impact on renal osteodystrophy. Nephrol Dial Transplant 2002;17 Suppl 2:30–4.

[26] Hadjidakis DJ, Androulakis II. Bone remodeling. Ann N Y Acad Sci 2006;1092:385–96. doi:10.1196/annals.1365.035.

[27] Lian JB, Ph D, Stein GS. DEVELOPMENT OF THE OSTEOBLAST PHENOTYPE : MOLECULAR MECHANISMS MEDIATING OSTEOBLAST GROWTH AND DIFFERENTIATION n.d.

[28] Boonrungsiman S, Gentleman E, Carzaniga R, Evans ND, McComb DW, Porter AE, *et al*. The role of intracellular calcium phosphate in osteoblast-mediated bone apatite formation. Proc Natl Acad Sci U S A 2012;109:14170–5. doi:10.1073/pnas.1208916109.

[29] Burckhardt P, Dawson-Hughes B, Weaver C, editors. Nutritional Influences on Bone Health. London: Springer London; 2010. doi:10.1007/978-1-84882-978-7.

[30] Brown EM. Extracellular Ca2+ sensing, regulation of parathyroid cell function, and role of Ca2+ and other ions as extracellular (first) messengers. Physiol Rev 1991;71:371–411.

[31] Nakahama K-I. Cellular communications in bone homeostasis and repair. Cell Mol Life Sci 2010;67:4001–9. doi:10.1007/s00018-010-0479-3.

[32] Manolagas SC. Birth and death of bone cells: basic regulatory mechanisms and implications for the pathogenesis and treatment of osteoporosis. Endocr Rev 2000;21:115–37. doi:10.1210/edrv.21.2.0395.

[33] Peterson DR, Heideger WJ, Beach KW. Calcium homeostasis: the effect of parathyroid hormone on bone membrane electrical potential difference. Calcif Tissue Int 1985;37:307–11.

[34] H.H.Mitchell, T.S.Hamilton, F.R.Steggerda HWB. The chemical composition of the adult human body and its bearing on the biochemistry of growth. J Biol Chem 1945;158:625–37.

[35] Beattie JH, Avenell a. Trace element nutrition and bone metabolism. Nutr Res Rev 1992;5:167–88. doi:10.1079/NRR19920013.

[36] Zofková I, Nemcikova P, Matucha P. Trace elements and bone health. Clin Chem Lab Med 2013;0:1–7. doi:10.1515/cclm-2012-0868.

[37] Bigi A, Foresti E, Gregorini R, Ripamonti A, Roveri N, Shah JS. The role of magnesium on the structure of biological apatites. Calcif Tissue Int 1992;50:439–44.

[38] Bigi A, Boanini E, Capuccini C, Gazzano M. Strontium-substituted hydroxyapatite nanocrystals. Inorganica Chim Acta 2007;360:1009–16. doi:10.1016/j.ica.2006.07.074.

[39] Paul W, Sharma CP. Effect of calcium, zinc and magnesium on the attachment and spreading of osteoblast like cells onto ceramic matrices. J Mater Sci Mater Med 2007;18:699–703. doi:10.1007/s10856-006-0005-1.

[40] Verberckmoes SC, De Broe ME, D'Haese PC. Dose-dependent effects of strontium on osteoblast function and mineralization. Kidney Int 2003;64:534–43. doi:10.1046/j.1523-1755.2003.00123.x.

[41] Yamaguchi M. Role of zinc in bone formation and bone resorption. J Trace Elem Exp Med 1998;11:119–35. doi:10.1002/(SICI)1520-670X(1998)11:2/3<119::AID-JTRA5>3.0.CO;2-3.

[42] LeGeros RZ. Calcium phosphate-based osteoinductive materials. Chem Rev 2008;108:4742–53.

[43] Boanini E, Gazzano M, Bigi a. Ionic substitutions in calcium phosphates synthesized at low temperature. Acta Biomater 2010;6:1882–94. doi:10.1016/j.actbio.2009.12.041.

[44] Dahl S., Allain P, Marie P., Mauras Y, Boivin G, Ammann P, *et al*. Incorporation and distribution of strontium in bone. Bone 2001;28:446–53. doi:10.1016/S8756-3282(01)00419-7.

[45] Marie PJ, Ammann P, Boivin G, Rey C. Mechanisms of action and therapeutic potential of strontium in bone. Calcif Tissue Int 2001;69:121–9.

[46] KAY MI, YOUNG RA, POSNER AS. Crystal Structure of Hydroxyapatite. Nature 1964;204:1050–2. doi:10.1038/2041050a0.

[47] J.C.Elliott. Structure and Chemistry of the Apatites and Other Calcium Orthophosphates. Amsterdam: Elsevier; 1994.

[48] Le L. Silicon Incorporation in Hydroxylapatite Obtained by Controlled Crystallization 2004:2300–8.

[49] Vallet-Regi M, Arcos D. Silicon substituted hydroxyapatites. A method to upgrade calcium phosphate based implants. J Mater Chem 2005;15:1509. doi:10.1039/b414143a.

[50] LeGeros RZ. Calcium phosphates in oral biology and medicine. Monogr Oral Sci 1991;15:1–201.

[51] Roveri N, Battistella E, Bianchi CL, Foltran I, Foresti E, Iafisco M, *et al*. Surface Enamel Remineralization: Biomimetic Apatite Nanocrystals and Fluoride Ions Different Effects. J Nanomater 2009;2009:1–9. doi:10.1155/2009/746383.

[52] Okazaki M, Takahashi J, Kimura H, Aoba T. Crystallinity, solubility, and dissolution rate behavior of fluoridated CO3 apatites. J Biomed Mater Res 1982;16:851–60. doi:10.1002/jbm.820160610.

[53] O'Donnell MD, Fredholm Y, de Rouffignac a, Hill RG. Structural analysis of a series of strontium-substituted apatites. Acta Biomater 2008;4:1455–64. doi:10.1016/j.actbio.2008.04.018.

[54] Miyaji F, Kono Y, Suyama Y. Formation and structure of zinc-substituted calcium hydroxyapatite. Mater Res Bull 2005;40:209–20. doi:10.1016/j.materresbull.2004.10.020.

[55] Nakamura S, Matsumoto T, Sasaki J-I, Egusa H, Lee KY, Nakano T, *et al*. Effect of calcium ion concentrations on osteogenic differentiation and hematopoietic stem cell niche-related protein expression in osteoblasts. Tissue Eng Part A 2010;16:2467–73.

[56] Maeno S, Niki Y, Matsumoto H, Morioka H, Yatabe T, Funayama A, *et al*. The effect of calcium ion concentration on osteoblast viability, proliferation and differentiation in monolayer and 3D culture. Biomaterials 2005;26:4847–55. doi:10.1016/j.biomaterials.2005.01.006.

[57] Barradas AMC, Fernandes HAM, Groen N, Chai YC, Schrooten J, van de Peppel J, *et al*. A calcium-induced signaling cascade leading to osteogenic differentiation of human bone marrow-derived mesenchymal stromal cells. Biomaterials 2012;33:3205–15. doi:10.1016/j.biomaterials.2012.01.020.

[58] Masanori Kanatani, Toshitsugu Sugimoto, Masaaki Fukase TF. Effect of elevated extracellular calcium on the proliferation of osteoblastic MC3T3-E1 cells:its direct and indirect effects via monocytes. Biochem Biophys Res Commun 1991;181:1425–30. doi:http://dx.doi.org/10.1016/0006-291X(91)92098-5.

[59] Zhang R, Lu Y, Ye L, Yuan B, Yu S, Qin C, *et al*. Unique roles of phosphorus in endochondral bone formation and osteocyte maturation. J Bone Miner Res 2011;26:1047–56. doi:10.1002/jbmr.294.

[60] Hayashibara T, Hiraga T, Sugita A, Wang L, Hata K, Ooshima T, *et al*. Regulation of Osteoclast Differentiation and Function by Phosphate: Potential Role of Osteoclasts in the Skeletal Abnormalities in Hypophosphatemic Conditions. J Bone Miner Res 2007;22. doi:10.1359/JBMR.070709.

[61] Habibovic P, Bassett DC, Doillon CJ, Gerard C, McKee MD, Barralet JE. Collagen biomineralization in vivo by sustained release of inorganic phosphate ions. Adv Mater 2010;22:1858–62. doi:10.1002/adma.200902778.

[62] Saita Y, Takagi T, Kitahara K, Usui M, Miyazono K, Ezura Y, *et al*. Lack of Schnurri-2 expression associates with reduced bone remodeling and osteopenia. J Biol Chem 2007;282:12907–15. doi:10.1074/jbc.M611203200.

[63] Saltman PD, Strause LG. The role of trace minerals in osteoporosis. J Am Coll Nutr 1993;12:384–9.

[64] Gentleman E, Stevens MM, Hill RG, Brauer DS. Surface properties and ion release from fluoride-containing bioactive glasses promote osteoblast differentiation and mineralization in vitro. Acta Biomater 2013;9:5771–9. doi:10.1016/j.actbio.2012.10.043.

[65] Ohno M, Kimoto K, Toyoda T, Kawata K, Arakawa H. Fluoride-treated bio-resorbable synthetic hydroxyapatite promotes proliferation and differentiation of human osteoblastic MG-63 cells. J Oral Implantol 2013;39:154–60. doi:10.1563/AAID-JOI-D-10-00175.

[66] Farley JR, Tarbaux N, Hall S, Baylink DJ. Mitogenic action(s) of fluoride on osteoblast line cells: determinants of the response in vitro. J Bone Miner Res 1990;5 Suppl 1:S107–13. doi:10.1002/jbmr.5650051371.

[67] Wang Y, Zhang S, Zeng X, Ma LL, Weng W, Yan W, *et al*. Osteoblastic cell response on fluoridated hydroxyapatite coatings. Acta Biomater 2007;3:191–7. doi:10.1016/j.actbio.2006.10.002.

[68] Yoon B-H, Kim H-W, Lee S-H, Bae C-J, Koh Y-H, Kong Y-M, *et al*. Stability and cellular responses to fluorapatite-collagen composites. Biomaterials 2005;26:2957–63. doi:10.1016/j.biomaterials.2004.07.062.

[69] Kim H-W, Lee E-J, Kim H-E, Salih V, Knowles JC. Effect of fluoridation of hydroxyapatite in hydroxyapatite-polycaprolactone composites on osteoblast activity. Biomaterials 2005;26:4395–404. doi:10.1016/j.biomaterials.2004.11.008.

[70] Zhang WG, Wang LZ, Liu Z. [The influence of fluoride on the development of the osteoblast phenotype in rat calvarial osteoblasts: an in vitro study]. Shanghai Kou Qiang Yi Xue 1998;7:88–93.

[71] Zou S, Ireland D, Brooks R a, Rushton N, Best S. The effects of silicate ions on human osteoblast adhesion, proliferation, and differentiation. J Biomed Mater Res B Appl Biomater 2009;90:123–30. doi:10.1002/jbm.b.31262.

[72] Reffitt D., Ogston N, Jugdaohsingh R, Cheung HF., Evans B a. ., Thompson RP., *et al*. Orthosilicic acid stimulates collagen type 1 synthesis and osteoblastic differentiation in human osteoblast-like cells in vitro. Bone 2003;32:127–35. doi:10.1016/S8756-3282(02)00950-X.

[73] Yamaguchi M, Weitzmann MN. Zinc stimulates osteoblastogenesis and suppresses osteoclastogenesis by antagonizing NF-κB activation. Mol Cell Biochem 2011;355:179–86. doi:10.1007/s11010-011-0852-z.

[74] Cen X, Wang R, Wu Z. [Zinc promotes proliferation and differentiation of osteoblast in rats in vitro]. Zhonghua Yu Fang Yi Xue Za Zhi 1999;33:221–3.

[75] Seo H-J, Cho Y-E, Kim T, Shin H-I, Kwun I-S. Zinc may increase bone formation through stimulating cell proliferation, alkaline phosphatase activity and collagen synthesis in osteoblastic MC3T3-E1 cells. Nutr Res Pract 2010;4:356–61. doi:10.4162/nrp.2010.4.5.356.

[76] Moonga BS, Dempster DW. Zinc is a potent inhibitor of osteoclastic bone resorption in vitro. J Bone Miner Res 1995;10:453–7. doi:10.1002/jbmr.5650100317.

[77] Li X, Senda K, Ito A, Sogo Y, Yamazaki A. Effect of Zn and Mg in tricalcium phosphate and in culture medium on apoptosis and actin ring formation of mature osteoclasts. Biomed Mater Bristol Engl 2008;3:045002. doi:10.1088/1748-6041/3/4/045002.

[78] Holloway WR, Collier FM, Herbst RE, Hodge JM, Nicholson GC. Osteoblast-mediated effects of zinc on isolated rat osteoclasts: inhibition of bone resorption and enhancement of osteoclast number. Bone 1996;19:137–42.
[79] Bonnelye E, Chabadel A, Saltel F, Jurdic P. Dual effect of strontium ranelate: stimulation of osteoblast differentiation and inhibition of osteoclast formation and resorption in vitro. Bone 2008;42:129–38. doi:10.1016/j.bone.2007.08.043.
[80] Amini AR, Laurencin CT, Nukavarapu SP. Bone tissue engineering: recent advances and challenges. Crit Rev Biomed Eng 2012;40:363–408.
[81] Bohner M. Resorbable biomaterials as bone graft substitutes. Mater Today 2010;13:24–30. doi:10.1016/S1369-7021(10)70014-6.
[82] Navarro M, Michiardi a, Castaño O, Planell J a. Biomaterials in orthopaedics. J R Soc Interface 2008;5:1137–58. doi:10.1098/rsif.2008.0151.
[83] Cao W, Hench LL. Bioactive materials. Ceram Int 1996;22:493–507. doi:10.1016/0272-8842(95)00126-3.
[84] Bruder SP, Kraus KH, Goldberg VM, Kadiyala S. The effect of implants loaded with autologous mesenchymal stem cells on the healing of canine segmental bone defects. J Bone Joint Surg Am 1998;80:985–96.
[85] Goshima J, Goldberg VM, Caplan AI. The osteogenic potential of culture-expanded rat marrow mesenchymal cells assayed in vivo in calcium phosphate ceramic blocks. Clin Orthop Relat Res 1991:298–311.
[86] Eniwumide JO, Yuan H, Cartmell SH, Meijer GJ, de Bruijn JD. Ectopic bone formation in bone marrow stem cell seeded calcium phosphate scaffolds as compared to autograft and (cell seeded) allograft. Eur Cell Mater 2007;14:30–8; discussion 39.
[87] Li J, Habibovic P, Yuan H, van den Doel M, Wilson CE, de Wijn JR, *et al*. Biological performance in goats of a porous titanium alloy-biphasic calcium phosphate composite. Biomaterials 2007;28:4209–18. doi:10.1016/j.biomaterials.2007.05.042.
[88] Giannoni P, Ph D, Scaglione S, Daga A, Ilengo C, Sci B, *et al*. Short-Time Survival and Engraftment of Bone Marrow Stromal Cells in an Ectopic Model of Bone Regeneration 2010;16.
[89] Eyckmans J, Roberts SJ, Schrooten J, Luyten FP. A clinically relevant model of osteoinduction: a process requiring calcium phosphate and BMP/Wnt signalling. J Cell Mol Med 2010;14:1845–56. doi:10.1111/j.1582-4934.2009.00807.x.
[90] Takahashi Y, Yamamoto M, Tabata Y. Enhanced osteoinduction by controlled release of bone morphogenetic protein-2 from biodegradable

sponge composed of gelatin and beta-tricalcium phosphate. Biomaterials 2005;26:4856–65. doi:10.1016/j.biomaterials.2005.01.012.

[91] Murakami N, Saito N, Takahashi J, Ota H, Horiuchi H, Nawata M, *et al*. Repair of a proximal femoral bone defect in dogs using a porous surfaced prosthesis in combination with recombinant BMP-2 and a synthetic polymer carrier. Biomaterials 2003;24:2153–9. doi:10.1016/S0142-9612(03)00041-3.

[92] Liang G, Yang Y, Oh S, Ong JL, Zheng C, Ran J, *et al*. Ectopic osteoinduction and early degradation of recombinant human bone morphogenetic protein-2-loaded porous beta-tricalcium phosphate in mice. Biomaterials 2005;26:4265–71. doi:10.1016/j.biomaterials.2004.10.035.

[93] Boden SD, Zdeblick TA, Sandhu HS, Heim SE. The use of rhBMP-2 in interbody fusion cages. Definitive evidence of osteoinduction in humans: a preliminary report. Spine (Phila Pa 1976) 2000;25:376–81.

[94] Zara JN, Siu RK, Zhang X, Shen J, Ngo R, Lee M, *et al*. High doses of bone morphogenetic protein 2 induce structurally abnormal bone and inflammation in vivo. Tissue Eng Part A 2011;17:1389–99. doi:10.1089/ten.TEA.2010.0555.

[95] Carragee EJ, Hurwitz EL, Weiner BK. A critical review of recombinant human bone morphogenetic protein-2 trials in spinal surgery: emerging safety concerns and lessons learned. Spine J 2011;11:471–91. doi:10.1016/j.spinee.2011.04.023.

[96] Lapczyna H, Galea L, Wüst S, Bohner M, Jerban S, Sweedy A, *et al*. Effect of grain size and microporosity on the in vivo behaviour of β-tricalcium phosphate scaffolds. Eur Cell Mater 2014;28:299–319.

[97] Bashoor-Zadeh M, Baroud G, Bohner M. Simulation of the in vivo resorption rate of β-tricalcium phosphate bone graft substitutes implanted in a sheep model. Biomaterials 2011;32:6362–73. doi:10.1016/j.biomaterials.2011.05.030.

[98] Yuan H, Kurashina K, de Bruijn JD, Li Y, de Groot K, Zhang X. A preliminary study on osteoinduction of two kinds of calcium phosphate ceramics. Biomaterials 1999;20:1799–806.

[99] Yuan H, Yang Z, Li Y, Zhang X, De Bruijn JD, De Groot K. Osteoinduction by calcium phosphate biomaterials. J Mater Sci Mater Med 1998;9:723–6.

[100] Habibovic P, Yuan H, van den Doel M, Sees TM, van Blitterswijk CA, de Groot K. Relevance of osteoinductive biomaterials in critical-sized orthotopic defect. J Orthop Res 2006;24:867–76. doi:10.1002/jor.20115.

[101] Yang R, Ye F, Cheng L, Wang J, Lu X, Shi Y, *et al*. Osteoinduction by Ca-P biomaterials implanted into the muscles of mice. J Zhejiang Univ Sci B 2011;12:582–90. doi:10.1631/jzus.B1000204.

[102] Yuan H, de Bruijn JD, Zhang X, van Blitterswijk C a, de Groot K. Bone induction by porous glass ceramic made from Bioglass (45S5). J Biomed Mater Res 2001;58:270–6.

[103] Yuan H, Li Y, de Bruijn JD, de Groot K, Zhang X. Tissue responses of calcium phosphate cement: a study in dogs. Biomaterials 2000;21:1283–90.

[104] Barbieri D, Yuan H, Luo X, Farè S, Grijpma DW, de Bruijn JD. Influence of polymer molecular weight in osteoinductive composites for bone tissue regeneration. Acta Biomater 2013:8–10. doi:10.1016/j.actbio.2013.07.026.

[105] Barbieri D, Renard AJS, de Bruijn JD, Yuan H. Heterotopic bone formation by nano-apatite containing poly(D,L-lactide) composites. Eur Cell Mater 2010;19:252–61.

[106] Le Nihouannen D, Saffarzadeh A, Gauthier O, Moreau F, Pilet P, Spaethe R, *et al*. Bone tissue formation in sheep muscles induced by a biphasic calcium phosphate ceramic and fibrin glue composite. J Mater Sci Mater Med 2008;19:667–75. doi:10.1007/s10856-007-3206-3.

[107] Hasegawa S, Neo M, Tamura J, Fujibayashi S, Takemoto M, Shikinami Y, *et al*. In vivo evaluation of a porous hydroxyapatite/poly-DL-lactide composite for bone tissue engineering. J Biomed Mater Res A 2007;81:930–8. doi:10.1002/jbm.a.31109.

[108] Fujibayashi S, Neo M, Kim H-M, Kokubo T, Nakamura T. Osteoinduction of porous bioactive titanium metal. Biomaterials 2004;25:443–50. doi:10.1016/S0142-9612(03)00551-9.

[109] Yuan H, Fernandes H, Habibovic P, de Boer J, Barradas AMC, de Ruiter A, *et al*. Osteoinductive ceramics as a synthetic alternative to autologous bone grafting. Proc Natl Acad Sci U S A 2010;107:13614–9. doi:10.1073/pnas.1003600107.

[110] Lord MS, Foss M, Besenbacher F. Influence of nanoscale surface topography on protein adsorption and cellular response. Nano Today 2010;5:66–78. doi:10.1016/j.nantod.2010.01.001.

[111] Chan CK, Kumar TSS, Liao S, Murugan R, Ngiam M, Ramakrishnan S. Biomimetic nanocomposites for bone graft applications. Nanomedicine (Lond) 2006;1:177–88. doi:10.2217/17435889.1.2.177.

[112] Zhang J, Luo X, Barbieri D, Barradas AMC, de Bruijn JD, van Blitterswijk CA, *et al*. The size of surface microstructures as an osteogenic factor in calcium

phosphate ceramics. Acta Biomater 2014;10:3254–63. doi:10.1016/j.actbio.2014.03.021.

[113] Nishimura N, Kawai T. Effect of microstructure of titanium surface on the behaviour of osteogenic cell line MC3T3-E1. J Mater Sci Mater Med 1998;9:99–102.

[114] Ramaglia L, Capece G, di Spigna G, Esposito D, Postiglione L. In vitro expression of osteoblastic phenotype on titanium surfaces. Minerva Stomatol 2010;59:259–66, 267–70.

[115] Takemoto M, Fujibayashi S, Neo M, Suzuki J, Matsushita T, Kokubo T, *et al*. Osteoinductive porous titanium implants: effect of sodium removal by dilute HCl treatment. Biomaterials 2006;27:2682–91. doi:10.1016/j.biomaterials.2005.12.014.

[116] Costa-Rodrigues J, Fernandes A, Lopes M a, Fernandes MH. Hydroxyapatite surface roughness: complex modulation of the osteoclastogenesis of human precursor cells. Acta Biomater 2012;8:1137–45. doi:10.1016/j.actbio.2011.11.032.

[117] Davison NL, Luo X, Schoenmaker T, Everts V, Yuan H, Barrère-de Groot F, *et al*. Submicron-scale surface architecture of tricalcium phosphate directs osteogenesis in vitro and in vivo. Eur Cell Mater 2014;27:281–97; discussion 296–7.

[118] Davison NL, Gamblin A-L, Layrolle P, Yuan H, de Bruijn JD, Barrère-de Groot F. Liposomal clodronate inhibition of osteoclastogenesis and osteoinduction by submicrostructured beta-tricalcium phosphate. Biomaterials 2014;35:5088–97. doi:10.1016/j.biomaterials.2014.03.013.

[119] Davison NL, ten Harkel B, Schoenmaker T, Luo X, Yuan H, Everts V, *et al*. Osteoclast resorption of beta-tricalcium phosphate controlled by surface architecture. Biomaterials 2014;35:7441–51. doi:10.1016/j.biomaterials.2014.05.048.

[120] Barradas AMC, Yuan H, van Blitterswijk CA, Habibovic P. Osteoinductive biomaterials: current knowledge of properties, experimental models and biological mechanisms. Eur Cell Mater 2011;21:407–29; discussion 429.

[121] Pietak AM, Reid JW, Stott MJ, Sayer M. Silicon substitution in the calcium phosphate bioceramics. Biomaterials 2007;28:4023–32. doi:10.1016/j.biomaterials.2007.05.003.

[122] Lin K, Xia L, Li H, Jiang X, Pan H, Xu Y, *et al*. Enhanced osteoporotic bone regeneration by strontium-substituted calcium silicate bioactive ceramics. Biomaterials 2013;34:10028–42. doi:10.1016/j.biomaterials.2013.09.056.

[123] Lusvardi G, Malavasi G, Menabue L, Menziani MC, Pedone a, Segre U, *et al*. Properties of zinc releasing surfaces for clinical applications. J Biomater Appl 2008;22:505–26. doi:10.1177/0885328207079731.

[124] Oh S, Won J, Kim H. Composite membranes of poly(lactic acid) with zinc-added bioactive glass as a guiding matrix for osteogenic differentiation of bone marrow mesenchymal stem cells. J Biomater Appl 2012;27:413–22. doi:10.1177/0885328211408944.

[125] Oh S-A, Kim S-H, Won J-E, Kim J-J, Shin US, Kim H-W. Effects on growth and osteogenic differentiation of mesenchymal stem cells by the zinc-added sol-gel bioactive glass granules. J Tissue Eng 2011;2010:475260. doi:10.4061/2010/475260.

[126] Ito A, Kawamura H, Otsuka M, Ikeuchi M, Ohgushi H, Ishikawa K, *et al*. Zinc-releasing calcium phosphate for stimulating bone formation. Mater Sci Eng C 2002;22:21–5.

[127] Capuccini C, Torricelli P, Sima F, Boanini E, Ristoscu C, Bracci B, *et al*. Strontium-substituted hydroxyapatite coatings synthesized by pulsed-laser deposition: in vitro osteoblast and osteoclast response. Acta Biomater 2008;4:1885–93. doi:10.1016/j.actbio.2008.05.005.

[128] Vestermark MT, Hauge E-M, Soballe K, Bechtold JE, Jakobsen T, Baas J. Strontium doping of bone graft extender. Acta Orthop 2011;82:614–21. doi:10.3109/17453674.2011.618909.

[129] Hing KA, Revell PA, Smith N, Buckland T. Effect of silicon level on rate, quality and progression of bone healing within silicate-substituted porous hydroxyapatite scaffolds. Biomaterials 2006;27:5014–26. doi:10.1016/j.biomaterials.2006.05.039.

[130] Tang Y, Chappell HF, Dove MT, Reeder RJ, Lee YJ. Zinc incorporation into hydroxylapatite. Biomaterials 2009;30:2864–72. doi:10.1016/j.biomaterials.2009.01.043.

[131] Roy M, Fielding G a., Bandyopadhyay A, Bose S. Effects of zinc and strontium substitution in tricalcium phosphate on osteoclast differentiation and resorption. Biomater Sci 2013;1:74. doi:10.1039/c2bm00012a.

[132] Li X, Sogo Y, Ito A, Mutsuzaki H, Ochiai N, Kobayashi T, *et al*. The optimum zinc content in set calcium phosphate cement for promoting bone formation in vivo. Mater Sci Eng C Mater Biol Appl 2009;29:969–75. doi:10.1016/j.msec.2008.08.021.

[133] Snead D, Barre P, Bajpai PK, Taylor a, Reynolds D, Mehling B, *et al*. The use of a zinc based bioceramic as an osteoconductive agent in the rat model. Biomed Sci Instrum 1995;31:141–6.

[134] Yamada Y, Ito A, Kojima H, Sakane M, Miyakawa S, Uemura T, *et al*. Inhibitory effect of Zn2+ in zinc-containing beta-tricalcium phosphate on resorbing activity of mature osteoclasts. J Biomed Mater Res A 2008;84:344–52. doi:10.1002/jbm.a.31265.

[135] Ito a, Otsuka M, Kawamura H, Ikeuchi M, Ohgushi H, Sogo Y, *et al*. Zinc-containing tricalcium phosphate and related materials for promoting bone formation. Curr Appl Phys 2005;5:402–6. doi:10.1016/j.cap.2004.10.006.

[136] Li X, Senda K, Ito A, Sogo Y, Yamazaki A. Difference in Osteoclast Responses to Tricalcium Phosphate in Culture Medium Supplemented with Zinc and to Zinc-Containing Tricalcium Phosphate. Bioceram Dev Appl 2010;1:1–4. doi:10.4303/bda/D101106.

[137] Looney M, O'Shea H, Boyd D. Preliminary evaluation of therapeutic ion release from Sr-doped zinc-silicate glass ceramics. J Biomater Appl 2013;27:511–24. doi:10.1177/0885328211413621.

[138] Du RL, Chang J, Ni SY, Zhai WY, Wang JY. Characterization and in vitro bioactivity of zinc-containing bioactive glass and glass-ceramics. J Biomater Appl 2006;20:341–60. doi:10.1177/0885328206054535.

[139] Storrie H, Stupp SI. Cellular response to zinc-containing organoapatite: an in vitro study of proliferation, alkaline phosphatase activity and biomineralization. Biomaterials 2005;26:5492–9. doi:10.1016/j.biomaterials.2005.01.043.

[140] Johal KK, Mendoza-Suárez G, Escalante-García JI, Hill RG, Brook IM. In vivo response of strontium and zinc-based ionomeric cement implants in bone. J Mater Sci Mater Med 2002;13:375–9.

[141] Aina V, Bergandi L, Lusvardi G, Malavasi G, Imrie FE, Gibson IR, *et al*. Sr-containing hydroxyapatite: morphologies of HA crystals and bioactivity on osteoblast cells. Mater Sci Eng C Mater Biol Appl 2013;33:1132–42. doi:10.1016/j.msec.2012.12.005.

[142] Yang G, Song L, Jiang Q, Wang X, Zhao S, He F. Effect of strontium-substituted nanohydroxyapatite coating of porous implant surfaces on implant osseointegration in a rabbit model. Int J Oral Maxillofac Implants n.d.;27:1332–9.

[143] Wong KL, Wong CT, Liu WC, Pan HB, Fong MK, Lam WM, *et al*. Mechanical properties and in vitro response of strontium-containing hydroxyapatite/polyetheretherketone composites. Biomaterials 2009;30:3810–7. doi:10.1016/j.biomaterials.2009.04.016.

[144] Ni G-X, Yao Z-P, Huang G-T, Liu W-G, Lu WW. The effect of strontium incorporation in hydroxyapatite on osteoblasts in vitro. J Mater Sci Mater Med 2011;22:961–7. doi:10.1007/s10856-011-4264-0.

[145] Isaac J, Nohra J, Lao J, Jallot E, Nedelec JM, Berdal A, *et al*. Effects of strontium-doped bioactive glass on the differentiation of cultured osteogenic cells. Eur Cell Mater 2011;21:130–43.

[146] Sekine K, Sakama M, Hamada K. Evaluation of strontium introduced apatite cement as the injectable bone substitute developments. Conf Proc IEEE Eng Med Biol Soc 2013;2013:858–61. doi:10.1109/EMBC.2013.6609636.

[147] Cardemil C, Elgali I, Xia W, Emanuelsson L, Norlindh B, Omar O, *et al*. Strontium-doped calcium phosphate and hydroxyapatite granules promote different inflammatory and bone remodelling responses in normal and ovariectomised rats. PLoS One 2013;8:e84932. doi:10.1371/journal.pone.0084932.

[148] Li Y, Li Q, Zhu S, Luo E, Li J, Feng G, *et al*. The effect of strontium-substituted hydroxyapatite coating on implant fixation in ovariectomized rats. Biomaterials 2010;31:9006–14. doi:10.1016/j.biomaterials.2010.07.112.

[149] Thormann U, Ray S, Sommer U, Elkhassawna T, Rehling T, Hundgeburth M, *et al*. Bone formation induced by strontium modified calcium phosphate cement in critical-size metaphyseal fracture defects in ovariectomized rats. Biomaterials 2013;34:8589–98. doi:10.1016/j.biomaterials.2013.07.036.

[150] Gentleman E, Fredholm YC, Jell G, Lotfibakhshaiesh N, Donnell MDO, Hill RG, *et al*. The effects of strontium-substituted bioactive glasses on osteoblasts and osteoclasts in vitro. Biomaterials 2010;31:3949–56. doi:10.1016/j.biomaterials.2010.01.121.

[151] Wong CT, Lu WW, Chan WK, Cheung KMC, Luk KDK, Lu DS, *et al*. In vivo cancellous bone remodeling on a strontium-containing hydroxyapatite (sr-HA) bioactive cement. J Biomed Mater Res A 2004;68:513–21. doi:10.1002/jbm.a.20089.

[152] Boanini E, Torricelli P, Fini M, Bigi a. Osteopenic bone cell response to strontium-substituted hydroxyapatite. J Mater Sci Mater Med 2011;22:2079–88. doi:10.1007/s10856-011-4379-3.

[153] Landi E, Tampieri A, Celotti G, Sprio S, Sandri M, Logroscino G. Sr-substituted hydroxyapatites for osteoporotic bone replacement. Acta Biomater 2007;3:961–9. doi:10.1016/j.actbio.2007.05.006.

[154] Yoon B-H, Kim H-W, Lee S-H, Bae C-J, Koh Y-H, Kong Y-M, *et al*. Stability and cellular responses to fluorapatite-collagen composites. Biomaterials 2005;26:2957–63. doi:10.1016/j.biomaterials.2004.07.062.

[155] Monjo M, Lamolle SF, Lyngstadaas SP, Rønold HJ, Ellingsen JE. In vivo expression of osteogenic markers and bone mineral density at the surface of fluoride-modified titanium implants. Biomaterials 2008;29:3771–80. doi:10.1016/j.biomaterials.2008.06.001.

[156] Inoue M, Rodriguez AP, Nagai N, Nagatsuka H, LeGeros RZ, Tsujigiwa H, *et al*. Effect of fluoride-substituted apatite on in vivo bone formation. J Biomater Appl 2011;25:811–24. doi:10.1177/0885328209357109.

[157] Cooper LF, Zhou Y, Takebe J, Guo J, Abron A, Holmén A, *et al*. Fluoride modification effects on osteoblast behavior and bone formation at TiO2 grit-blasted c.p. titanium endosseous implants. Biomaterials 2006;27:926–36. doi:10.1016/j.biomaterials.2005.07.009.

[158] Julien M, Khairoun I, LeGeros RZ, Delplace S, Pilet P, Weiss P, *et al*. Physico-chemical-mechanical and in vitro biological properties of calcium phosphate cements with doped amorphous calcium phosphates. Biomaterials 2007;28:956–65. doi:10.1016/j.biomaterials.2006.10.018.

[159] Otsuka M, Oshinbe A, Legeros RZ, Tokudome Y, Ito A, Otsuka K, *et al*. Efficacy of the injectable calcium phosphate ceramics suspensions containing magnesium, zinc and fluoride on the bone mineral deficiency in ovariectomized rats. J Pharm Sci 2008;97:421–32. doi:10.1002/jps.21131.

[160] Ito T, Racquel Z, Takemasa M, Tokudome Y, Uchino T, Ito A, *et al*. Effect of calcium phosphate compound (MZF-CaP) with and without fluoride in preventing bone loss in ovariectomized rats. Int J Drug Deliv 2013;5:412–9. doi:10.5138/ijdd.v5i4.1088.

[161] Habibovic P, Barralet JE. Bioinorganics and biomaterials: bone repair. Acta Biomater 2011;7:3013–26. doi:10.1016/j.actbio.2011.03.027.

[162] Patel N, Best SM, Bonfield W, Gibson IR, Hing KA, Damien E, *et al*. A comparative study on the in vivo behavior of hydroxyapatite and silicon substituted hydroxyapatite granules. J Mater Sci Mater Med 2002;13:1199–206.

[163] Hing KA, Wilson LF, Buckland T. Comparative performance of three ceramic bone graft substitutes. Spine J n.d.;7:475–90. doi:10.1016/j.spinee.2006.07.017.

[164] Pimenta L, Pesántez CFA, Oliveira L. Silicon Matrix Calcium Phosphate as a Bone Substitute: Early Clinical and Radiological Results in a Prospective Study With 12-Month Follow-up. SAS J 2008;2:62–8. doi:10.1016/S1935-9810(08)70020-3.

[165] Mieszawska AJ, Fourligas N, Georgakoudi I, Ouhib NM, Belton DJ, Perry CC, *et al*. Osteoinductive silk-silica composite biomaterials for bone regeneration. Biomaterials 2010;31:8902–10. doi:10.1016/j.biomaterials.2010.07.109.

[166] Bohner M. Silicon-substituted calcium phosphates - a critical view. Biomaterials 2009;30:6403–6. doi:10.1016/j.biomaterials.2009.08.007.

[167] Coathup MJ, Samizadeh S, Fang YS, Buckland T, Hing KA, Blunn GW. The osteoinductivity of silicate-substituted calcium phosphate. J Bone Joint Surg Am 2011;93:2219–26. doi:10.2106/JBJS.I.01623.

[168] Fujii E, Ohkubo M, Tsuru K, Hayakawa S, Osaka A, Kawabata K, *et al*. Selective protein adsorption property and characterization of nano-crystalline zinc-containing hydroxyapatite. Acta Biomater 2006;2:69–74. doi:10.1016/j.actbio.2005.09.002.

[169] Buchanan FJ, editor. Degradation Rate of Bioresorbable Materials. Cambridge: Woodhead Publishing limited; 2008.

[170] Driessens FC. Physiology of hard tissues in comparison with the solubility of synthetic calcium phosphates. Ann N Y Acad Sci 1988;523:131–6.

[171] Klein CP, de Blieck-Hogervorst JM, Wolke JG, de Groot K. Studies of the solubility of different calcium phosphate ceramic particles in vitro. Biomaterials 1990;11:509–12.

[172] Kwon S, Jun Y, Hong S, Kim H. Synthesis and dissolution behavior of β-TCP and HA/β-TCP composite powders. J Eur Ceram Soc 2003;23:1039–45. doi:10.1016/S0955-2219(02)00263-7.

[173] Dorozhkin S V. A Review on the Dissolution Models of Calcium Apatites 2002;8974:4–9.

[174] Bohner M, Galea L, Doebelin N. Calcium phosphate bone graft substitutes: Failures and hopes. J Eur Ceram Soc 2012;32:2663–71. doi:10.1016/j.jeurceramsoc.2012.02.028.

[175] Schilling AF, Linhart W, Filke S, Gebauer M, Schinke T, Rueger JM, *et al*. Resorbability of bone substitute biomaterials by human osteoclasts. Biomaterials 2004;25:3963–72. doi:10.1016/j.biomaterials.2003.10.079.

[176] Kanatani M, Sugimoto T, Fukase M, Fujita T. Effect of elevated extracellular calcium on the proliferation of osteoblastic MC3T3-E1 cells:its direct and indirect effects via monocytes. Biochem Biophys Res Commun 1991;181:1425–30.

[177] Zaidi M, Datta HK, Patchell A, Moonga B, MacIntyre I. “Calcium-activated” intracellular calcium elevation: a novel mechanism of osteoclast regulation. Biochem Biophys Res Commun 1989;163:1461–5.

[178] Hamdan M, Moseke C, Blanco L, Barralet JE, Lopez-carbacos E, Gbureck U. Biomaterials Strontium modified biocements with zero order release kinetics. Biomaterials 2008;29:4691–7. doi:10.1016/j.biomaterials.2008.08.026.

[179] Pan HB, Li ZY, Lam WM, Wong JC, Darvell BW, Luk KDK, *et al*. Solubility of strontium-substituted apatite by solid titration. Acta Biomater 2009;5:1678–85. doi:10.1016/j.actbio.2008.11.032.

[180] Fukui N, Sato T, Kuboki Y, Aoki H. Bone tissue reaction of nano-hydroxyapatite/collagen composite at the early stage of implantation. Biomed Mater Eng 2008;18:25–33.

[181] Du C, Cui FZ, Feng QL, Zhu XD, de Groot K. Tissue response to nano-hydroxyapatite/collagen composite implants in marrow cavity. J Biomed Mater Res 1998;42:540–8.

[182] Venkatasubbu GD, Ramasamy S, Ramakrishnan V, Kumar J. Hydroxyapatite-Alginate Nanocomposite as Drug Delivery Matrix for Sustained Release of Ciprofloxacin. J Biomed Nanotechnol 2011;7:759–67. doi:10.1166/jbn.2011.1350.

[183] Li H, Gong M, Yang A, Ma J, Li X, Yan Y. Degradable biocomposite of nano calcium-deficient hydroxyapatite-multi(amino acid) copolymer. Int J Nanomedicine 2012;7:1287–95. doi:10.2147/IJN.S28978.

[184] Huang M, Feng J, Wang J, Zhang X, Li Y, Yan Y. Synthesis and characterization of nano-HA/PA66 composites. J Mater Sci Mater Med 2003;14:655–60.

[185] Barbieri D, de Bruijn JD, Luo X, Farè S, Grijpma DW, Yuan H. Controlling dynamic mechanical properties and degradation of composites for bone regeneration by means of filler content. J Mech Behav Biomed Mater 2013;20:162–72. doi:10.1016/j.jmbbm.2013.01.012.

[186] Singh S, Ray SS. Polylactide based nanostructured biomaterials and their applications. J Nanosci Nanotechnol 2007;7:2596–615.

[187] Beslikas T, Gigis I, Goulios V, Christoforides J, Papageorgiou GZ, Bikiaris DN. Crystallization study and comparative in vitro-in vivo hydrolysis of PLA reinforcement ligament. Int J Mol Sci 2011;12:6597–618. doi:10.3390/ijms12106597.

[188] Lasprilla AJR, Martinez G a R, Lunelli BH, Jardini AL, Filho RM. Poly-lactic acid synthesis for application in biomedical devices - a review. Biotechnol Adv 2012;30:321–8. doi:10.1016/j.biotechadv.2011.06.019.

[189] Deng X, Hao J, Wang C. Preparation and mechanical properties of nanocomposites of poly(D,L-lactide) with Ca-deficient hydroxyapatite nanocrystals. Biomaterials 2001;22:2867–73.

[190] Nejati E, Mirzadeh H, Zandi M. Synthesis and characterization of nano-hydroxyapatite rods/poly(l-lactide acid) composite scaffolds for bone tissue engineering. Compos Part A Appl Sci Manuf 2008;39:1589–96. doi:10.1016/j.compositesa.2008.05.018.

[191] Lin P-L, Fang H-W, Tseng T, Lee W-H. Effects of hydroxyapatite dosage on mechanical and biological behaviors of polylactic acid composite materials. Mater Lett 2007;61:3009–13. doi:10.1016/j.matlet.2006.10.064.

[192] Wei G, Ma PX. Structure and properties of nano-hydroxyapatite/polymer composite scaffolds for bone tissue engineering. Biomaterials 2004;25:4749–57. doi:10.1016/j.biomaterials.2003.12.005.

[193] Lim L-T, Auras R, Rubino M. Processing technologies for poly(lactic acid). Prog Polym Sci 2008;33:820–52. doi:10.1016/j.progpolymsci.2008.05.004.

[194] Gunning MA, Geever LM, Killion JA, Lyons JG, Higginbotham CL. Improvement in mechanical properties of grafted polylactic acid composite fibers via hot melt extrusion. Polym Compos 2014;35:1792–7. doi:10.1002/pc.22833.

[195] Kawamura H, Ito A, Miyakawa S, Layrolle P, Ojima K, Ichinose N, *et al*. Stimulatory effect of zinc-releasing calcium phosphate implant on bone formation in rabbit femora. J Biomed Mater Res 2000;50:184–90. doi:10.1002/(SICI)1097-4636(200005)50:2<184::AID-JBM13>3.0.CO;2-3.

[196] Staiger MP, Pietak AM, Huadmai J, Dias G. Magnesium and its alloys as orthopedic biomaterials: A review. Biomaterials 2006;27:1728–34. doi:10.1016/j.biomaterials.2005.10.003.

[197] Kuang G-M, Yau WP, Wu J, Yeung KWK, Pan H, Lam WM, *et al*. Strontium exerts dual effects on calcium phosphate cement: Accelerating the degradation and enhancing the osteoconductivity both in vitro and in vivo. J Biomed Mater Res A 2015;103:1613–21. doi:10.1002/jbm.a.35298.

[198] Ikeuchi M, Ito A, Dohi Y, Ohgushi H, Shimaoka H, Yonemasu K, *et al*. Osteogenic differentiation of cultured rat and human bone marrow cells on the surface of zinc-releasing calcium phosphate ceramics. J Biomed Mater Res A 2003;67:1115–22. doi:10.1002/jbm.a.10041.

[199] Yang F, Yang D, Tu J, Zheng Q, Cai L, Wang L. Strontium enhances osteogenic differentiation of mesenchymal stem cells and in vivo bone formation by activating Wnt/catenin signaling. Stem Cells 2011;29:981–91. doi:10.1002/stem.646.

[200] Nuttall ME, Gimble JM. Is there a therapeutic opportunity to either prevent or treat osteopenic disorders by inhibiting marrow adipogenesis? Bone 2000;27:177–84.

[201] Mark Percival. Bone Health & Osteoporosis. Appied Nutr Sci Reports 1999;5:1–6.

[202] Reginster JY, Seeman E, De Vernejoul MC, Adami S, Compston J, Phenekos C, *et al*. Strontium ranelate reduces the risk of nonvertebral fractures in postmenopausal women with osteoporosis: Treatment of Peripheral Osteoporosis (TROPOS) study. J Clin Endocrinol Metab 2005;90:2816–22. doi:10.1210/jc.2004-1774.

[203] Tadashi Kokubo. Bioceramics and Their Clinical Applications. 1st ed. London: CRC Press; 2008.

[204] Vitamin and mineral requirements in human nutrition : report of a joint FAO/WHO expert consultation chapter 12. Bangkok,Thailand: 1998.

[205] Eberle J, Schmidmayer S, Erben RG, Stangassinger M, Roth HP. Skeletal effects of zinc deficiency in growing rats. J Trace Elem Med Biol 1999;13:21–6. doi:10.1016/S0946-672X(99)80019-4.

[206] RELEA P, REVILLA M, RIPOLL E, ARRIBAS I, VILLA LF, RICO H. Zinc, Biochemical Markers of Nutrition, and Type I Osteoporosis. Age Ageing 1995;24:303–7. doi:10.1093/ageing/24.4.303.

[207] Atik OS. Zinc and senile osteoporosis. J Am Geriatr Soc 1983;31:790–1.

[208] Ishikawa K, Miyamoto Y, Yuasa T, Ito A, Nagayama M, Suzuki K. Fabrication of Zn containing apatite cement and its initial evaluation using human osteoblastic cells. Biomaterials 2002;23:423–8.

[209] Doty SB, Jones KW, Kraner HW, Shroy RE, Hanson AL. Proton microprobe analysis of zinc in skeletal tissues. Nucl Instruments Methods 1981;181:159–64. doi:10.1016/0029-554X(81)90599-1.

[210] Mansilla E, Marín GH, Drago H, Sturla F, Salas E, Gardiner C, *et al*. Bloodstream cells phenotypically identical to human mesenchymal bone marrow stem cells circulate in large amounts under the influence of acute large skin damage: new evidence for their use in regenerative medicine. Transplant Proc 2006;38:967–9. doi:10.1016/j.transproceed.2006.02.053.

[211] Minguell JJ, Erices A, Conget P, Onget PAC. Mesenchymal Stem Cells. Exp Biol Med 2001;226:507–20.

[212] Boyce BF, Yao Z, Zhang Q, Guo R, Lu Y, Schwarz EM, *et al*. New roles for osteoclasts in bone. Ann N Y Acad Sci 2007;1116:245–54. doi:10.1196/annals.1402.084.

[213] Arinzeh TL, Tran T, Mcalary J, Daculsi G. A comparative study of biphasic calcium phosphate ceramics for human mesenchymal stem-cell-induced bone formation. Biomaterials 2005;26:3631–8. doi:10.1016/j.biomaterials.2004.09.035.

[214] Wang C, Duan Y, Markovic B, Barbara J, Howlett CR, Zhang X, *et al*. Phenotypic expression of bone-related genes in osteoblasts grown on calcium phosphate ceramics with different phase compositions. Biomaterials 2004;25:2507–14.

[215] Kurashina K, Kurita H, Wu Q, Ohtsuka a, Kobayashi H. Ectopic osteogenesis with biphasic ceramics of hydroxyapatite and tricalcium phosphate in rabbits. Biomaterials 2002;23:407–12.

[216] Marchisio M, Di Carmine M, Pagone R, Piattelli A, Miscia S. Implant surface roughness influences osteoclast proliferation and differentiation. J Biomed Mater Res B Appl Biomater 2005;75:251–6. doi:10.1002/jbm.b.30287.

[217] Brinkmann J, Hefti T, Schlottig F, Spencer ND, Hall H. Response of osteoclasts to titanium surfaces with increasing surface roughness: an in vitro study. Biointerphases 2012;7:34. doi:10.1007/s13758-012-0034-x.

[218] Ross AM, Jiang Z, Bastmeyer M, Lahann J. Physical aspects of cell culture substrates: topography, roughness, and elasticity. Small 2012;8:336–55. doi:10.1002/smll.201100934.

[219] Watari S, Hayashi K, Wood JA, Russell P, Nealey PF, Murphy CJ, *et al*. Modulation of osteogenic differentiation in hMSCs cells by submicron topographically-patterned ridges and grooves. Biomaterials 2012;33:128–36. doi:10.1016/j.biomaterials.2011.09.058.

[220] McNamara LE, McMurray RJ, Biggs MJP, Kantawong F, Oreffo ROC, Dalby MJ. Nanotopographical control of stem cell differentiation. J Tissue Eng 2010;2010:120623. doi:10.4061/2010/120623.

[221] Schwartz Z, Lohmann CH, Oefinger J, Bonewald LF, Dean DD, Boyan BD. Implant surface characteristics modulate differentiation behavior of cells in the osteoblastic lineage. Adv Dent Res 1999;13:38–48.

[222] Fratzl P, Gupta HS, Paschalis EP, Roschger P. Structure and mechanical quality of the collagen mineral nano-composite in bone. J Mater Chem 2004;14:2115. doi:10.1039/b402005g.

[223] Xin R, Leng Y, Wang N. HRTEM Study of the Mineral Phases in Human Cortical Bone. Adv Eng Mater 2010;12:B552–7. doi:10.1002/adem.200980080.

[224] Hong SI, Hong SK, Kohn DH. Nanostructural analysis of trabecular bone. J Mater Sci Mater Med 2009;20:1419–26. doi:10.1007/s10856-009-3708-2.

[225] Reis RL, Weiner S, editors. Learning from nature how to design new implantable biomaterialsis: from biomineralization fundamentals to biomimetic materials and processing routes. vol. 171. Dordrecht: Kluwer Academic Publishers; 2005. doi:10.1007/1-4020-2648-X.

[226] Shehab D, Elgazzar AH, Collier BD. Heterotopic ossification. J Nucl Med 2002;43:346–53.
[227] Verheyen CC, de Wijn JR, van Blitterswijk CA, de Groot K, Rozing PM. Hydroxylapatite/poly(L-lactide) composites: an animal study on push-out strengths and interface histology. J Biomed Mater Res 1993;27:433–44. doi:10.1002/jbm.820270404.
[228] Luo X, Barbieri D, Davison N, Yan Y, de Bruijn JD, Yuan H. Zinc in calcium phosphate mediates bone induction: in vitro and in vivo model. Acta Biomater 2014;10:477–85. doi:10.1016/j.actbio.2013.10.011.
[229] Landis WJ. The strength of a calcified tissue depends in part on the molecular structure and organization of its constituent mineral crystals in their organic matrix. Bone 1995;16:533–44.
[230] Shorr E, Carter AC. The usefulness of strontium as an adjuvant to calcium in the remineralization of the skeleton in man. Bull Hosp Joint Dis 1952;13:59–66.
[231] Chavassieux P. Bone effects of fluoride in animal models in vivo. A review and a recent study. J Bone Miner Res 1990;5 Suppl 1:S95–9.
[232] Lau KH, Baylink DJ. Molecular mechanism of action of fluoride on bone cells. J Bone Miner Res 1998;13:1660–7. doi:10.1359/jbmr.1998.13.11.1660.
[233] Marie PJ, Hott M. Short-term effects of fluoride and strontium on bone formation and resorption in the mouse. Metabolism 1986;35:547–51.
[234] Riggs BL, Hodgson SF, Hoffman DL, Kelly PJ, Johnson KA, Taves D. Treatment of primary osteoporosis with fluoride and calcium. Clinical tolerance and fracture occurrence. JAMA 1980;243:446–9.
[235] Riggs BL, Seeman E, Hodgson SF, Taves DR, O'Fallon WM. Effect of the fluoride/calcium regimen on vertebral fracture occurrence in postmenopausal osteoporosis. Comparison with conventional therapy. N Engl J Med 1982;306:446–50. doi:10.1056/NEJM198202253060802.
[236] Gutowska I, Baranowska-Bosiacka I, Safranow K, Jakubowska K, Olszewska M, Telesiński a, *et al*. Fluoride in low concentration modifies expression and activity of 15 lipoxygenase in human PBMC differentiated monocyte/macrophage. Toxicology 2012;295:23–30. doi:10.1016/j.tox.2012.02.014.
[237] D.R. Simpson. substitution in apatite： low temperature fluoride-hydroxyl apatite. Am Mineral 1968;vol.53:1953–64.
[238] Meurl S, Srupson DR. Fluoride in Apatite : Substitution of Monofluorophosphate for Orthophosphate. Am Miner 1975;60:134–8.

[239] Siparsky GL, Voorhees KJ, Miao F. Hydrolysis of Polylactic Acid (PLA) and Polycaprolactone (PCL) in Aqueous Acetonitrile Solutions : Autocatalysis. J Environ Polym Degrad 1998;6:31–41.

[240] Kokubo T, Takadama H. How useful is SBF in predicting in vivo bone bioactivity? Biomaterials 2006;27:2907–15. doi:10.1016/j.biomaterials.2006.01.017.

[241] Song G, Habibovic P, Bao C, Hu J, van Blitterswijk C a, Yuan H, *et al*. The homing of bone marrow MSCs to non-osseous sites for ectopic bone formation induced by osteoinductive calcium phosphate. Biomaterials 2013;34:2167–76. doi:10.1016/j.biomaterials.2012.12.010.

[242] Kondo N, Ogose A, Tokunaga K, Umezu H, Arai K, Kudo N, *et al*. Osteoinduction with highly purified beta-tricalcium phosphate in dog dorsal muscles and the proliferation of osteoclasts before heterotopic bone formation. Biomaterials 2006;27:4419–27. doi:10.1016/j.biomaterials.2006.04.016.

[243] Akiyama N, Takemoto M, Fujibayashi S, Neo M, Hirano M, Nakamura T. Difference between dogs and rats with regard to osteoclast-like cells in calcium-deficient hydroxyapatite-induced osteoinduction. J Biomed Mater Res A 2011;96:402–12. doi:10.1002/jbm.a.32995.

[244] Kimoto K, Okudera T, Okudera H, Nordquist WD, Krutchkoff DJ. Part I: crystalline fluorapatite-coated hydroxyapatite, physical properties. J Oral Implantol 2011;37:27–33. doi:10.1563/AAID-JOI-D-09-00118.1.

[245] Teti A. Mechanisms of osteoclast-dependent bone formation. Bonekey Rep 2013;2. doi:10.1038/bonekey.2013.183.

[246] Takeshita S, Fumoto T, Matsuoka K, Park K, Aburatani H, Kato S, *et al*. Osteoclast-secreted CTHRC1 in the coupling of bone resorption to formation. J Clin Invest 2013;123:3914–24. doi:10.1172/JCI69493DS1.

[247] Spicer PP, Kretlow JD, Young S, Jansen JA, Kasper FK, Mikos AG. Evaluation of bone regeneration using the rat critical size calvarial defect. Nat Protoc 2012;7:1918–29. doi:10.1038/nprot.2012.113.

[248] Loty C, Sautier J, Boulekbache H, Kokubo T, Kim H, Forest N. In vitro bone formation on a bone-like apatite layer prepared by a biomimetic process on a bioactive glass – ceramic 1999.

[249] Kokubo T. Formation of biologically active bone-like apatite on metals and polymers by a biomimetic process. Thermochim Acta 1996;280-281:479–90. doi:10.1016/0040-6031(95)02784-X.

[250] Surgery O. Apatite coating on ceramics , metals and polymers utilizing a biological process 1990:233–8.

[251] Wang L, Zhang B, Bao C, Habibovic P, Hu J, Zhang X. Ectopic osteoid and bone formation by three calcium-phosphate ceramics in rats, rabbits and dogs. PLoS One 2014;9:e107044. doi:10.1371/journal.pone.0107044.

[252] Habibovic P, Gbureck U, Doillon CJ, Bassett DC, van Blitterswijk C a, Barralet JE. Osteoconduction and osteoinduction of low-temperature 3D printed bioceramic implants. Biomaterials 2008;29:944–53. doi:10.1016/j.biomaterials.2007.10.023.

[253] Ma PX, Choi JW. Biodegradable polymer scaffolds with well-defined interconnected spherical pore network. Tissue Eng 2001;7:23–33. doi:10.1089/107632701300003269.

[254] Tanaka M, Sato K, Kitakami E, Kobayashi S, Hoshiba T, Fukushima K. Design of biocompatible and biodegradable polymers based on intermediate water concept. Polym J 2014;47:114–21. doi:10.1038/pj.2014.129.

[255] Luo X, Barbieri D, Passanisi G, Yuan H, de Bruijn JD. Influence of fluoride in poly(d,l-lactide)/apatite composites on bone formation. J Biomed Mater Res B Appl Biomater 2015;103:841–52. doi:10.1002/jbm.b.33255.

[256] Peng S, Liu XS, Wang T, Li Z, Zhou G, Luk KDK, *et al*. In vivo anabolic effect of strontium on trabecular bone was associated with increased osteoblastogenesis of bone marrow stromal cells. J Orthop Res 2010;28:1208–14. doi:10.1002/jor.21127.

[257] Purac Biomaterials. Inherent viscosity and molecular weight correlations. Datasheet 03 2010:Rev. NO. 1.

[258] Li ZY, Lam WM, Yang C, Xu B, Ni GX, Abbah S a, *et al*. Chemical composition, crystal size and lattice structural changes after incorporation of strontium into biomimetic apatite. Biomaterials 2007;28:1452–60. doi:10.1016/j.biomaterials.2006.11.001.

[259] Verberckmoes SC, Behets GJ, Oste L, Bervoets a R, Lamberts L V, Drakopoulos M, *et al*. Effects of strontium on the physicochemical characteristics of hydroxyapatite. Calcif Tissue Int 2004;75:405–15. doi:10.1007/s00223-004-0260-4.

[260] Christoffersen J, Christoffersen MR, Kolthoff N, Bärenholdt O. Effects of strontium ions on growth and dissolution of hydroxyapatite and on bone mineral detection. Bone 1997;20:47–54.

[261] Rokidi S, Koutsoukos PG. Crystal growth of calcium phosphates from aqueous solutions in the presence of strontium. Chem Eng Sci 2012;77:157–64. doi:10.1016/j.ces.2012.02.049.

[262] Andrew J. Peacock ARC. Polymer chemistry: properties and applications. 2006.

[263] Makadia HK, Siegel SJ. Poly Lactic-co-Glycolic Acid (PLGA) as Biodegradable Controlled Drug Delivery Carrier. Polymers (Basel) 2011;3:1377–97. doi:10.3390/polym3031377.

[264] Blomqvist J, Mannfors B, Pietilä L-O. Amorphous cell studies of polyglycolic, poly(L-lactic), poly(L,D-lactic) and poly(glycolic/L-lactic) acids. Polymer (Guildf) 2002;43:4571–83. doi:10.1016/S0032-3861(02)00312-9.

[265] Korsmeyer RW, Gurny R, Doelker E, Buri P, Peppas NA. Mechanisms of solute release from porous hydrophilic polymers. Int J Pharm 1983;15:25–35. doi:10.1016/0378-5173(83)90064-9.

[266] Welldon KJ, Findlay DM, Evdokiou A, Ormsby RT, Atkins GJ. Calcium induces pro-anabolic effects on human primary osteoblasts associated with acquisition of mature osteocyte markers. Mol Cell Endocrinol 2013;376:85–92. doi:10.1016/j.mce.2013.06.013.

[267] Karageorgiou V, Kaplan D. Porosity of 3D biomaterial scaffolds and osteogenesis. Biomaterials 2005;26:5474–91. doi:10.1016/j.biomaterials.2005.02.002.

[268] Reginster J-. Strontium Ranelate in Osteoporosis. Curr Pharm Des 2002;8:1907–16. doi:10.2174/1381612023393639.

[269] Meunier PJ, Roux C, Ortolani S, Diaz-Curiel M, Compston J, Marquis P, *et al*. Effects of long-term strontium ranelate treatment on vertebral fracture risk in postmenopausal women with osteoporosis. Osteoporos Int 2009;20:1663–73. doi:10.1007/s00198-008-0825-6.

[270] Carnevale V, Del Fiacco R, Romagnoli E, Fontana A, Cipriani C, Pepe J, *et al*. Effects of strontium ranelate administration on calcium metabolism in female patients with postmenopausal osteoporosis and primary hyperparathyroidism. Calcif Tissue Int 2013;92:15–22. doi:10.1007/s00223-012-9659-5.

[271] Reginster J-Y, Felsenberg D, Boonen S, Diez-Perez A, Rizzoli R, Brandi M-L, *et al*. Effects of long-term strontium ranelate treatment on the risk of nonvertebral and vertebral fractures in postmenopausal osteoporosis: Results of a five-year, randomized, placebo-controlled trial. Arthritis Rheum 2008;58:1687–95. doi:10.1002/art.23461.

[272] D'Haese PC, Schrooten I, Goodman WG, Cabrera WE, Lamberts L V, Elseviers MM, *et al*. Increased bone strontium levels in hemodialysis patients with osteomalacia. Kidney Int 2000;57:1107–14. doi:10.1046/j.1523-1755.2000.00938.x.

[273] Schrooten I, Elseviers MM, Lamberts L V, De Broe ME, D'Haese PC. Increased serum strontium levels in dialysis patients: an epidemiological survey. Kidney Int 1999;56:1886–92. doi:10.1046/j.1523-1755.1999.00740.x.

[274] Osborne V, Layton D, Perrio M, Wilton L, Shakir SAW. Incidence of venous thromboembolism in users of strontium ranelate: an analysis of data from a prescription-event monitoring study in England. Drug Saf 2010;33:579–91. doi:10.2165/11533770-000000000-00000.

[275] Kramkimel N, Sibon C, Le Beller C, Saiag P, Mahé E. Bullous DRESS in a patient on strontium ranelate. Clin Exp Dermatol 2009;34:e349–50. doi:10.1111/j.1365-2230.2009.03302.x.

[276] Iyer D, Buggy Y, O'Reilly K, Searle M. Strontium ranelate as a cause of acute renal failure and dress syndrome. Nephrology (Carlton) 2009;14:624. doi:10.1111/j.1440-1797.2009.01125.x.

[277] Bergmann J-F. Strontium ranelate(Protelos®): who really benefits of the doubt? Presse Med 2011;40:893–4. doi:10.1016/j.lpm.2011.07.011.

[278] Jonville-Béra a P, Crickx B, Aaron L, Hartingh I, Autret-Leca E. Strontium ranelate-induced DRESS syndrome: first two case reports. Allergy 2009;64:658–9. doi:10.1111/j.1398-9995.2009.01940.x.

[279] European medicines agency. Recommendation to restrict the use of Protelos/Osseor (strontium ranelate)； CHMP confirms recommendation from the PRAC 2013.

[280] European medicines agency. European Medicines Agency recommends that Protelos / Osseor remain available but with further restrictions 2014.

[281] European medicines agency. Summary of the European public assessment report (EPAR) for Protelos 2014:0–2.

[282] Torricelli P, Fini M, Giavaresi G, Giardino R. In vitro models to test orthopedic biomaterials in view of their clinical application in osteoporotic bone. Int J Artif Organs 2004;27:658–63.

[283] Kim H-W, Koh Y-H, Kong Y-M, Kang J-G, Kim H-E. Strontium substituted calcium phosphate biphasic ceramics obtained by a powder precipitation method. J Mater Sci Mater Med 2004;15:1129–34. doi:10.1023/B:JMSM.0000046395.76435.60.

[284] El Feki H, Rey C, Vignoles M. Carbonate ions in apatites: infrared investigations in the upsilon 4 CO3 domain. Calcif Tissue Int 1991;49:269–74.

[285] Ripamonti U. Osteoinduction in porous hydroxyapatite implanted in heterotopic sites of different animal models. Biomaterials 1996;17:31–5. doi:10.1016/0142-9612(96)80752-6.

[286] Yuan H, van Blitterswijk CA, de Groot K, de Bruijn JD. Cross-species comparison of ectopic bone formation in biphasic calcium phosphate (BCP) and hydroxyapatite (HA) scaffolds. Tissue Eng 2006;12:1607–15. doi:10.1089/ten.2006.12.1607.

[287] Li Y, Feng G, Gao Y, Luo E, Liu X, Hu J. Strontium ranelate treatment enhances hydroxyapatite-coated titanium screws fixation in osteoporotic rats. J Orthop Res 2010;28:578–82. doi:10.1002/jor.21050.

[288] Delannoy P, Bazot D, Marie PJ. Long-term treatment with strontium ranelate increases vertebral bone mass without deleterious effect in mice. Metabolism 2002;51:906–11. doi:10.1053/meta.2002.33360.

[289] Buehler J, Chappuis P, Saffar J., Tsouderos Y, Vignery A. Strontium ranelate inhibits bone resorption while maintaining bone formation in alveolar bone in monkeys (Macaca fascicularis). Bone 2001;29:176–9. doi:10.1016/S8756-3282(01)00484-7.

[290] Marie PJ, Hott M, Modrowski D, De Pollak C, Guillemain J, Deloffre P, *et al*. An uncoupling agent containing strontium prevents bone loss by depressing bone resorption and maintaining bone formation in estrogen-deficient rats. J Bone Miner Res 1993;8:607–15. doi:10.1002/jbmr.5650080512.

[291] Bain SD, Jerome C, Shen V, Dupin-Roger I, Ammann P. Strontium ranelate improves bone strength in ovariectomized rat by positively influencing bone resistance determinants. Osteoporos Int 2009;20:1417–28. doi:10.1007/s00198-008-0815-8.

[292] Beck G. Inorganic phosphate regulates multiple genes during osteoblast differentiation, including Nrf2. Exp Cell Res 2003;288:288–300. doi:10.1016/S0014-4827(03)00213-1.

[293] Renkema KY, Alexander RT, Bindels RJ, Hoenderop JG. Calcium and phosphate homeostasis: concerted interplay of new regulators. Ann Med 2008;40:82–91. doi:10.1080/07853890701689645.

[294] Mundy GR, Guise T a. Hormonal control of calcium homeostasis. Clin Chem 1999;45:1347–52.

[295] Cummings SR, Kelsey JL, Nevitt MC, O'Dowd KJ. Epidemiology of osteoporosis and osteoporotic fractures. Epidemiol Rev 1985;7:178–208.

[296] Fini M, Giavaresi G, Torricelli P, Krajewski a., Ravaglioli a., Belmonte MM, et al. Biocompatibility and osseointegration in osteoporotic bone. J Bone Jt Surg 2001;83:139–43. doi:10.1302/0301-620X.83B1.10162.

[297] Fini M, Giavaresi G, Torricelli P, Borsari V, Giardino R, Nicolini a, *et al*. Osteoporosis and biomaterial osteointegration. Biomed Pharmacother 2004;58:487–93. doi:10.1016/j.biopha.2004.08.016.

[298] Luo X, Barbieri D, Zhang Y, Yan Y, Bruijn J de, Yuan H. Strontium-Containing Apatite/Poly Lactide Composites Favoring Osteogenic Differentiation and in Vivo Bone Formation. ACS Biomater Sci Eng 2015;1:85–93. doi:10.1021/ab500005e.

[299] Castañeda S, Calvo E, Largo R, González-González R, de la Piedra C, Díaz-Curiel M, *et al*. Characterization of a new experimental model of osteoporosis in rabbits. J Bone Miner Metab 2008;26:53–9. doi:10.1007/s00774-007-0797-1.

[300] Baofeng L, Zhi Y, Bei C, Guolin M, Qingshui Y, Jian L. Characterization of a rabbit osteoporosis model induced by ovariectomy and glucocorticoid. Acta Orthop 2010;81:396–401. doi:10.3109/17453674.2010.483986.

[301] Isaksson H, Harjula T, Koistinen A, Iivarinen J, Sepp̈anen K, Arokoski JPA, *et al*. Collagen and mineral deposition in rabbit cortical bone during maturation and growth: Effects on tissue properties. J Orthop Res 2010;28:1626–33. doi:10.1002/jor.21186.

[302] Kato M, Toyoda H, Namikawa T, Hoshino M, Terai H, Miyamoto S, *et al*. Optimized use of a biodegradable polymer as a carrier material for the local delivery of recombinant human bone morphogenetic protein-2 (rhBMP-2). Biomaterials 2006;27:2035–41. doi:10.1016/j.biomaterials.2005.10.007.

[303] Liu Y, de Groot K, Hunziker EB. BMP-2 liberated from biomimetic implant coatings induces and sustains direct ossification in an ectopic rat model. Bone 2005;36:745–57. doi:10.1016/j.bone.2005.02.005.

[304] Hartmann N, Martrette JM, Westphal A. Estrogen modulates estrogen receptor α and β expression, osteogenic activity, and apoptosis in mesenchymal stem cells (MSCs) of osteoporotic mice. J Cell Biochem 2001;81:144–55. doi:10.1002/jcb.1096.

[305] Turgeman G, Zilberman Y, Zhou S, Kelly P, Moutsatsos IK, Kharode YP, *et al*. Systemically administered rhBMP-2 promotes MSC activity and reverses bone and cartilage loss in osteopenic mice. J Cell Biochem 2002;86:461–74. doi:10.1002/jcb.10231.

[306] Julius Wolff. The Law of Bone Remodeling. Berlin Heidelberg New York: Springer; 1986.

[307] Burkhardt R, Kettner G, Böhm W, Schmidmeier M, Schlag R, Frisch B, *et al*. Changes in trabecular bone, hematopoiesis and bone marrow vessels in aplastic anemia, primary osteoporosis, and old age: a comparative histomorphometric study. Bone 1987;8:157–64.

[308] Justesen J, Stenderup K, Ebbesen EN, Mosekilde L, Steiniche T, Kassem M. Adipocyte tissue volume in bone marrow is increased with aging and in patients with osteoporosis. Biogerontology 2001;2:165–71.

[309] Meunier P, Aaron J, Edouard C, Vignon G. Osteoporosis and the replacement of cell populations of the marrow by adipose tissue. A quantitative study of 84 iliac bone biopsies. Clin Orthop Relat Res 1971;80:147–54.

[310] Patsch JM, Li X, Baum T, Yap SP, Karampinos DC, Schwartz A V, *et al*. Bone marrow fat composition as a novel imaging biomarker in postmenopausal women with prevalent fragility fractures. J Bone Miner Res 2013;28:1721–8. doi:10.1002/jbmr.1950.

[311] Rosen CJ, Bouxsein ML. Mechanisms of disease: is osteoporosis the obesity of bone? Nat Clin Pract Rheumatol 2006;2:35–43. doi:10.1038/ncprheum0070.

[312] Rodríguez JP, Astudillo P, Ríos S, Pino AM. Involvement of adipogenic potential of human bone marrow mesenchymal stem cells (MSCs) in osteoporosis. Curr Stem Cell Res Ther 2008;3:208–18.

[313] Pino AM, Rosen CJ, Rodríguez JP. In osteoporosis, differentiation of mesenchymal stem cells (MSCs) improves bone marrow adipogenesis. Biol Res 2012;45:279–87. doi:10.4067/S0716-97602012000300009.

[314] Astudillo P, Ríos S, Pastenes L, Pino AM, Rodríguez JP. Increased adipogenesis of osteoporotic human-mesenchymal stem cells (MSCs) characterizes by impaired leptin action. J Cell Biochem 2008;103:1054–65. doi:10.1002/jcb.21516.

[315] Saidak Z, Haÿ E, Marty C, Barbara A, Marie PJ. Strontium ranelate rebalances bone marrow adipogenesis and osteoblastogenesis in senescent osteopenic mice through NFATc/Maf and Wnt signaling. Aging Cell 2012;11:467–74. doi:10.1111/j.1474-9726.2012.00804.x.

[316] Włodarski KH, Galus R, Brodzikowska A, Włodarski PK. The adipocyte component of bone marrow in heterotopic bone induced by demineralized incisor grafts. Folia Histochem Cytobiol 2012;50:444–9. doi:10.5603/19755.

[317] Peng S, Zhang G, Zhang B-T, Guo B, He Y, Bakker AJ, *et al*. The beneficial effect of icaritin on osteoporotic bone is dependent on the treatment initiation timing in adult ovariectomized rats. Bone 2013;55:230–40. doi:10.1016/j.bone.2013.02.012.

[318] Fielding G, Bose S. SiO2 and ZnO dopants in three-dimensionally printed tricalcium phosphate bone tissue engineering scaffolds enhance

osteogenesis and angiogenesis in vivo. Acta Biomater 2013;9:9137–48. doi:10.1016/j.actbio.2013.07.009.

[319] Qiao Y, Zhang W, Tian P, Meng F, Zhu H, Jiang X, *et al*. Stimulation of bone growth following zinc incorporation into biomaterials. Biomaterials 2014;35:6882–97. doi:10.1016/j.biomaterials.2014.04.101.

[320] Baier M, Staudt P, Klein R, Sommer U, Wenz R, Grafe I, *et al*. Strontium enhances osseointegration of calcium phosphate cement: a histomorphometric pilot study in ovariectomized rats. J Orthop Surg Res 2013;8:16. doi:10.1186/1749-799X-8-16.

[321] Yuan H, Van Den Doel M, Li S, Van Blitterswijk CA, De Groot K, De Bruijn JD. A comparison of the osteoinductive potential of two calcium phosphate ceramics implanted intramuscularly in goats. J Mater Sci Mater Med 2002;13:1271–5.

[322] Shih Y-R V, Hwang Y, Phadke A, Kang H, Hwang NS, Caro EJ, *et al*. Calcium phosphate-bearing matrices induce osteogenic differentiation of stem cells through adenosine signaling. Proc Natl Acad Sci U S A 2014:1–6. doi:10.1073/pnas.1321717111.

[323] Ito A, Kawamura H, Miyakawa S, Layrolle P, Kanzaki N, Treboux G, *et al*. Resorbability and solubility of zinc-containing tricalcium phosphate. J Biomed Mater Res 2002;60:224–31. doi:10.1002/jbm.10068.

[324] Sila-Asna M, Bunyaratvej A, Maeda S, Kitaguchi H, Bunyaratavej N. Osteoblast differentiation and bone formation gene expression in strontium-inducing bone marrow mesenchymal stem cell. Kobe J Med Sci 2007;53:25–35.

[325] Li Z, Wang Y, Wang X, Lan A, Wu W. [Strontium ranelate promotes osteogenic differentiation of rat bone marrow mesenchymal stem cells by increasing bone morphogenetic protein-7 expression]. J South Med Univ 2011;31:1949–53.

[326] Kim K, Jeon Y, Lee J, Ahn S, Lee S, Cho D, *et al*. The Effect of Silicon Ion on Proliferation and Osteogenic Differentiation of Human ADSCs. Tissue Eng Regen Med 2010;7:171–7.

[327] Davison NL, Harkel B, Al G, Luo X, Layrolle P, Schoenmaker T, *et al*. OsteoinducTve , Resorbable Tricalcium Phosphate Achieved Through Submicrostructural Control of Osteoclasts 2012;608:241879.

[328] Stubblefield E, Mueller GC, Stubblefieldt E. Effects of Sodium Chloride Concentration on Growth , Biochemical Composition , and Metabolism of HeLa Cells. Cancer Res 1960;20:1646–55.

[329] Barralet J, Gbureck U, Habibovic P, Vorndran E, Gerard C, Doillon CJ. Angiogenesis in calcium phosphate scaffolds by inorganic copper ion release. Tissue Eng Part A 2009;15:1601–9. doi:10.1089/ten.tea.2007.0370.

[330] Yilma AN, Singh SR, Dixit S, Dennis VA. Anti-inflammatory effects of silver-polyvinyl pyrrolidone (Ag-PVP) nanoparticles in mouse macrophages infected with live Chlamydia trachomatis. Int J Nanomedicine 2013;8:2421–32. doi:10.2147/IJN.S44090.

[331] Ewald A, Hösel D, Patel S, Grover LM, Barralet JE, Gbureck U. Silver-doped calcium phosphate cements with antimicrobial activity. Acta Biomater 2011;7:4064–70. doi:10.1016/j.actbio.2011.06.049.

[332] Kumar R, Münstedt H. Silver ion release from antimicrobial polyamide/silver composites. Biomaterials 2005;26:2081–8. doi:10.1016/j.biomaterials.2004.05.030.

[333] Reginster JY, Meunier PJ. Strontium ranelate phase 2 dose-ranging studies: PREVOS and STRATOS studies. vol. 14 Suppl 3. 2003. doi:10.1007/s00198-002-1349-0.

[334] Murphy S, Boyd D, Moane S, Bennett M. The effect of composition on ion release from Ca-Sr-Na-Zn-Si glass bone grafts. J Mater Sci Mater Med 2009;20:2207–14. doi:10.1007/s10856-009-3789-y.

[335] Barradas AMC, Yuan H, van der Stok J, Le Quang B, Fernandes H, Chaterjea A, *et al*. The influence of genetic factors on the osteoinductive potential of calcium phosphate ceramics in mice. Biomaterials 2012;33:5696–705. doi:10.1016/j.biomaterials.2012.04.021.

[336] Castro AGB, Almeida JC, Salvado IMM, Margaça FM a., Fernandes MHV. A novel hybrid material with calcium and strontium release capability. Mater Lett 2012;88:12–5. doi:10.1016/j.matlet.2012.08.022.

[337] Ahn HW, Fulton B, Moxon D, Jeffery EH. Interactive effects of fluoride and aluminum uptake and accumulation in bones of rabbits administered both agents in their drinking water. J Toxicol Environ Health 1995;44:337–50. doi:10.1080/15287399509531963.

[338] Leeuwenkamp OR, van der Vijgh WJ, Hüsken BC, Lips P, Netelenbos JC. Human pharmacokinetics of orally administered strontium. Calcif Tissue Int 1990;47:136–41.

[339] Wiesmann H, Tkotz T, Joos U, Zierold K, Stratmann UDO, Szuwart T, *et al*. Magnesium in Newly Formed Dentin Mineral of Rat Incisor 1997;12:380–3.

[340] Li C, Paris O, Siegel S, Roschger P, Paschalis EP, Klaushofer K, *et al*. Strontium is incorporated into mineral crystals only in newly formed bone

during strontium ranelate treatment. J Bone Miner Res 2010;25:968–75. doi:10.1359/jbmr.091038.

[341] Janning C, Willbold E, Vogt C, Nellesen J, Meyer-Lindenberg a., Windhagen H, *et al*. Magnesium hydroxide temporarily enhancing osteoblast activity and decreasing the osteoclast number in peri-implant bone remodelling. Acta Biomater 2010;6:1861–8. doi:10.1016/j.actbio.2009.12.037.

[342] Xia W, Grandfield K, Schwenke A, Engqvist H. Synthesis and release of trace elements from hollow and porous hydroxyapatite spheres. Nanotechnology 2011;22:305610. doi:10.1088/0957-4484/22/30/305610.

[343] Olesberg JT, Cao C, Yager JR, Prineas JP, Coretsopoulos C, Arnold M a., *et al*. Optical Microsensor for Continuous Glucose Measurements in Interstitial Fluid. In: Coté GL, Priezzhev A V., editors. vol. 6094, 2006, p. 609403–609403 – 10. doi:10.1117/12.646751.

[344] Wang J, Zhang X. Needle-type dual microsensor for the simultaneous monitoring of glucose and insulin. Anal Chem 2001;73:844–7.

[345] Chen OT-C, Wang S. A medical microsensor for blood glucose monitoring. Proc. 1997 IEEE Int. Symp. Circuits Syst. Circuits Syst. Inf. Age ISCAS '97, vol. 4, IEEE; 1997, p. 2761–4. doi:10.1109/ISCAS.1997.612897.

[346] Verron E, Khairoun I, Guicheux J, Bouler J-M. Calcium phosphate biomaterials as bone drug delivery systems: a review. Drug Discov Today 2010;15:547–52. doi:10.1016/j.drudis.2010.05.003.

[347] Ginebra M-P, Traykova T, Planell J a. Calcium phosphate cements: competitive drug carriers for the musculoskeletal system? Biomaterials 2006;27:2171–7. doi:10.1016/j.biomaterials.2005.11.023.

[348] Bose S, Fielding G, Tarafder S, Bandyopadhyay A. Understanding of dopant-induced osteogenesis and angiogenesis in calcium phosphate ceramics. Trends Biotechnol 2013;31:594–605. doi:10.1016/j.tibtech.2013.06.005.

[349] Gérard C, Bordeleau L-J, Barralet J, Doillon CJ. The stimulation of angiogenesis and collagen deposition by copper. Biomaterials 2010;31:824–31. doi:10.1016/j.biomaterials.2009.10.009.

[350] Bacáková L, Mares V, Bottone MG, Pellicciari C, Lisá V, Svorcík V. Growth and differentiation of the vascular smooth muscle and endothelial cells cultured on fluorine ion-implanted polystyrene. Gen Physiol Biophys 1999;18 Suppl 1:53–6.

[351] Kose N, Otuzbir A, Pekşen C, Kiremitçi A, Doğan A. A silver ion-doped calcium phosphate-based ceramic nanopowder-coated prosthesis increased infection resistance. Clin Orthop Relat Res 2013;471:2532–9. doi:10.1007/s11999-013-2894-x.

[352] Lee JS, Murphy WL. Functionalizing calcium phosphate biomaterials with antibacterial silver particles. Adv Mater 2013;25:1173–9. doi:10.1002/adma.201203370.

[353] Wong KKY, Cheung SOF, Huang L, Niu J, Tao C, Ho C-M, *et al*. Further evidence of the anti-inflammatory effects of silver nanoparticles. ChemMedChem 2009;4:1129–35. doi:10.1002/cmdc.200900049.

[354] Nadworny PL, Wang J, Tredget EE, Burrell RE. Anti-inflammatory activity of nanocrystalline silver in a porcine contact dermatitis model. Nanomedicine 2008;4:241–51. doi:10.1016/j.nano.2008.04.006.

[355] Lansdown ABG. Silver in health care: antimicrobial effects and safety in use. Curr Probl Dermatol 2006;33:17–34. doi:10.1159/000093928.

[356] Kanczler JM, Oreffo ROC. Osteogenesis and angiogenesis: the potential for engineering bone. Eur Cell Mater 2008;15:100–14.

[357] Fellah BH, Josselin N, Chappard D, Weiss P, Layrolle P. Inflammatory reaction in rats muscle after implantation of biphasic calcium phosphate micro particles. J Mater Sci Mater Med 2007;18:287–94. doi:10.1007/s10856-006-0691-8.

[358] Fellah BH, Delorme B, Sohier J, Magne D, Hardouin P, Layrolle P. Macrophage and osteoblast responses to biphasic calcium phosphate microparticles. J Biomed Mater Res A 2010;93:1588–95. doi:10.1002/jbm.a.32663.

[359] Koike N, Fukumura D, Gralla O, Au P, Schechner JS, Jain RK. Tissue engineering: creation of long-lasting blood vessels. Nature 2004;428:138–9. doi:10.1038/428138a.

[360] Carano RAD, Filvaroff EH. Angiogenesis and bone repair. Drug Discov Today 2003;8:980–9.

[361] Gerber HP, Ferrara N. Angiogenesis and bone growth. Trends Cardiovasc Med 2000;10:223–8.

[362] Rey C, Combes C, Drouet C, Glimcher MJ. Bone mineral: update on chemical composition and structure. Osteoporos Int 2009;20:1013–21. doi:10.1007/s00198-009-0860-y.

[363] Racquel Z. LeGeros, John LeGeros DM. Calcium phosphate-based materials containing zinc, magnesium, fluoride and carbonate, 2009. doi:patent US 20090068285 A1.

[364] Wei Xia, Carl Lindahl, Håkan ENGQVIST, Peter Thomsen JL. Ion substituted calcium phosphate coatings, 2010. doi:patent WO 2010126436 A1.

[365] Gerber T. Inorganic resorbable bone substitute material and production method, 2009. doi:patent CA 2398517 C.

[366] Hedera P, Peltier A, Fink JK, Wilcock S, London Z, Brewer GJ. Myelopolyneuropathy and pancytopenia due to copper deficiency and high zinc levels of unknown origin II. The denture cream is a primary source of excessive zinc. Neurotoxicology 2009;30:996–9. doi:10.1016/j.neuro.2009.08.008.

SUMMARY

Autograft, which contains growth factors such as BMP and osteogenic cells, is the "gold standard" of bone graft yet it is limited in quantity and may cause harvest site morbidity. Synthetic bone substitutes are not limited in quantity but are not as efficient. The most promising subsets are calcium phosphate materials since they allow direct bone binding and growth on their surface (i.e. osteoconduction).

However, many synthetic orthopaedic materials alone cannot induce adequate osteogenesis at the desired sites, i.e. critical size defects. In this regard, there is a growing interest to improve the bone forming ability of synthetic bone substitutes with external additions such as osteogenic cells and growth factors. The surface microstructure of biomaterials has also been shown to be a controllable parameter related to their bone forming ability.

The inorganic phase of bone contains trace elements such as **zinc (Zn)**, **strontium (Sr)** and **fluoride (F),** which have been shown to regulate the proliferation and differentiation of bone cells in vitro. Therefore, by incorporating trace elements in synthetic bone substitutes, it may be possible to provide a release of the doped trace element, in this way affecting the surrounding cellular responses and subsequently promote their bone forming ability.

In this thesis we aimed to improve the bone forming ability of synthetic calcium phosphate materials by incorporating various trace elements. Three trace elements (Zn, Sr and F) were studied, with an emphasis on their effect on the biological performance of calcium phosphate materials in vivo using an ectopic model.

The effect of trace element addition on cellular behaviour has been shown in the past decades. Less clear is to which extent trace elements can affect bone formation by synthetic bone substitutes and to which extent these effects can be ascribed to the release of the doped ions. Starting with Zn (**Chapter 2**), we found that the addition of Zn in TCP enhanced the osteogenic differentiation of human bone marrow stromal cells (hBMSCs), influenced osteoclastogenesis and triggered *de novo* bone formation (i.e. osteoinduction) after 12-week intramuscular implantation in dogs. Adding Zn to tricalcium phosphate (TCP) also caused a reduction of grain and pore size from 3 μm to about 1μm, which has been reported to be related to material-directed osteoinduction. The observed osteoinductivity due to Zn addition can therefore not solely be attributed to the Zn release but could also have been due to these physical changes of the TCP. The results therefore indicated that the addition of Zn provoked multiple variances that might have contributed to the inductive bone

formation. In this regard, we aimed for better designed materials with fewer parameters altered to distinguish the role of doped ions.

In **Chapter 3 and 4**, composite models were proposed to exclude the role of surface topography. The trace element was first introduced into apatite particles and a polymer matrix (i.e. polylactide) was used to embed the ion-containing particles. In this way, we excluded the surface difference provoked by ion substitution from these ion-containing composites.

We found that the addition of fluoride in apatite decreased its solubility, leading to suppressed ion release and in vivo resorption of F-apatite/polylactide composite and consequently resulted in lower osteoinductivity in sheep (**Chapter 3**). In contrast, Sr increased the solubility of apatite and hence the release of Sr^{2+}, Ca^{2+} and PO_4^{3-} ions (**Chapter 4**). Moreover, it was shown that when Sr-containing apatite was introduced in two different polylactide matrices, only the highly amorphous polylactide (PDL04) supporting higher release of all three ions allowed the osteoinduction to occur after 12-week intramuscular implantation in dogs. These results indicate that the ion release from these composites is not only controlled by the chemical stability of the doped apatite but also the water affinity of the polylactide matrices. Further, it pointed out that the addition of trace elements is always paralleled with the changes in the release of Ca^{2+} and PO_4^{3-} and that sufficient release of Ca^{2+} and PO_4^{3-} might be necessary for bone induction to occur.

In **Chapter 5**, the release of Sr from Sr-apatite/PDL04 composites was shown to be dose-dependent and consistent for up to 24 weeks in vitro, indicating the implantation of such materials may provide long-term sustained delivery of the ions. Mouse bone marrow stromal cells (mBMSc) grown on these materials showed up-regulated osteogenic differentiation without the addition of growth factors. When the composites were studied with the combination of rhBMP-2 in a heterotopic model in rabbits, more bone was formed on composites with higher Sr content, suggesting the Sr addition in synthetic materials could enhance their bone forming ability.

Bone formation in osteoporotic (OP) patients is impaired, which might result in poor osteo-integration and surgical failure when implanting bone graft materials. Although Sr-containing composites were shown to enhance the osteogenic differentiation of mBMSc and in vivo bone formation (**Chapter 5**), it was yet to be clarified whether or not an osteogenic stimulus such as Sr could be effective in OP individuals. In **Chapter 6**, we showed that the addition of Sr could elevate the bone forming potential of materials in OP animals to the level equal to healthy animals, indicating the effectiveness of Sr addition to locally enhance the bone growth on implants in OP individuals.

In this thesis, we showed the potential of trace element addition in enhancing the bone forming ability of synthetic calcium phosphate materials. This enhancement, however, can only be partly attributed to the release of the doped ions and/or the release of calcium and phosphate ions, while the physicochemical changes provoked by the ion substitution, including surface topography, chemical stability and resorbability, may also have played a role. The findings presented herein help to better understand the role of doped ions in ion-containing materials and could ultimately lead to enhance bone regenerating synthetic bone substitutes.

SAMENVATTING

Een autogeen bottransplantaat bevat groeifactoren, zoals BMP's en osteogene cellen, en is daarom de huidige gouden standaard als bot vervangend materiaal. Echter, autogene bottransplantaten zijn beperkt beschikbaar en kunnen morbiditeit veroorzaken op de donor locatie. Synthetische bot vervangende materialen zijn niet beperkt in hun beschikbaarheid, maar bevatten geen BMP's en osteogene cellen, en zijn daarom minder efficiënt dan autogene bottransplantaten. De meest veelbelovende synthetische bot vervangende materialen zijn calcium fosfaat materialen, omdat deze materialen hebben aangetoond zich aan bot te kunnen binden, en als matrix kunnen fungeren voor botregeneratie (e.g. osteoconductie).

Synthetische bot vervangende materialen kunnen zelf geen osteogenese induceren (osteoinductie), waardoor deze materialen nog niet gebruikt kunnen worden bij het genezen van o.a. grote botdefecten. Er is daarom een toenemende belangstelling om de osteogene eigenschappen van deze materialen te verbeteren. Dit kan gedaan worden door osteogene cellen en/of groeifactoren aan deze materialen toe te voegen, maar het is ook mogelijk de microporositeit, oplosbaarheid en andere materiaal karakteristieken van een synthetische bot vervangend materiaal zo aan te passen dat deze osteoinductieve eigenschappen krijgt.

De anorganische fase van bot bevat spore elementen waaronder **zink (Zn)**, **Strontium (Sr)** en **Fluoride (F)**. Het is aangetoond dat deze spore elementen in vitro de proliferatie en differentiatie van botcellen reguleren. De osteoinductieve eigenschappen van een synthetische bot vervangend materialen zou mogelijk verbeterd kunnen worden door incorporatie van deze spore elementen in deze materialen. De geleidelijke afgifte van spore elementen tijdens de degradatie van een synthetisch bot vervangend materiaal zou een omliggende cellulaire response kunnen inleiden die osteoinductie tot gevolg kan hebben.

Bij ons onderzoek, beschreven in dit proefschrift, is geprobeerd de osteoinductieve eigenschappen van synthetische bot vervangende materialen te verbeteren door de incorporatie van verschillende spore elementen in deze materialen. Drie spore elementen (Zn, Sr, F) zijn hierbij onderzocht , waarbij voornamelijk gekeken is naar de osteoinductieve eigenschappen van deze materialen in een ectopisch model.

Het effect van spore elementen op het gedrag van cellen is al eerder aangetoond. Minder duidelijk is in hoeverre het toevoegen van spore elementen aan bot vervangende materialen van invloed is op de osteoinductiviteit, en in hoeverre dit effect kan worden toegeschreven aan de afgifte van de toegevoegde spore elementen aan het omliggende (bot) weefsel, tijdens de degradatie van het materiaal. In **hoofdstuk 2** hebben we laten zien dat Zn verrijkt tri-calciumfosfaat na 12 weken i.m. implantatie in honden, de osteogene differentiatie van humane beenmerg cellen stimuleert en invloed heeft op de osteoclastgenesis, en daarmee *de novo* botformatie induceert. Echter, het verrijken van Zn aan tri-calciumfosfaat is ook de oorzaak van veranderende materiaal karakteristieken, waaronder een reductie van de microporositeit van het materiaal. Het is bekend dat de reductie van microporositeit gerelateerd is aan materiaal gerelateerde osteoinductie. De gevonden osteoinductiviteit kan daarom niet alleen worden toegeschreven aan het toevoegde Zn, omdat deze kan ook gerelateerd zijn aan de kleinere microporositeit of andere veranderde materiaal karakteristieken. De resultaten laten zien dat het toevoegen van Zn meerdere materiaal karakteristieken heeft aangepast die kunnen hebben bijgedragen aan de osteoinductiviteit van het materiaal. Er is daarom in latere experimenten gebruik gemaakt van materialen waar minder eigenschappen aan zijn veranderd om zo alleen de rol van de toegevoegde spore elementen te kunnen onderzoeken.

In **hoofdstuk 3 en 4** worden composiet materialen onderzocht die de rol van de microporositeit, of andere materiaal karakteristieken, op de osteoinductiviteit van een materiaal uitsluiten, waardoor alleen de rol van toegevoegde spore elementen kan worden onderzocht. Hiervoor zijn spore elementen toegevoegd aan een granulaat van calcium fosfaat die vervolgens zijn ingebed in een matrix van poly-melkzuur. Door de matrix van poly-melkzuur zijn veranderingen aan de microporositeit, en andere materiaal karakteristieken, ondervangen waardoor alleen naar het effect van het toegevoegde spore element gekeken kan worden. Het toevoegen van F aan granulaat van calciumfosfaat verminderd de oplosbaarheid van het granulaat. Een verminderde oplosbaarheid van het granulaat leidt tot een verminderde in-vivo resorptie van het fluor-calciumfosfaat / poly-melkzuur composiet, een verminderde afgifte van spore elementen in het omliggende weefsel en daarmee een verminderde osteoinductiviteit (**hoofdstuk 3**). In tegenstelling tot F wordt de oplosbaarheid van calciumfosfaat granulaat verhoogd als Sr wordt toegevoegd, waarmee dus ook een verhoogde afgifte van Sr, Ca en PO_4^{3-} ionen wordt gerealiseerd (**hoofdstuk 4**). Na 12 weken i.m. implantatie in honden is aangetoond dat wanneer met Sr verrijkt calciumfosfaat granulaat wordt toegevoegd aan twee verschillende polymere matrixen, alleen de amorfe poly-melkzuur (PDL04) een hogere afgifte van al de drie

ionen te zien gaf, die verantwoordelijk zijn voor de gevonden osteoinductie. De resultaten laten zien dat de afgifte van ionen door deze composieten niet alleen bepaald worden door de chemische stabiliteit van het verrijkte calciumfosfaat, maar ook door de affiniteit met water van de poly-melkzuur matrixen. Verder heeft het ook laten zien dat het toevoegen spore elementen altijd gelieerd is met veranderingen in de afgifte van Ca^{2+} en PO_4^{3-} ionen, en dat de afgifte van deze ionen bepalend kan zijn voor osteoinductie.

Hoofdstuk 5 laat zien dat de afgifte van Sr vanuit een Sr verrijkt calciumfosfaat / PDL04 composiet, dosis afhankelijk is, en consistent verloopt gedurende 24 weken in vitro. Dit is een indicatie dat het implanteren van deze materialen ook een langdurige afgifte van Sr ionen zal laten zien. Muis beenmergcellen gekweekt op deze materialen laten osteogene differentiatie zien, ook zonder de toevoeging van groeifactoren. Wanneer de composieten bestudeerd werden in combinatie met rhBMP-2 in een heterotopic model in konijnen, werd meer bot werd gevormd op composieten met een hoog Sr concentratie. Dit suggereert dat het toevoegen van Sr aan synthetische bot vervangende materialen de osteoinductiviteit kan verbeteren.

Osteogenese bij patiënten met osteoporose is sterk verminderd. Dit kan resulteren in een slechte integratie van een bot vervangend materiaal in het omliggende botweefsel en daarmee het mislukken van de chirurgische procedure. Hoewel Sr verrijkte composieten hebben aangetoond de osteogene differentiatie te stimuleren van mBMSc en in vivo botformatie (**hoofdstuk 5**), zal het nog moeten worden aangetoond of een osteogene stimulatie zoals het toevoegen van Sr, effectief is op patiënten met osteoporose. In **hoofdstuk 6** hebben we laten zien dat het toevoegen van Sr verhoogde botgroei kan laten zien op implantaten bij proefdieren met osteoporose, welke vergelijkbaar is met de botgroei van gezonde proefdieren, wat indicatief is voor de effectiviteit van het toevoegen van Sr op de botgroei bij patiënten met osteoporose.

In dit proefschrift hebben we laten zien dat het toevoegen van spore elementen aan synthetische bot vervangende materialen de osteoinductieve eigenschappen van deze materialen kan verbeteren. Deze verbetering kan maar ten dele worden toegeschreven aan de toegevoegde spore elementen, omdat materiaal karakteristieken zoals de afgifte van Ca_{2+} en PO_4^{3-} ionen, microporositeit, oplosbaarheid, en andere materiaal karakteristieken, mogelijk ook een rol spelen. De bevindingen beschreven in dit proefschrift helpen het beter begrijpen te krijgen naar de rol van spore elementen bij osteogenese en kan uiteindelijk leiden naar verbeterde osteoinductiviteit van synthetische bot vervangende materialen.

ACKNOWLEDGEMENTS

My PhD and the make of this thesis will not be possible without the help of all my friends, my colleagues, and my family. As a Chinese, I have dreamed of long speeches that can be used in such scenario for years just in case if I finally have to say something. Now the time comes and I forgot all the planned drafts. In the end it actually has nothing to do with the language but is because it is so difficult to contain all the supports I got from every one of you, all the tears and laughter that worthy mention, and, of course, to include all the names in such a narrow page.

Master Yuan, thank you for giving me this opportunity to pursue my PhD in the Netherlands. I still remember the first time we went to the countryside for an animal study almost 10 years ago. With the earthy smell in the air, you taught me the first lesson about how a real scientific life is: it is not playing with glass tubes in a tidy lab or pointing at graphs in front of an office desk. A real scientist is like a soldier in the frontline, ready to walk in the mud, not afraid of blood and flesh and capable of standing hours and hours at the post in the operation room. With your passion for work, you made yourself the best example and inspired everyone in the group keep moving forward to the goal. Thank you for your hospitality when I first arrived in the Netherlands and your guidance in the lab, in the noisy kitchen and in my life path.

Prof. de Bruijn, you are a strict scientist and at the same time such a kind boss! I am so grateful that I did my PhD at Xpand under your supervision. You persistently lead the company with a positive attitude and you also care about the personal development of the employees. You taught me how to manage and schedule a PhD's life wisely and how to think logically and scientifically. Thank you for all your criticisms in scientific discussions and for your huge patience in correcting my manuscripts repeatedly. And, thank you for bringing us out of office to the faraway cities, the countryside and the great sails!

Now my PhD fellows, Davide, on my first day in Xpand, you introduced me the history of R&D group upstairs, in Meeting Room 2, and that was how I started my PhD life. I learnt a lot from you these years and it is such an intriguing experience to work with a serious Italian. Thank you for all the fiery discussions we had and I appreciate every piece of your input. Thank you for driving Yuxi and me home on rainy days and for the delicious pasta you and Pan Zhen cooked for us!

Noel, you and I are so different people. But our common passion on cookies and other wonderful food united us! Please do not give up baking. I believe a cake that can be easily forgotten is not a good cake. Although that brownie you brought to the

office was smoking, I did see a lot of potential of its phenotypes. I bet you can handle baking very well, just as good as you handle the cells. You know it takes time.

Rongquan and Luuk, I wish you good luck in your future research!

Florence, you are a skilful manager who always kindly asks for my availability before distributing any tasks. Working with you really makes me feel my work is meaningful! Also thank you for helping Yuxi on her assignment! To Vincent, it is never boring chatting with you. Thank you for keeping our lab instruments running in good condition and also thanks for fixing my bicycle pump. I wish you recover as soon as possible so we can try more exotic food that only Chinese and French eat! And some day you will show me your bicycle collections! To the production team, Remco, Ruiqing and Jurren, you are probably the most accurate and tidy people in the company. Thank you for your supervision in the processing lab and clean room. To Pieter, Rens, Ruud, Wendy, Jordy, Eloise and Marijn, I enjoyed the office time we spent together with the peacocks, mosquitofishes and shrimps! Viola, the life in the Netherlands has been so much easier with your help! I cannot thank you enough for what you have done for Yuxi and me. Ulrike, thank you for all the stickers you insert in my study reports which certainly improved the good documentation practice. To Eko, Linda, Elise, Monica and Jinyi, I wish you every success in your new careers! To all of you working in Xpand and Cellcotec, thank you for your kindness to me all these years and all the cakes you brought to the office! Anyhow I am not good at phrases so I will bring cakes!

I also would like to thank Prof. Grijpma and Prof. Habibovic for your critics to the scientific issues and your suggestions to my career. Karin, thank you for all the mails and phone calls you made to help me pursuing my PhD! I am grateful to Prof Yan, my first supervisor in China, for your care on me and your support in my research.

Baba and Mama, please forgive my obstinacy in the past. Even though I have been unruly since young, you loved me selflessly. When I decided to go abroad, you supported me without any hesitation. It is from you that I learnt the meaning of patience and kindness. I wish you are happy and proud to see this book!

Yuxi, thank you for being here with me. Since our attachment to each other is growing stronger every day, shall we fit your ring finger with some shining thing?

Yo-yo, among all the creatures in this world I love you most. Part of your fearlessness is now living inside me and it encouraged me get through difficulties in life and the long, dark winter nights here. I missed you a lot. *May you live happily and play all day in doggie heaven.*

List of publications

- **Luo X**, Barbieri D, Davison N, Yan Y, de Bruijn JD, Yuan H. Zinc in calcium phosphate mediates bone induction: in vitro and in vivo model. Acta biomaterialia 10/2013; 10(1): 477–85.
- **Luo X**, Barbieri D, Passanisi G, Yuan H, de Bruijn JD. Influence of fluoride in poly(d,l-lactide)/apatite composites on bone formation. Journal of Biomedical Materials Research Part B Applied Biomaterials 08/2014; 103(4)
- **Luo X**, Barbieri D, Zhang Y, Yan Y, de Bruijn JD, Yuan H. Strontium-containing apatite/poly-lactide composites provide strontium-rich environment favouring osteogenic differentiation and in vivo bone formation. ACS biomaterials science and engineering 2015, 1 (2), pp 85–932014.
- **Luo X**, Barbieri D, Duan R, Yuan H, de Bruijn JD. Strontium-containing apatite/polylactide composites enhance bone formation in osteopenic rabbits. Acta Biomaterialia 07/2015; 26: 331-37.
- **Luo X**, Barbieri D, Zhang Y, Yan Y, Yuan H, de Bruijn JD. The impact of polymer matrix composition on the ion release and osteoinductivity of Sr-containing apatite/polylactide composites. Submitted
- Zhang J, **Luo X**, Barbieri D, Barradas AMC, de Bruijn JD, van Blitterswijk CA, Yuan H. The size of surface microstructures as an osteogenic factor in calcium phosphate ceramics. Acta Biomater. 2014 Jul;10(7):3254–63.
- Davison NL, **Luo X**, Schoenmaker T, Everts V, Yuan H, Barrère-de Groot F, de Bruijn JD. Submicron-scale surface architecture of tricalcium phosphate directs osteogenesis in vitro and in vivo. Eur Cell Mater. 2014 Jan;27(0):281–97
- Wang L, **Luo X**, Barbieri D, Bao C, Yuan H. Controlling surface microstructure of calcium phosphate ceramic from random to custom-design. Ceram Int. 2014 Jul ;40(6):7889–97.
- Barbieri D, Yuan H, **Luo X**, Farè S, Grijpma DW, de Bruijn JD. Influence of polymer molecular weight in osteoinductive composites for bone tissue regeneration. Acta Biomater. 2013 Jul 31;8–10.
- Barbieri D, de Bruijn JD, **Luo X**, Farè S, Grijpma DW, Yuan H. Controlling dynamic mechanical properties and degradation of composites for bone regeneration by means of filler content. J Mech Behav Biomed Mater. 2013 Apr;20:162–72.
- Davison NL, ten Harkel B, Schoenmaker T, **Luo X**, Yuan H, Everts V, et al. Osteoclast resorption of beta-tricalcium phosphate controlled by surface architecture. Biomaterials 2014;35:7441–51.

Accepted conference abstracts

- 9th World Biomaterials Conference (WBC), 2012, Chengdu
  - Oral presentation “Effect of strontium substitution in apatite on apatite/poly(L-D, L-lactide) composites ”
  - Poster presentation “Improved bone formation with zinc containing calcium phosphates ” ---Rapid Fire Poster Awards
- 25th European Conference on Biomaterials (ESB) , 2013, Madrid
  - Poster presentation “Inhibition of osteoclastogenesis with Fluoride-containing apatite/PLA composites”
- 26th Symposium and Annual Meeting of the International Society for Ceramics in Medicine (Bioceramics), 2014, Barcelona,
  - Oral presentation “Influence of fluoride in poly(D,L-lactide)/apatite composite on bone induction”
- Consortium meeting of The Netherlands Institute for Regenerative Medicine（NIRM), 2013, Utrecht
  - Poster presentation “Strontium-substituted apatite/PLA nano-composites allowing dose-dependent strontium release”

About the author

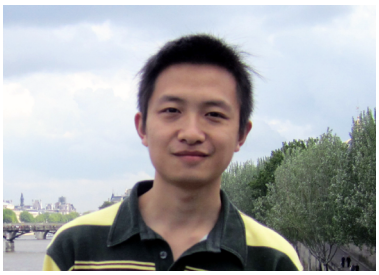

Xiaoman Luo was born on May 22nd, 1984 in Chengdu, China. He spent most of his childhood quietly with all kinds of insects he could find on the balcony and claimed that he would be a scientist in the future, just like all other boys of that age in primary school. Stubbornly, he carried this claim to Sichuan University, where he obtained his bachelor degree in Polymer Science and Engineering on 2005. After the graduation, he worked in Sichuan Guona Technology Co., Ltd. as a synthesis operator and later as an assistant researcher in biomaterials. 3 years later he went back to Sichuan University to study biomaterial science in Prof. Yan's group. He joined Xpand Biotechnology in 2010 as a PhD student under the supervision of Dr. Yuan and Prof. de Bruijn. Supported by all his friends and Shifu, and his lovely wife, he joyfully sees that his childhood claim is still stumbling with him on the path of science.